AN ABSTRACT OF THE DISSERTATION OF

LOUIS IRWIN GORDON for the DOCTOR OF PHILOSOPHY

in Chemical Oceanography presented on 20 November 1972

A STUDY OF CARBON DIOXIDE PARTIAL PRESSURES IN SURFACE WATERS OF THE PACIFIC OCEAN

Redacted for privacy

Abstract approved: _____
Dr. P. Kilho Park

An instrument system for continuous semi-automated measurement of the partial pressure of carbon dioxide in the oceans has been developed. This simple, portable, and reliable system was applied to studies of surface waters and to depths of 55 m in the North Pacific. It employs a non-dispersive infrared gas analyzer to measure concentrations of carbon dioxide in air streams equilibrated with the seawater. Using simplified models of the analytical system, response times were calculated which agreed with the observed response times within a factor of 2. With the system response time of 40 seconds, horizontal surface PCO_2 features of one kilometer or larger dimensions may be faithfully observed from a ship traveling at a speed of ten knots.

The system was calibrated against standards furnished by the CO_2 Project Laboratory at the Scripps Institution of Oceanography. A generalized calibration scheme which included compensation for the analyzer nonlinearity was developed to permit use of the analyzer over almost any desired concentration range. The system has a precision of ±1% and an estimated accuracy of ± 5%.

The correction formula was derived to evaluate the error in measured PCO_2 which arises when a seawater sample is heated, during sampling, under the restraints of constant salinity, alkalinity, and total carbon dioxide concentration. The resultant correction is approximately +4%/°C in agreement with one empirically derived correction in the literature of +4.5%/°C. It is in disagreement with several other corrections which have been used.

Between October 1968 and March-April 1969, the surface PCO_2 in the subarctic North Pacific Ocean was observed to increase by an average of 60 ppm. This was attributed to winter mixing of deep, high PCO_2 waters into the surface layers and diminished photosynthetic activity. An additional rise of 18 ppm in PCO_2 occurred in a 30-45 day period in March-April 1969 largely because of spring warming of the surface waters. The 60 ppm rise from October to March-April reversed the role of the surface ocean waters from that of sources to sinks for atmospheric CO_2.

Mapping of summertime surface PCO_2 distributions in the Pacific Ocean was extended into the subarctic Pacific and the Bering Sea. High surface PCO_2 was directly observed along the Aleutian Island arc probably as the result of local upwelling or intense vertical mixing in and near the passes between the islands. The central Bering Sea and central subarctic Pacific were intense sinks and surface waters off the mouths of the Yukon and Kuskokwim Rivers were sources of carbon dioxide to the atmosphere.

PCO_2 was found to be a useful indicator and locater of upwelling and associated processes in the waters off Oregon. This was particularly true when PCO_2 was used in conjunction with other oceanographic variables. PCO_2 and pH were found to be coherent as would be expected theoretically. Theoretically calculated curves fitted the observed relationship well. PCO_2 and apparent oxygen utilization were also examined but found to be less coherent. PCO_2 and sigma-t were found to be coherent probably because of the coincident effects of the several oceanographic processes: mixing, photosynthesis, respiration and decay, heating, and atmospheric exchange.

The time variations in PCO_2 distributions in Oregon coastal waters were also examined and PCO_2 was found to vary by up to several hundred ppm in the space of two to five days. This variation was observed in small patches close inshore with horizontal scales on the order of tens of kilometers.

Finally, the comparisons of vertical sections of sigma-t and PCO_2 indicated the possible existence of a carbon trap on the shelf near the coast. The carbon trap is postulated to result from a cyclical process wherein part of the carbon dioxide entering via upwelling into the near coastal region is fixed into the biomass and/or sediments.

A Study of Carbon Dioxide Partial Pressures in Surface Waters of the Pacific Ocean

by

Louis Irwin Gordon

A DISSERTATION

submitted to

Oregon State University

in partial fulfillment of
the requirements for the
degree of

Doctor of Philosophy

June 1973

APPROVED:

Redacted for privacy

Professor of Oceanography in charge of major

Redacted for privacy

Dean of School of Oceanography

Redacted for privacy

Dean of Graduate School

Date thesis is presented 20 November 1972

Typed by Suelynn Williams for Louis Irwin Gordon

To Jackie, my wife

to Judy and Dee, my daughters

to Justin, my son

to Ella Gordon, my mother

and to my father, Morris Gordon

whose memory is blessed

with love and gratitude.

ACKNOWLEDGMENTS

I am deeply indebted to my major professor, P. Kilho Park, for making this work possible and for his seemingly infinite patience. I also owe a debt of gratitude to Prof. Harry Freund for much of the instrumentation background and constructive criticism of this work. Prof. Robert L. Smith has spent innumerable hours in discussion of problems associated with the upwelling process, the upwelling field work herein, and finally in reading and criticizing Chapter five on upwelling. My thanks go as well to the remaining members of my doctoral committee, Professors Raymond Simon and Norman Cutshall for their help and encouragement. The collaboration with Stephen Hager, Timothy Parsons, John Kelley, and Donald Hood on the publication of material from Chapters three and four has been a gratifying experience.

This work would not have been possible without the contributions of many other people. Dr. John Teal of the Woods Hole Oceanographic Institution lent the first air-water equilibrator which was used in the early stages of the project. Kent Kantz, Mike King, and Ed Seifert helped with the laboratory work. They, along with Saul Alvarez-Borrego, David Ball, Peter Becker, Richard Gates, and Stephen Hager helped shake down and operate the system during more than

220 days at sea. I am also grateful to the several captains, crews and scientific parties of the CNAV ENDEAVOUR, NOAAS SURVEYOR, and R/V YAQUINA for their tireless and enthusiastic support. The computer programs necessary to reduce the tremendous amount of data acquired in the laboratory and at sea and in the theoretical work were written with the cheerful and expert assistance of Lynn Jones and David Standley. Joyce Shane helped draft the many vertical sections presented.

This dissertation owes its ultimate fruition to the long hours of work and encouragement by Richard Tomlinson, Suelynn Williams, and Jaqueline Gordon.

This research was made possible by the financial support of the National Science Foundation under grant numbers GA 1281 and GA 12113 as well as the Office of Naval Research through contract N00014-67-A-0369-0007 under project NR 083-102.

TABLE OF CONTENTS

TABLE OF CONTENTS CONTINUED

LIST OF TABLES

LIST OF FIGURES

LIST OF FIGURES CONTINUED

LIST OF FIGURES CONTINUED

LIST OF FIGURES CONTINUED

LIST OF FIGURES CONTINUED

A STUDY OF CARBON DIOXIDE PARTIAL PRESSURES IN SURFACE WATERS OF THE PACIFIC OCEAN

CHAPTER 1

INTRODUCTION

1.1 General Remarks and Fundamental Background

The carbon dioxide partial pressure of seawater may be defined as the equilibrium partial pressure of carbon dioxide in a small volume of a gas phase in contact with a large volume of the seawater, the interface being a plane surface.

The carbon dioxide partial pressure (PCO_2) is related at equilibrium to the concentration of molecular CO_2 in solution (C_{CO_2}) by Henry's Law:

$$PCO_2 = \alpha\, C_{CO_2} \qquad (1.1)$$

α, the solubility coefficient, varies with the temperature and salinity of seawater and has been calculated or measured by several workers (Buch, 1951; Murray and Riley, 1971; Li and Tsui, 1971).

The molecular CO_2 concentration is determined by the poising of the various chemical equilibrium, and often non-equilibrium, processes which can take place in the seawater and which involve carbon dioxide, directly or indirectly.

These processes are of manifold variety. They will be reviewed only briefly here but the reader is referred to the many

recent, more complete treatments of the subject, many of which will be referenced as this review proceeds.

Biological processes affecting PCO_2. A process, or rather set of processes, which exerts an intense influence upon PCO_2 in seawater is the complex of biochemical reactions which consume or liberate CO_2 from place-to-place and time-to-time. These reactions are often summarized for many purposes by the hypothetical and empirically based model of Redfield for the formation and oxidation of a "typical" or "average" organic molecule:

$$(CH_2O)_{106} \cdot 16NH_3 \cdot H_3PO_4 + 138\,O_2 \underset{\text{photosynthesis}}{\overset{\text{oxidation}}{\rightleftharpoons}} 106CO_2 + 16HNO_3 + H_3PO_4 + 122H_2O \qquad (1.2)$$

This equation, developed by Redfield and his co-workers (Redfield, Ketchum, and Richards, 1963) has proven useful in many oceanographic studies of water movement at depth (see for example, Alvarez-Borrego and Park, 1971; Alvarez-Borrego et al., 1972; Pytkowicz and Kester, 1966; Sugiura and Yoshimura, 1964; Sugiura, 1965). It has also been valuable for interrelating carbon dioxide, oxygen, and plant nutrient variations in the oceans (cf. Stefánsson and Richards, 1963; Stefánsson, 1968; Park, 1967; Park et al., 1972;

Alvarez-Borrego et al., 1972). Several workers have been employing this model in studies leading toward modeling of the distributions of various chemical oceanographic variables (Wyrtki, 1962; Munk, 1966; Keeling and Bolin, 1968).

This model of Redfield, Ketchum, and Richards (RKR) describes an "average" set of biochemical reactions which in general do not reach equilibrium. At best they are in a steady state wherein solar energy is in part stored as potential energy in the form of plant-photosynthesized organic compounds. The changes produced by these processes are not in PCO_2 directly but in the amount of total inorganic carbon dioxide (TCO_2) which is present in seawater.

Inorganic chemistry of CO_2 in aqueous solutions and seawater. The next part of this review deals with the reactions between, and the partitioning of, TCO_2 among its various inorganic components. This subject area has been reviewed recently by several authors (Stumm and Morgan, 1970, Chapt. 4; Pytkowicz, 1968; Skirrow, 1965; Edsall, 1969; Garrells and Christ, 1965, Chapt. 3). Edsall (1969) treated the fundamental physical properties, thermodynamics, and kinetics of interconversion of carbon dioxide, carbonic acid, bicarbonate ion, and carbonate ion in water and other solvents. Stumm and Morgan (1970) and Garrels and Christ (1965) applied basic physical chemistry treatments to the behavior of carbon dioxide

chemistry in natural water and geochemical systems. Skirrow (1965) reviewed the aqueous physical chemistry of carbon dioxide with particular reference to the marine context while Pytkowicz (1968) emphasized the effects of hydrostatic pressure upon carbonate equilibria in the oceans. Because of the existence of these recent and very comprehensive reviews it seems unnecessary to give a detailed treatment here. However, the reader who is unfamiliar with the subject may perhaps follow more easily what comes later if a brief sketch of seawater carbon dioxide chemistry is presented.

Molecular CO_2 in aqueous solutions hydrates to form carbonic acid:

$$H_2O + CO_2(aq) = H_2CO_3 \qquad (1.3)$$

for which the Law of Mass Action may be applied to formulate an equilibrium constant:

$$K_h = [H_2CO_3]/[H_2O][CO_2] \qquad (1.4)$$

The square brackets denote activities of the various species. The activity of water is commonly considered to be constant and included in K_h so that the expression reduces to:

$$K_h = [H_2CO_3]/[CO_2] \qquad (1.5)$$

The kinetics of this reaction, in the forward direction particularly, are slow, among the slowest of the various reactions

discussed in this section. The forward rate constant is but 0.03 sec^{-1} (Edsall, 1969). The situation is considerably more complicated than this presentation would indicate and the reader is referred to the review by Edsall for a more thorough treatment. The most important complications are the existence of

$$CO_2(aq) + OH^- = HCO_3^- \qquad (1.6)$$

at pH above 7.5, and the possible contribution of

$$H_2O + CO_2(aq) = H^+ + HCO_3^- \qquad (1.7)$$

whose rate it is impossible to measure independently of (1.3).

The kinetics of the hydration and dehydration reactions are profoundly important for two reasons. They play an important role in the response time considerations of the PCO_2 measurement apparatus to be described in this work. They are also vitally important in life systems involving excretion of metabolic CO_2 in the lungs of animals. The latter have developed specific enzymes, carbonic anhydrases, to catalyze the hydration of CO_2 and the dehydration of HCO_3^- to circumvent the slow inorganic reaction rates (Forster et al., 1969).

H_2CO_3 acts as a diprotic acid in aqueous solution, dissociating in two steps

$$H_2CO_3 = H^+ + HCO_3^- \qquad (1.8)$$

and

$$HCO_3^- = H^+ + CO_3^{-2} \qquad (1.9)$$

for which one may write

$$K_1 = [H^+][HCO_3^-]/[H_2CO_3] \qquad (1.10)$$

and

$$K_2 = [H^+][CO_3^{-2}]/[HCO_3^-] \qquad (1.11)$$

respectively. The first dissociation constant pK_1 (the logarithm, base 10, of the reciprocal of K_1) is approximately 3.8; and pK_2 is approximately 10.3 at 25° C (Stumm and Morgan, 1970, p. 79).

For operational ease oceanographers generally redefine these equilibrium constants in several ways. The convention generally used is that followed by Lyman (1956) whose equilibrium constants will be used in this work. He rewrote Eq. (1.10) in terms of the sum of (CO_2) and (H_2CO_3) instead of $[H_2CO_3]$. The parentheses denote total concentrations instead of activities. The result

$$K_1 = [H^+][HCO_3^-]/((CO_2) + (H_2CO_3)) \qquad (1.12)$$

makes carbonic acid appear as a much weaker acid. This is because K_h is small, that is because $pK_h \sim 2.7$ for Eqs. (1.3) and (1.5) (Edsall, 1969) and only a few tenths of a percent of the sum of the $CO_2(aq)$ and H_2CO_3 present are in the form of H_2CO_3. The new

value for pK_1 becomes approximately 6.3 at 25°C.

Thus far we have been discussing solutions of CO_2 in distilled water. The presence in seawater of some 3.5 g/kg of dissolved salts introduces several complexities. These will necessitate further operational modifications to the expressions for the equilibrium constants. First, bicarbonate and carbonate ions apparently form ion pairs with specific cations present in seawater. Thus, only about 9% of the carbonate ion is thought to be present as free carbonate ion while the remainder forms ion pairs with magnesium (principally), sodium, and calcium (Garrels and Thompson, 1962). Bicarbonate ion forms ion pairs with the same cations but to a lesser degree, approximately 70% of the bicarbonate remaining in the unassociated form.

A further complexity is introduced by the large ionic concentration of seawater, equivalent to somewhat higher than a one-half molal solution. This causes diminished activities of ions, related to their free, or unassociated, concentrations by activity coefficients less than unity. Although the values of activity coefficients can be calculated (Stumm and Morgan, 1970) for very dilute solutions up to perhaps 0.03 molal total ionic concentrations, they are at best only approximately estimated at the concentration of seawater. This makes it difficult to work with Eqs. (1.10), (1.11), and (1.12) as we have written them thus far.

Furthermore, with the exception of hydrogen ion, whose activities in seawater can be precisely if not accurately measured, we seldom can measure or control bicarbonate and carbonate ion activities. What we usually can measure is the total carbon dioxide, TCO_2, which is present as molecular carbon dioxide, carbonic acid, free bicarbonate and carbonate ions, plus the bicarbonate and carbonate associated with cations in ion pairs, defined as:

$$TCO_2 = (CO_2) + (H_2CO_3) + (HCO_3^-)_{total} + (CO_3^{-2})_{total} \quad (1.13)$$

or alternatively we measure the carbonate alkalinity, CA:

$$CA = (HCO_3^-)_{total} + 2(CO_3^{-2})_{total} \quad (1.14)$$

The usual methods of measurement of TCO_2 or CA involve acidification, followed by extraction and measurement of the resultant CO_2 or measurement of the amount of acid required to neutralize all of the bicarbonate and carbonate ions present respectively. Both methods completely dissociate all ion pairs and measure the TCO_2 and CA (plus any other alkalinity present, eg. borate). The alternative, synthetic, method of study involves introducing a known amount of CO_2, HCO_3^-, and/or CO_3^{-2} into the seawater being studied. This method, too, gives control over only the total concentrations, and

not activities.

To simplify the problem analytically the expressions for the dissociation constants of carbon dioxide have often been rewritten by marine chemists in terms of hydrogen ion activity and total concentrations, free plus combined, of bicarbonate and carbonate ions:

$$K_1' = [H^+](HCO_3^-)/((CO_2) + (H_2CO_3)) \qquad (1.15)$$

$$K_2' = [H^+](CO_3^{-2})/(HCO_3^-) \qquad (1.16)$$

Both these forms and the values of K_1' and K_2' as functions of temperature and salinity used in this work are those of Lyman (1956).

Having so defined the dissociation constants of carbonic acid it becomes simpler to study the chemistry of carbon dioxide and carbonates in the oceans. Harvey (1955) and Skirrow (1965) present detailed treatments of the manipulations involved using the dissociation constants as written here and using the scheme devised by Buch (1951).

Stumm and Morgan (1970) develop further the graphical methods for study of the CO_2 system introduced by Deffeyes (1965) and for study of acid-base titrations by Gran (1952); the use of the latter technique has been strongly encouraged by Dyrssen and Sillén (1967).

Park (1969) discusses ten different measurement approaches

to the study of the CO_2 system in seawater, each of which employs observation of two or three of the variables, pH, PCO_2, TCO_2, and CA. The CA is derived from the total alkalinity, TA, of a seawater sample and includes, in addition to the CA defined earlier, the contribution arising from the presence of borate ion in seawater.

$$TA = CA + BA \tag{1.17}$$

The borate alkalinity (BA) may be estimated from the pH and salinity of the water sample and knowledge of the total boron to salinity ratio (cf. Skirrow, 1965). Park also investigated the effect upon the seawater CO_2 system of addition or subtraction of CO_2 by respiration and/or decay or photosynthesis as well as the effect of removal of carbonate ion by precipitation of calcium carbonate or the converse by dissolution of calcium carbonate.

It should be noted that provided that Eqs. (1.1), (1.13), (1.14), (1.15), (1.16), and (1.17) are valid and that the values of α, K_1', and K_2' are measured as functions of temperature, salinity, and if applicable, pressure, in a manner consistent with the use to be made of them, then measurement of any two of the variables, pH, PCO_2, TA, and TCO_2 serves to completely determine the poising of, or state of partitioning of CO_2 within, Eqs. (1.8) and (1.9), or (1.13) and (1.14). Implicit in the values of α, K_1' and K_2' used in any calculations will thus be a knowledge, or prior measurement of, the

temperature and salinity of the seawater as well (and pressure if the seawater came from appreciable depth).

The approach employing the measurement of pH and TA has been the most widely used until recent years. The relative ease of measurement of the pH of seawater using a glass electrode and of TA by measurement of the pH after addition of a known quantity of acid (Anderson and Robinson, 1946; Culberson et al., 1970) is a relatively simple procedure. However, the initial measurement of pH must be carried out with great care in both the sampling and the measurement itself (Strickland and Parsons, 1968, p. 29; Li et al., 1969; Pytkowicz et al., 1966).

These measurements, together with Eqs. (1.1), (1.13), (1.14), (1.15), (1.16), and (1.17) may be combined to give:

$$PCO_2 = CA[H^+]^2 / \left(K_1'\alpha([H^+] + 2K_2')\right) \qquad (1.18)$$

Thus the PCO_2 of a water sample may be computed from pH and alkalinity determinations.

Wong (1968) developed a precise method for the total extraction of CO_2 from seawater acidified with phosphoric acid and subsequent measurement of the CO_2 with an infrared gas analyzer. He then applied the technique to the study of TCO_2 distributions in the eastern Tropical Pacific Ocean. He calculated an evasion rate of CO_2 from the ocean of 24 ± 14 moles CO_2 $m^{-2}yr^{-1}$ and an atmospheric residence

time of CO_2 relative to exchange with the ocean of 4.5 years.

Both prior to the introduction of the Anderson-Robinson technique for measuring TA, and in more recent years, direct titrations have been widely employed. Skirrow (1965, p. 247) reviews the early work.

Edmond (1970) has developed a technique for titration of seawater in a closed volume, following the titration with a glass electrode. Using a digital computer for data processing and Gran's (1952) method he was able to determine both TA and TCO_2 with a single titration and thus completely determine the CO_2 system. He then applied the method to a study of the formation and dissolution of carbonate sedimentary minerals.

Park (1965ab), Park et al. (1964), and more recently Weiss (1970) have measured TCO_2 in seawater using gas chromatography. The methods are based upon that published by Swinnerton et al. (1962). The method has been applied by Park et al. (1969ab) to studies of Columbia River CO_2 chemistry and in this work as auxiliary data for the PCO_2 studies in the Bering Sea, subarctic Pacific Ocean, and off Oregon. Weiss (1970) has refined the instrumentation and applied TCO_2 measurements along with nitrogen and argon concentration measurements to a study of the origins of the brines of the Atlantis II and Discovery deeps in the Red Sea.

Intensive intercomparisons of the results of the various kinds

of precision measurements on the CO_2 system were carried out at the first GEOSECS (Geochemical Ocean Sections Study) intercalibration station in 1969 (Takahashi et al., 1970). (This work is part of the U. S. effort in the International Decade of Ocean Exploration being sponsored by the National Science Foundation.) Measurements were made by the pH-alkalinity method (Culberson, 1972; Culberson et al., 1970), titration method (Edmond, 1970), total CO_2 extraction method (Wong, 1968), gas chromatographic method (Weiss, 1970), and PCO_2-total CO_2 method (Li et al., 1969). The discrepancies between the results of the various methods were 1.5% between the alkalinities by direct titration and pH-alkalinity methods; 2% between the total CO_2 by titration and gas chromatographic methods. pH calculated from PCO_2 and gas chromatographic TCO_2 was 0.015 higher than the directly measured value while alkalinity calculated from the same variables was 2% smaller than the direct titration alkalinity and 3% smaller than the pH-alkalinity method. PCO_2 calculated from the pH-alkalinity measurements was 3-5% higher than directly measured PCO_2 values and TCO_2 calculated from pH-alkalinity was 2-5% higher than measured TCO_2. The results of this effort achieved a degree of refinement in methods and resultant accuracy and precision never before attained in studies of seawater CO_2 chemistry.

PCO_2 measurements in the oceans. The method of study of CO_2 in the oceans which is the basis of this work has not yet been discussed. That is the direct measurement of PCO_2. This is carried out by measurement of the concentration of CO_2, at known total pressure, in air previously equilibrated with seawater. The instruments universally employed for the measurements at this time are non-dispersive infrared gas analyzers. The review of this subject which follows will ignore the early studies of PCO_2 in the oceans based upon values calculated from pH and alkalinity measurements. Keeling et al. (1965) cite some references to this early work and the difficulties with it.

Skirrow (1965) reviews in some detail the early directly measured PCO_2 work, particularly that of Takahashi (1961) and Waterman (1965). These studies corroborated the previous indications given by the pH-alkalinity data of low PCO_2 in surface waters of the central ocean water masses and the higher PCO_2 in equatorial surface waters and waters at the margins of the basins, and furnished much additional data of an enhanced precision and accuracy.

Keeling and co-workers (1965; 1968; Keeling et al., 1965; Keeling and Waterman, 1968) published in succeeding years the results of several expeditions which covered much of the world oceans, particularly the Pacific and Indian Oceans. Based upon these

and the previous studies as well as general oceanographic considerations Keeling (1968) compiled a chart of the global oceanic distribution of PCO_2 in surface waters. The chart covered all three world oceans from 60° S latitude to 60° N in the Atlantic, 65° S to 37° N in the Pacific, and from the Equator to 55° S in the Indian Ocean. Although there are some gaps, the chart presents a comprehensive picture of the general distribution. All data available were integrated into the chart without regard to season or year but the majority of the data tend to be local summertime observations.

Additional workers have continued studies of distributions of PCO_2 on a regional basis. Kelley and Hood (Kelley, 1968, 1970; Kelley and Hood, 1971; Kelley, et al., 1971) have concentrated upon the Arctic and Bering Seas, and the northeast Pacific Ocean.

Japanese workers have also been active. Miyake and Sugimura (1969; Sugimura and Hirao, 1970) have made expeditions into the Pacific, Indian, and Antarctic Oceans. Akiyama (1968; 1969abc) has made several cruises in the northwestern Pacific Ocean and East China Sea.

PCO_2 measurements have been applied by many workers to specific oceanographic and related problems. Broecker and co-workers have studied the precipitation and degree of saturation of calcium carbonate in the oceans (Broecker and Takahashi, 1966; Li et al., 1969). Keeling (1965) and Kanwisher (1960) have studied the

exchange of CO_2 between the oceans and atmosphere on the basis of the gradient in partial pressure of CO_2 between them. Teal and Kanwisher (1966) have employed PCO_2 as a tool for estimating biological production in Massachusetts waters.

1.2 The Purpose and Scope of This Work

There were four objectives to this work. First was the design and construction of a semi-automated analysis system for the continuous measurement of PCO_2. It was to be applied to both continuous underway and vertical profiling observations. The data were to be comparable to those of other laboratories.

The second objective was to examine the time variations in the distributions of PCO_2 in surface ocean waters. The time scale of interest in this work was from a few days to months to seasonal.

The third objective was to extend present knowledge of directly measured, summer, surface seawater PCO_2 distributions into Pacific subarctic waters and the Bering Sea.

The last objective was to examine the utility of PCO_2 observations in studies of coastal processes. The coastal waters off the Pacific Northwest United States would constitute a particularly interesting locale for such studies. Here could be found the several oceanographic phenomena of a major river outflow plume, coastal upwelling, and intense biological activity.

Chapter two of this dissertation presents a description of the system which was constructed to meet the first objective. It represents a stage in the continual evolution of a portable, seagoing PCO_2 measurement system. It is semi-automatic and operates unattended for many hours while a ship is underway. It employs as calibration standards, gases which are traceable to those employed in at least two other laboratories, at the Scripps Institution of Oceanography and at the University of Alaska. Most of this chapter has been abstracted from a detailed description of the PCO_2 system (Gordon and Park, 1972d).

The second objective, of examining time variations in the subarctic Pacific Ocean, has partly been realized with the publication of data from two cruises in the subarctic Pacific aboard the NOAAS (National Oceanic and Atmospheric Administration Ship) SURVEYOR in September and October 1968 and aboard the CNAV (Canadian Naval Auxiliary Vessel) ENDEAVOUR on the Transpac Expedition of March and April 1969. Chapter three consists of the article reporting that data. It appeared in the Journal of the Oceanographical Society of Japan and was co-authored by P. K. Park, S. W. Hager, and T. R. Parsons (Gordon et al., 1971).

The third objective, of extending observations of surface PCO_2 distributions into the subarctic Pacific and Bering Sea, has been submitted to Marine Chemistry. The manuscript comprises chapter

four of this dissertation. This work was performed in collaboration with J. J. Kelley and D. W. Hood of the University of Alaska and with P. K. Park (Gordon et al., 1970). Part of these data had been collected aboard the NOAAS OCEANOGRAPHER by Kelley and Hood (1971).

Chapter five summarizes the results of studies off the coast of Oregon. The use of PCO_2 as an indicator of upwelling and associated processes is discussed and PCO_2 is theoretically related to pH and apparent oxygen utilization. The time scales of PCO_2 variations in the coastal waters are examined, and finally there is presented an indication of a carbon trap on the continental shelf off Oregon.

Chapter six briefly summarizes and restates the conclusions of this work.

Three appendices follow the body of this dissertation. The first describes the polynomials fitted to published values of the solubility of CO_2 and the dissociation constants of carbonic acid and boric acid in seawater as functions of temperature and salinity. The second appendix presents a glossary of those symbols and terms used in the dissertation more than in the one instance where first defined. Appendix III is a brief vita of the author.

CHAPTER 2

METHODS

In this chapter are first described the PCO_2 system itself, its response time to a step function in the PCO_2 of a seawater sample stream, and how it was calibrated. Corrections for two instrumental effects, the "pressure" and "humidity" effects, which arise in the operation of the system are discussed next. Then the unit in which the data are reported is defined and the method of data reduction is outlined. Another correction, for warming of the seawater stream, which has not been applied to any of the data, is discussed next. After citing references to the methods for obtaining auxiliary oceanographic data there appears the last section in which is described the calculation of two types of derived auxiliary data, apparent oxygen utilization and relative humidity.

2.1 Description of the PCO_2 System

This section describes the system designed for semi-automated continuous measurement of seawater carbon dioxide partial pressure (PCO_2). In operation, seawater flows through a seacock or is pumped to a seawater-air equilibrator. Air is circulated continuously through the equilibrator in a closed loop which also includes

an infrared gas analyzer (IRA). The carbon dioxide partial pressure in the air in the loop comes to equilibrium with that of the seawater and the concentration of CO_2 in the loop is measured by the IRA. The output of the IRA and the temperature and pH of the water in the equilibrator are recorded on a strip chart recorder. Auxiliary data necessary for the correction of instrumental errors are recorded manually on the strip chart. A suite of auxiliary chemical, biological, and physical measurements are made, appropriate to the particular oceanographic problem at hand.

Historical background. As early as 1961 the need was anticipated for a shipboard system capable of measuring PCO_2 in seawater continuously while underway, and on station, at depth. This system would be of great value in studies being planned in the Department, of the air-sea exchange of carbon dioxide and oxygen, coastal upwelling, the Columbia River plume, and of sharp hydrographic fronts near the sea surface.

In 1967 under the direction of Professor Park, I began design and construction of the Oregon State University (OSU) system. In June 1968 Dr. Park and I made the first measurements with the system, continuous underway surface measurements with no sampling from depth. Only PCO_2 was measured continuously while all auxiliary data required were recorded manually. Manual techniques were employed for all the chemical analyses performed in addition to the

PCO_2 observations.

Since that time continual improvements have been made in the system. Inlet water temperatures and pH are recorded continuously along with PCO_2. Nutrients can be measured continuously using a Technicon AutoAnalyzer® (Atlas et al., 1971). A submersible pump has been added to the system to provide vertical profiling capability to a depth of 100 meters.

The system performance and its reliability have been very high and virtually one hundred percent of each cruise's objectives have been attained. The system has been successfully installed and operated on the R/V YAQUINA of OSU, the NOAAS SURVEYOR of the National Oceanic and Atmospheric Administration, and the Canadian Naval Auxiliary Vessel ENDEAVOUR.

Table 2.1 lists the cruises and expeditions on which PCO_2 measurements have been made with the system and indicates the corresponding configurations of the system.

A detailed technical report describing the system has been published (Gordon and Park, 1972d).

General design considerations. The primary purpose of the PCO_2 system is to produce continuous underway observations of PCO_2 in surface waters and vertical profiles of PCO_2 to 100 meters. The system was designed to perform these tasks with a precision of ±5% or better, an accuracy of ±10% or better, and a response time of one

Table 2.1. Cruises on which PCO_2 data have been taken. The table is in two parts. a) Cruises, dates, equilibrator model and depth of pumping employed on the cruises and reference numbers for publications of cruise data are given. b) Lists the reference numbers and publications. A * denotes that the publication contains PCO_2 data.

a) Cruise	Dates	Area	Eq. Model	Depth of Pumping	Publication of data
Y6806-C	23 VI-3 VII 68	Off Oregon-Washington	WHOI	Surface	1,2,3,4
SURVEYOR	13 IX-23 X 68	Bering Sea & Pacific Subarctic	OSU-I	Surface	3,5,6
Y6812-A	14 XII 68	Columbia River	OSU-I	Surface	2,3,7
ENDEAVOUR-TRANSPAC	17 III-30 IV 69	Pacific Subarctic	OSU-I	Surface	6,8,9
Y6906-C (COOC-4)	18 VI-3 VII 69	Off Oregon-Washington	OSU-I	0-55 m	4,9,10
Y6908-A (COOC-6)	31 VII-12 VIII 69	Off Oregon-Washington	OSU-I	0-55 m	4,9,10
Y6910-E (COOC-10)	22-31 X 69	Off Oregon-Washington	OSU-I	0-55 m	9,10
Y7001-A	6-9 I 70	Off Oregon	OSU-I	0-55 m	11
Y7001-C	25-26 I 70	Off Oregon	OSU-I	0-55 m	11
Y7005-A	4-10 V 70	Off Oregon	OSU-I	0-55 m	11
Y7006-A	16-29 VI 70	Off Oregon	OSU-I	0-55 m	11
YALOC 70	17 VII-25 VIII 70	Pacific Subarctic	OSU-II	0-100 m	11
Y7103-E	28-31 III 71	Off Oregon	OSU-II	0-100 m	12
Y7106-B	12-16 VI 71	Columbia River & Off Oregon	OSU-II	0-100 m	12

b)
1. Ball (1970) and Gordon and Park (1968)*
2. Barstow et al. (1969)
3. Gordon and Park (1972a)*
4. Pillsbury and Bottero (1971) and Pillsbury (1972)
5. Alvarez-Borrego (1970), Alvarez-Borrego and Park (1971), Gordon et al. (1970)*
6. Gordon et al. (1971)*
7. Park et al. (1969b)*
8. Barraclough et al. (1969), Fisheries Research Board of Canada (1970)*, Parsons and Anderson (1970), Seki (1970), Stephens (1970), and Wickett (1969)
9. Gordon and Park (1972b)*
10. Wyatt et al. (1970)
11. Wyatt et al. (1971) and Gordon and Park (1972c)*
12. Wyatt et al. (1972), Kantz (1973)* and Kantz et al. (1972)*

minute or less. A precision of ±1% was achieved, estimated accuracy was ±5%, and the 99% response time was estimated as approximately three minures.

A short response time was desired in order to resolve patchy horizontal distributions of the various chemical variables and sharp hydrographic fronts that are often encountered off Oregon and elsewhere. The PCO_2 record of the present system was designed to have a response time of one minute or less as noted earlier. It proved to have a response time[1] of approximately 40 seconds.

To what horizontal distance does this response time correspond? A ship travelling at a speed of ten knots moves a distance of 300 meters in one minute. With a 40 second response time the ship moves through a horizontal distance of 200 meters. If the ship encounters an infinitely sharp front between two water types of uniform PCO_2, the system will have responded to within 1% of the difference between the two water types in four and a half response times, three minutes, corresponding to the ship having passed 900 meters beyond the front. Thus the system can only resolve horizontal features, with 99% response, which are on the order of a kilometer in extent and will have a lag in position on the order of one

---

[1]Response time is defined here as the time required for the system to respond to a step function in PCO_2 to within 1/e of the difference between the two levels of PCO_2. e is the base of the Naperian logarithm system.

kilometer.

Several supplemental measurements are required in addition to PCO_2, both as necessary data to correct for various instrumental effects and as auxiliary data to provide the general oceanographical background for interpreting the PCO_2 results. Where possible these measurements were incorporated on the same data records as the raw PCO_2 data.

To enable work on expeditions of other institutions, and because the OSU marine facilities are located 55 miles distant from the shore laboratories, portability of the system was important. The present system may be dismantled in the shore laboratory and packed aboard a truck in one hour. It can be transferred from the truck to the ship in less than a half hour using a crane. Installation in the ship's laboratory requires approximately eight man-hours. Two additional men are required for the lab-to-truck and truck-to-ship transfers. These are in addition to the two analysts usually responsible for the system at sea.

For shipment by commercial carrier to a remote port, the system is disassembled to its basic components facilitating more careful packing. Shipping weight approximates one ton for supplies for a six-week cruise, while the volume for shipping purposes amounts to approximately 4.25 cubic meters.

A potential problem was that most shipboard electrical

power supplies were likely to present difficulties with not only line voltage but line frequency transients as well. For this reason the sensitive components of the system were protected with a stabilizer of the "frequency changer" or AC-DC-AC type.

Component reliability and simple circuitry were stressed in the design to simplify maintenance and service demands upon the operators at sea. Advantage was taken of existing technology as much as possible and commercially available components were used when these were not prohibitively expensive. The factor of cost versus resources had to be faced, and the system constructed for less than $10,000 if possible. The eventual cost for components and parts, excluding overhead and labor considerations, was approximately $10,500.

General description of the system. A block diagram of the PCO_2 system is given in Fig. 2.1. A Mine Safety Appliances Model 200 LIRA infrared analyzer (IRA) continuously measures the carbon dioxide concentration in either a standard gas, outside air, or in air equilibrated with seawater. The equilibrator shown in Fig. 2.2 was constructed of acrylic plastic for the latter purpose. It follows a design by Teal and Kanwisher of the Woods Hole Oceanographic Institution, WHOI (Teal and Kanwisher, 1966). (Dr. Teal lent us an equilibrator which was employed on cruise Y6806C. It is denoted by "WHOI" in Table 2.1.) To accelerate the rate of equilibration of the air with the

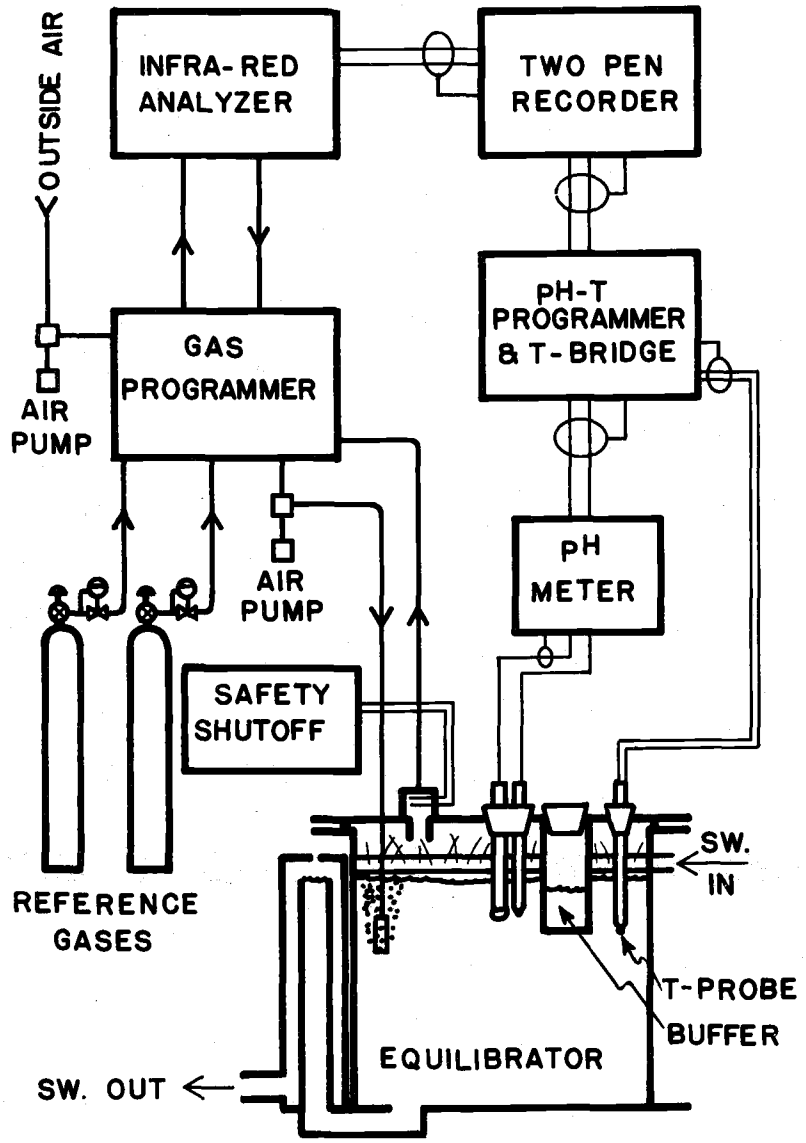

Fig. 2.1. Block diagram of the PCO_2 system. Air connections are shown with heavy lines, the arrows indicating direction of flow. Electrical connections are shown with light lines, in general being made with two-conductor, shielded cable. The infrared analyzer, recorder, gas programmer, pH-T programmer, pH meter, and equilibrator are described in the text. The air pumps are Neptune Dyna-Pumps, Model 3-SS, and are located on the programmer chassis. The reference gases are contained in compressed gas cylinders fitted with standard two-stage gas regulators; the latter are generally adjusted to deliver 1.4 decibars pressure (two pounds-per-square-inch, gage pressure).

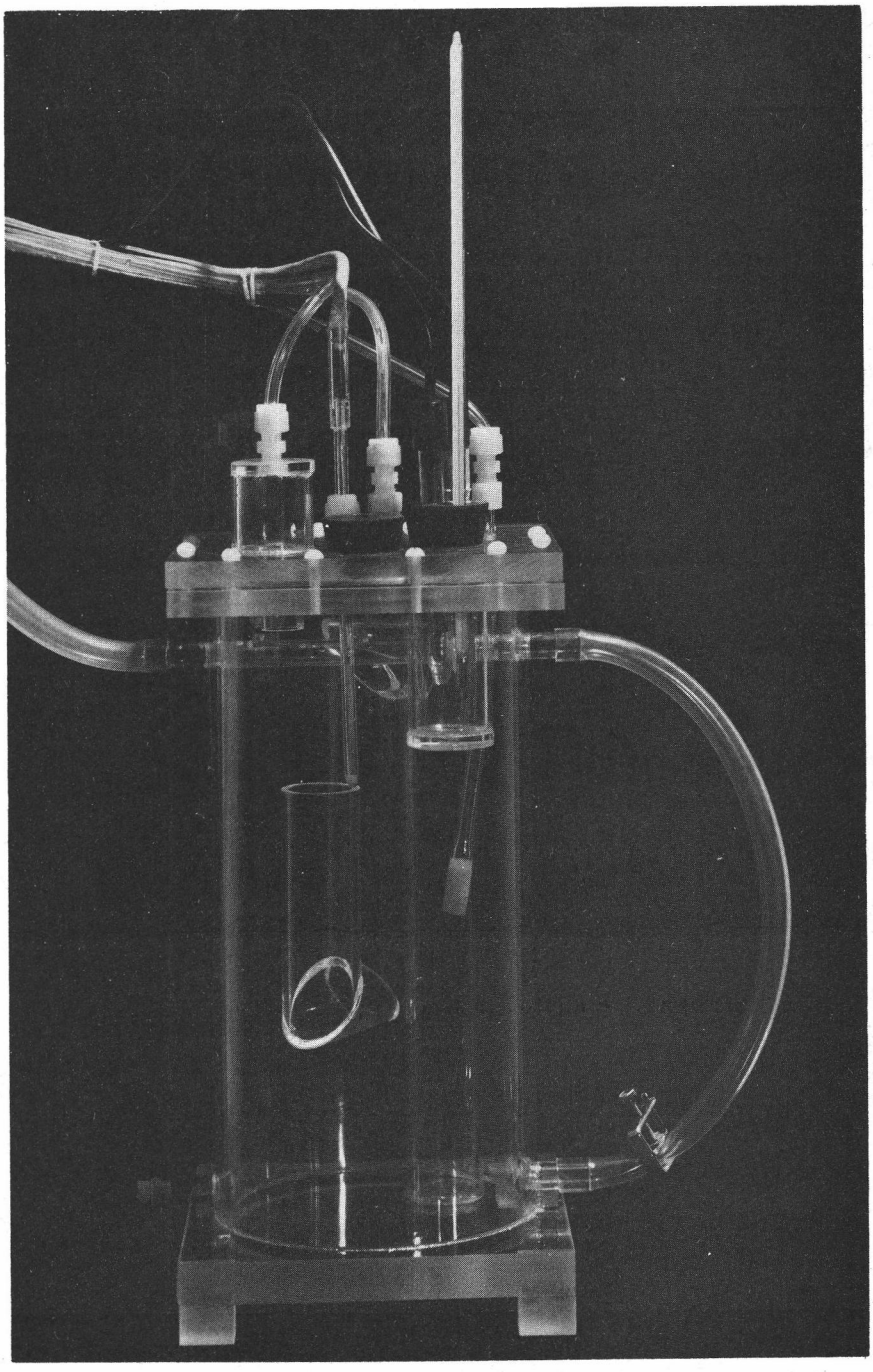

Fig. 2.2. The 4 liter OSU equilibrator. This is the first equilibrator constructed at OSU and is referred to in Table 2.1a as the OSU-I equilibrator. In overall geometry it is similar to the WHOI equilibrator. (Photograph by Jeffrey M. Stander)

water it employs both a rapidly renewed thin film of water on the top and sides of the equilibrator and a dispersion of fine air bubbles produced by a fritted glass diffuser on the air stream inlet to the equilibrator.

The pH of the seawater in the equilibrator is continuously measured with a glass electrode and a pH meter, while a thermistor probe monitors the water temperature. A Tygon® tube, fitted with a pinch clamp, at the bottom of the equilibrator serves for drawing off discrete samples for dissolved oxygen, nutrient, pH and alkalinity, and salinity determinations.

A gas programmer controls the flow of gases to the gas analyzer in either an automatically timed, or manually controlled, sequence of standard gases and sample streams. The gas flow scheme is shown in Fig. 2.3.

To prevent water being inadvertantly admitted to the IRA as a result of malfunctions or human error, there is also incorporated a safety shutoff system which senses the presence of liquid water in the air stream. The safety shutoff then closes two solenoid valves isolating the equilibrator, and shuts off the air pumps.

The output of the IRA is recorded by one pen of a two-pen strip-chart recorder. The second recorder pen records the output of the thermistor probe and pH meter alternately.

Not shown in these diagrams but described by Gordon and

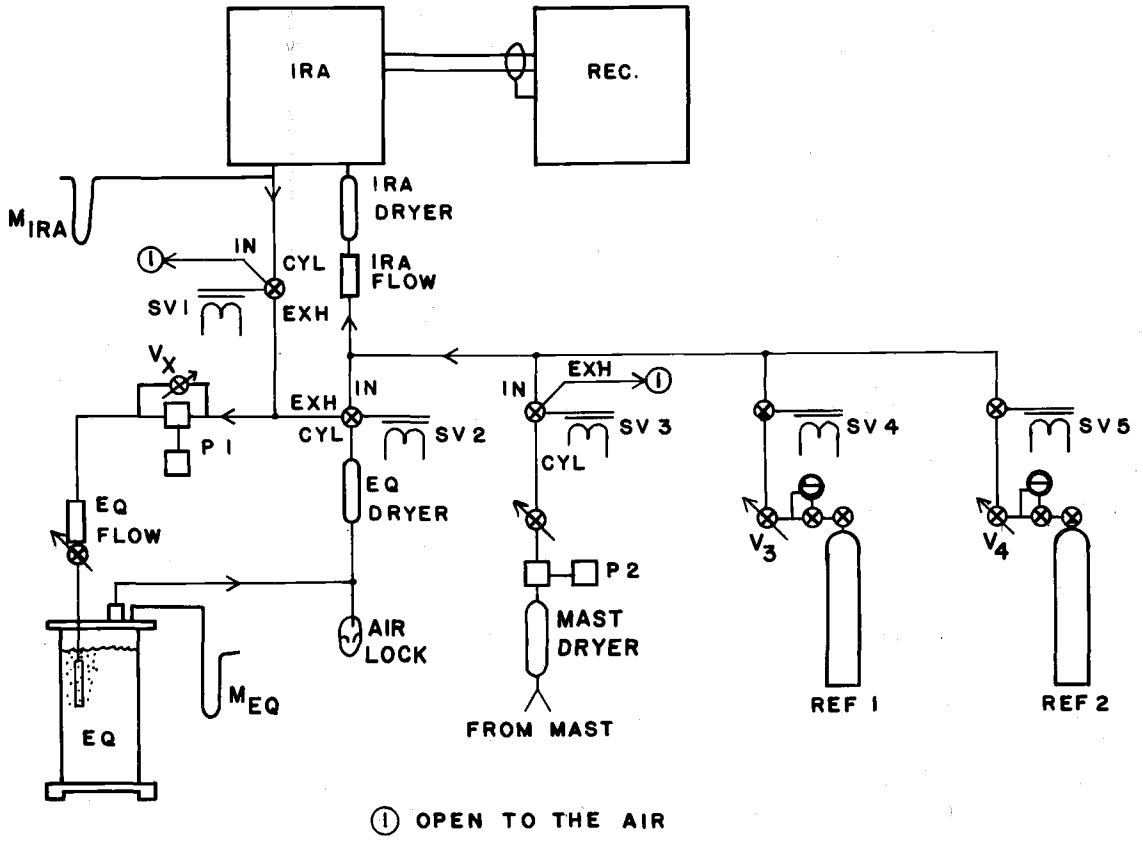

Fig. 2.3. PCO_2 gas flow schematic diagram. The abbreviations used are: CYL, IN, EXH, the ports so marked on the solenoid valves (SV); EQ, equilibrator; FLOW, flowmeter; IRA, infrared analyzer; P 1, pump number one; REC, recorder; REF 1, reference gas number one; SV 1, solenoid valve number one; V 1, manually operated valve number one; M_{eq} identifies the manometer used to measure the difference between the pressure in the equilibrator and the ambient atmospheric pressure; M_{IRA} identifies the manometer used to measure the difference between the pressure in the IRA cell and the ambient atmospheric pressure. The various components are described in detail in Gordon and Park (1972d).

Park (1972d) is a simple, submersible pumping system for sampling to depths of 100 meters.

2.2 The Response Time of the PCO_2 System

In this section a simplified calculation of the system response time is made. Then the calculated response is compared with the results of several experiments.

First of all it is assumed that the water in the equilibrator is mixed rapidly relative to the rate at which water flows through the equilibrator. This assumption is reasonable because looking through the clear walls of the equilibrator one observes a great amount of turbulent motion in the water while the system is operating. The numerous bubbles of the injected air stream are the visual indicators of motion. For the model in Fig. 2.4a for the aqueous phase, one has

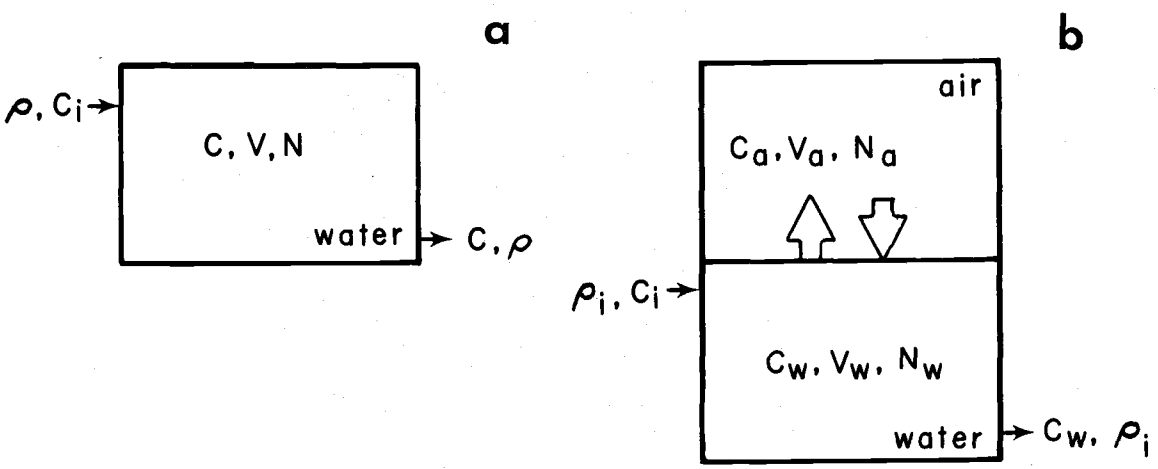

Fig. 2.4. Models for calculating the equilibrator response time. a. The first case considers only the water phase. b. The second case includes an air phase but assumes that the air-water exchange rate is infinitely fast. For nomenclature see the text.

the relationships: 1) from the definition of concentration

$$C \equiv \frac{N}{V} \tag{2.1}$$

where C, N, and V are concentration, number of CO_2 molecules, and volume in a phase, respectively; 2) the rate of change of concentration of CO_2 in the water phase is

$$\frac{dC}{dt} = \frac{1}{V}\frac{dN}{dt} = \frac{1}{V}(\rho C_i - \rho C) \tag{2.2}$$

where t and ρ represent time and water flow rate respectively. The subscript i indicates the incoming water stream. The condition has been used that the incoming and outgoing water flow rates are equal since the volume of water in the equilibrator remains constant. On the assumption that the water in the equilibrator is well mixed, the concentration of CO_2 in the outgoing water is at all times equal to the concentration of CO_2 in the water within the equilibrator. Furthermore the concentration within the equilibrator is uniform.

Eq. (2.2) can be rearranged to the form

$$\frac{dC}{dt} + \frac{\rho}{V} C = \frac{\rho}{V} C_i \tag{2.3}$$

This is a textbook example first order differential equation which has as its solution (Sokolnikoff and Redheffer, 1958, p. 23-24)

$$C = \frac{\rho}{V} \exp\left(-\frac{\rho}{V}\right) \int \exp\left(\frac{\rho}{V}t\right) C_i dt + B\frac{\rho}{V} \exp\left(\frac{\rho}{V}t\right) \qquad (2.4)$$

B is a constant of integration which must be evaluated from the boundary conditions.

To do this, consider the response of the equilibrator to a step function in C_i. This is a case which would correspond to a continuous underway oceanographic survey in which the ship crosses a sharp hydrographic front between two water masses, each with its almost uniform PCO_2. Then set $C_i \neq C_i(t)$ but constant for $t > 0$, and C_i, at $t \leq 0$, equal to C_o, (also constant).

The integrated form of Eq. (2.4) is then

$$C = C_i + B\frac{\rho}{V} \exp\left(-\frac{\rho}{V}t\right) \qquad (2.5)$$

To evaluate A, set $C = C_o$ and $t = 0$ and solve for B, finding

$$B = \frac{V}{\rho}(C_o - C_i) \qquad (2.6)$$

Substituting for B from Eq. (2.6) into Eq. (2.5) obtain

$$C = C_o + (C_i - C_o)\left[1 - \exp\left(-\frac{\rho}{V}t\right)\right] \qquad (2.7)$$

Figure 2.5 illustrates the response. Observe that at $t = 0$, $C = C_o$; as $t \to \infty$, C approaches C_i exponentially.

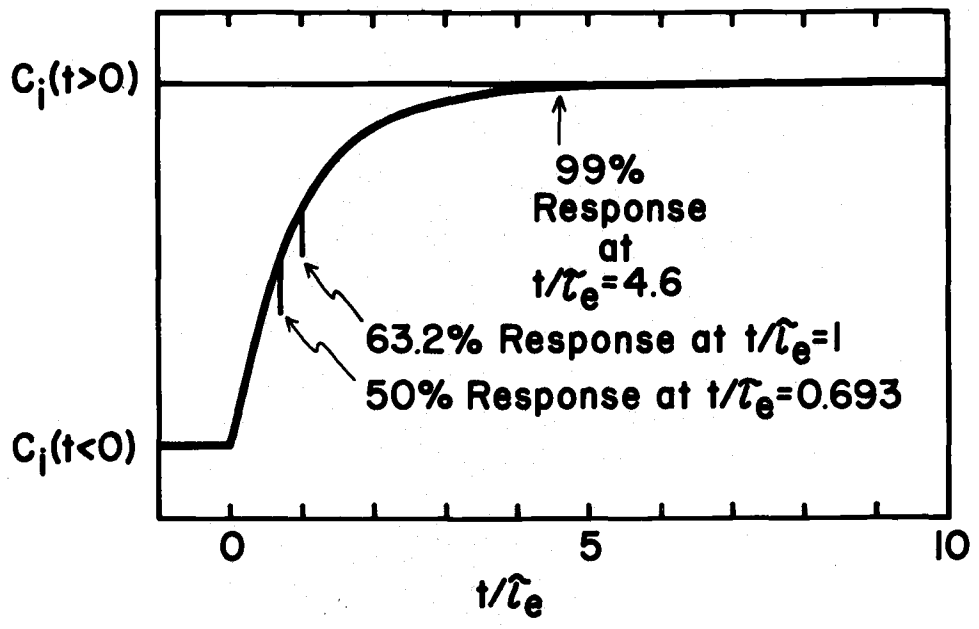

Fig. 2.5. The equilibrator air-stream response to a step function in PCO_2 of the incoming water. The curve is the exponential response predicted by the model for the equilibrator assuming infinitely fast mixing in the water and air phases, fast exchange of CO_2 between the water and the air, and no exchange of CO_2 between the dissolved species. $C_i(t > 0)$, the concentration of CO_2 in the water after time zero may be greater or less than $C_i(t < 0)$, the concentration before time zero.

To calculate the response time of the concentration C, that is for C to approach C_i to within 1/e of $(C_o - C_i)$, where e is the base of the Naperian logarithm system, substitute C from Eq. (2.7) into

$$\frac{C - C_i}{C_o - C_i} = \frac{1}{e} \qquad (2.8)$$

Now define $\tau = t$ under this condition and obtain

$$\tau = V/\rho \qquad (2.9)$$

which may be evaluated for the system operating parameters. The system operates with a water flow rate of four and one half to seven

liters/minute. The seawater volume of the newest equilibrator is 1.2 liters. Thus τ ranges from 15.5 down to 9.9 seconds for these water flow rates. This is the time for the seawater in the equilibrator to be sufficiently flushed out so that the concentration of molecular CO_2 comes to within 1/e or 37% of its final value. In 4.5τ or from 44 to 70 seconds, the concentration has come to within 99% of its final value (see Fig. 2.5). Table 2.2 lists responses in terms of the percent approach to the final value when time is expressed as multiples of the response time, whether expressed as the 50%, 1/e, or 99% response time.

Table 2.2. Values of $[1 - \exp(-t/\tau)] \cdot 100$ for t equal to integral multiples of τ for τ defined as the 50% response time, τ_{50}, 1/e response time, τ_e, and the 99% response time τ_{99}.

	$(1-e^{-t/\tau})\ 100\ (\%)$		
t	τ_{50}	τ_e	τ_{99}
0.5τ	29.3	39.3	90.9
τ	50.0	63.2	99.0
2τ	75.0	86.5	99.99
3τ	87.5	95.0	99.999,9
4τ	93.8	98.2	99.999,999
5τ	96.9	99.3	99.999,999,99

To obtain the response time for the air in the equilibrator air loop one can employ further simplifications. First, assume that the

rate of exchange of CO_2 between the gas phase and the molecular CO_2 fraction of the total CO_2 in the seawater is much faster than the flushing rate of the water.[2] Then treat the CO_2 in the gas phase as part of that in the water and modify the flushing calculations to include the air phase as part of the volume to be flushed. Referring to Fig. 2.4b one can obtain by assuming that the concentrations of CO_2 in the gas phase and of the molecular CO_2 fraction of the total CO_2 in the water are approximately equal,[3]

$$C = C_w \cong C_a, \quad V = V_a + V_w, \quad \text{and} \quad N = N_a + N_w \qquad (2.10)$$

where C, V, and N have the same role in Eq. (2.10) as before. The subscripts a and w apply to the air and water phases respectively.

The response time of the concentration of CO_2 in the air (and the water) can now be calculated from

$$\tau_a = (V_a + V_w)/\rho \qquad (2.11)$$

---

[2] In a relatively quiescent state the simplification, that the rate of exchange of CO_2 between the water and the air is fast, would certainly not be true. The exchange would be limited by diffusion in both phases, but particularly so in the laminar layer in the water at the air-water interface. In the equilibrator this slow step is virtually eliminated. There are rapidly and continuously generated large areas of new air-water interface. The air bubbling through the glass frit into the water and the spray through the air and onto the top and walls of the air space in the equilibrator do this very effectively.

[3] This assumption that the concentrations of molecular CO_2 in the seawater and the air phases are about equal is borne out by examination of the solubility data for CO_2 in seawater (Murray and Riley, 1971; or Harvey, 1955, p. 168).

where τ has been subscripted to distinguish it from that calculated in Eq. (2.9).

A series of experiments was carried out to measure the response time of the system. The equilibrator used was the 4 liter model and the results are tabulated in Table 2.3. There were four experiments designed to measure the response time as a function of the water and air flow rates. The equilibrator was operated with cold and warm water from the taps in the laboratory. The original source of the water was the City of Corvallis water intake on the Willamette River. This river is high in PCO_2 and low in salinity (Park et al., 1969; Kantz et al., 1972; Kantz, 1973).

Table 2.3. Calculated and observed equilibrator response times.

Expt. No.	ρ_w (l/min)	ρ_a (l/min)	τ_t (min)	τ_w (min)	τ_{PCO_2} (min)	τ_{a+w} (min)	τ_t/τ_w	τ_{PCO_2}/τ_{a+w}
1	4.6	1.0	1.1	0.85	(7.0)	1.05	1.3	(6.7)
2	9.1	1.0	0.7	0.42	1.1	0.52	1.7	2.1
3	4.6	2.0	1.1	0.85	2.1	1.05	1.3	2.0
4	8.2	2.0	0.6	0.47	1.0	0.58	1.4	1.7

The cold water flow was adjusted to give the desired rate for the experiment. Then the warm water tap was opened to cause the temperature and PCO_2 traces to move almost offscale at the upscale edge of the recorder chart. After a steady upscale trace was obtained the hot water tap was closed and response curves for the temperature

and PCO_2 obtained. The 1/e response times obtained under each of four sets of water and air flow rates were measured.

The first experiment was abortive because the Drierite® in one of the air stream drying columns was defective. The data is retained, however, because it demonstrates the magnitude of the effect which can arise from this cause.

Consider first the temperature data obtained with the thermistor probe in the equilibrator. Note that Experiment 1 is valid for the temperature response. The estimated thermistor response time is about one second (see Gordon and Park, 1972d). This is much faster than the flushing time of the water in the equilibrator as may be seen for the values of τ_w in Table 2.3. These vary from 25 to 51 seconds. τ_w has been calculated from Eq. (2.9) using 3.88 liters for the value of V. The observed temperature response times are all somewhat larger than the calculated times indicating that either there is another somewhat slow step in the temperature measurement system or that the experimental data contain systematic errors. Estimated accuracies for the equilibrator water volume, water flow rate and τ_t are all approximately ± 10% of the values. Therefore, although the observed τ is systematically 40% greater than the calculated response time, it is difficult to draw firm conclusions with data of this order of accuracy. The tentative conclusion is that the flushing time for water in the equilibrator is satisfactorily predicted by the model.

Next the PCO_2 response times are examined. The observed τ_{PCO_2} values given in Table 2.3 have been calculated allowing for the nonlinear response of the IRA. They are the 1/e response times for the concentration of CO_2 in the air stream passing through the IRA, not for the recorder trace measured linearly on the chart. The calculated response times, τ_{a+w}, have been calculated from Eq. (2.11) using 4.75 liters for $V_a + V_w$. This includes an added 0.1 liters for the volume of the IRA cell plus the estimated free volume of the drying tube.

Once again the observed response times are greater than predicted, now by a factor of two. Therefore one must search for additional slow steps in the system to account for this, and modify or reject the model.

It is evident that the Drierite® can adversely affect the system response time. It is quite possible that even though the "bad" Drierite® of Experiment 1 was replaced by a "good" batch for the remaining experiments, the Drierite® still is responsible for a major part of the discrepancy. At this time there is insufficient data to test the possibility.

One should consider hydration of molecular CO_2 as an additional slow step because the rate constant for this reaction is only approximately 0.03 sec^{-1} at 25° C and pH 7 (Kern, 1960, p. 17; Edsall, 1969, p. 20), roughly the conditions of these experiments.

However, considering both the crudity of the experiments and the uncertainty in the hydration rate constants a further refinement of the model seems unjustified at this time.

Note that when the water-flow rate is decreased by a factor of two as between Experiments 2 and 4 versus Experiment 3, τ_{PCO_2} increases by a factor of two. But when the air-flow rate is varied by a factor of two as between Experiment 4 versus Experiment 2, τ_{PCO_2} remains almost constant. The certain conclusion is that whatever the dominant processes in limiting the response of the system, they are more water-flow dependent than air-flow dependent. Flushing of the IRA cell and drying tubes is only air-flow dependent, although they are of such small volumes that their flushing times are only 2 seconds or thereabouts. Hydration of CO_2 should be independent of either air- or water-flow rate but sensitive to temperature and certainly to pH (Kern, 1960, p. 17; Edsall, 1969, p. 20).

In conclusion, the response time for the 4 liter equilibrator (OSU-I) is apparently two minutes with the usual operating conditions employed. A response time of 0.44 minutes for the smaller, OSU-II, equilibrator now in use was calculated. The actual response time for this equilibrator has not been directly measured in the above manner, but it may be larger than the calculated τ by a factor of two. If so, its response time is of the order of 0.88 minutes or 52 seconds. A response time to a slug of prepurified nitrogen or high PCO_2 air

introduced into the air loop of 40 seconds has been observed which is close to this figure.

2.3 Calibration of the PCO_2 System

There are two objectives to be attained in calibrating the PCO_2 system. The first is to establish an absolute calibration. The second is to correct for the nonlinearity of the IRA.

Calibration of the OSU system and standard gases was achieved as outlined in Figure 2.6 and as follows:

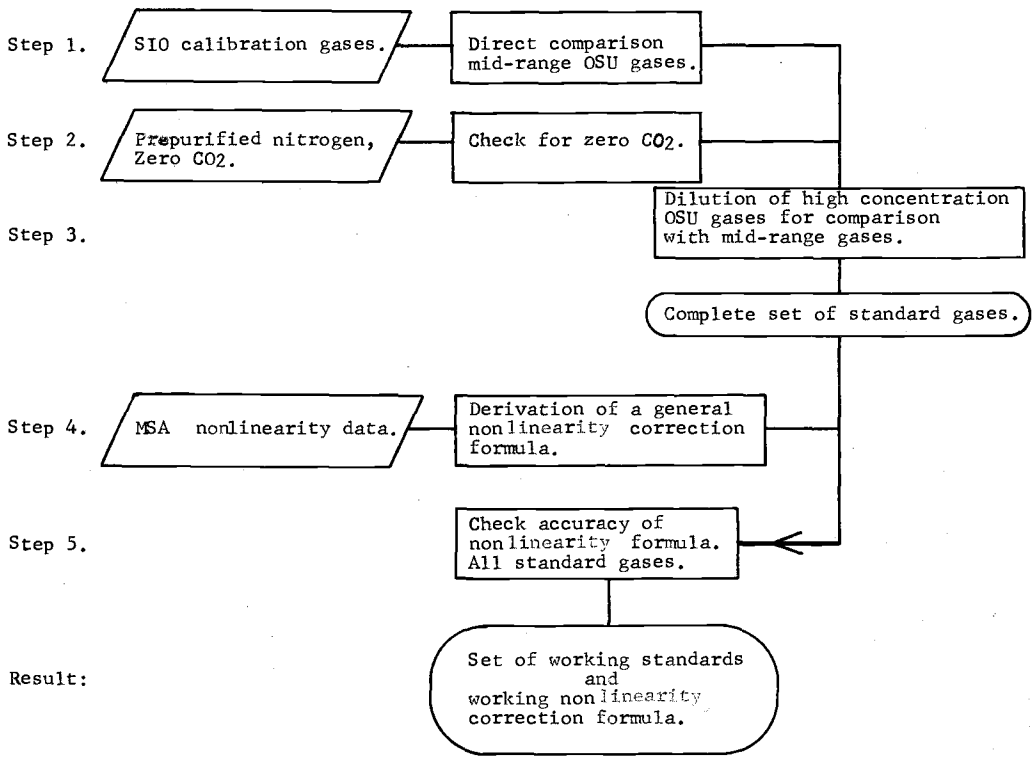

Fig. 2.6. Flow chart of the scheme employed for calibrating a set of working CO_2 standards and deriving a correction formula for the nonlinearity of the IRA. The scheme is explained in the text. Parallelograms denote input data; rectangles, steps in the overall scheme; and rounded boxes, the desired goals.

Step 1. Establishment of the absolute calibration of a scale comparable to that being used by other workers in the field. This was achieved with the help of Dr. C. D. Keeling and Mr. A. Bainbridge of the Scripps Institution of Oceanography. They kindly supplied three cylinders of carbon dioxide-nitrogen mixtures which they had carefully analyzed in the range of 286 to 260 ppm CO_2. The basis of these analyses was precise constant-volume manometric measurement (Bainbridge, 1969; Guenther, 1971). These gases are referred to in this dissertation as "SIO gases."

All of the OSU gases lying between the range of 265 and 380 ppm CO_2 were then directly compared with the three SIO calibration gases. Because the concentration range between the highest and lowest SIO gases was quite small, less than 70 ppm, the effect of the nonlinearity of the IRA was negligible. This permitted establishment of a set of OSU gases of limited concentration range as secondary reference gases for further work, without concern for nonlinearity problems.

Concentrations obtained in these comparisons are shown in Table 2.4 together with additional analyses described later. This set of secondary reference gases consisted of numbers 1, 3, 4, 5, 8, 13, and 14. This is the method of calibration called "direct" in Table 2.4.

Step 2. Establishment of a zero gas. A reference gas of zero or known near-zero CO_2 concentration is required to adjust the low end

Table 2.4. Accepted concentrations of CO_2 standards.

OSU Number	Cylinder Number	Nominal Concentration (ppm)	Accepted Concentration (ppm ± av. dev. ppm)	Standards Employed	Method of Standardization Employed	Number of Comparisons	Number of Analyses
1	M 47174	265	265.5 ± 0.2	SIO	Direct	7	1
2	M 41825	610	655.0 ± 0.4	OSU	Dilution	10	2
3	M 37606	320	318.9 ± 0.3	SIO	Direct	4	1
4	M 34153	310	327.6 ± 0.6	SIO	Direct		
5	M 33422	360	363.8 ± 0.1	SIO	Direct	6	1
6	NCG 2540862	0	≤0.2 (taken as 0)	---	Absorption of any CO_2 with Lithasorb®	2	1
7	M 7279	228	219.0 ± 1.0	OSU	Direct		3
8	M 13235	352	352.3 ± 0.1	SIO	Direct	8	1
9	AIRCO 3751	342	348.55				
10	AIRCO 2420	286	281.65 ±0.2	Concentrations supplied by A. Bainbridge (1969), SIO			
11	AIRCO 18208	309	309.21				
12	NCG 3983	1350	1381.2 ± 0.4	OSU	Dilution		2
13	M 21027T	270	264.3 ± 0.25	SIO	Direct	8	1
14	M 13183T	332	326.8 ± 0.25	SIO	Direct	4	1
15	M 48648	220	215.1 ± 1.2	OSU	Direct	7	1
16	M 30485	215	208.5 ± 0.4	OSU	Direct	9	1
17	M 19498	390	387.4 ± 0.8	OSU	Direct		2
18	M 56961	389	386.5 ± 0.8	OSU	Direct		2
19	M 37644	600	605.4 ± 0.8	OSU	Direct	6	1

of the range of the IRA or to dilute high concentration reference gases so as to measure their concentrations. Zero concentration calibration gas is readily available in the form of pre-purified dry nitrogen supplied by many vendors. The tanks used in the present study were checked for zero carbon dioxide content by passing the nitrogen through Lithasorb®. The Lithasorb® completely removed carbon dioxide from test gases containing quite large concentrations of CO_2. There was a maximum of 0.2 ppm carbon dioxide in the nitrogen. Therefore, the carbon dioxide concentration in the nitrogen was taken as equal to zero.

Step 3. Establishment of high concentration standards. PCO_2 values in excess of 1200 ppm-atm were expected in these studies. To increase the range of standard gas concentrations, gases of high concentrations (610 and 1350 ppm-atm nominal concentrations) were calibrated by dilution with pre-purified nitrogen in the apparatus shown in Fig. 2.7. The method consists of passing the reference gas to be diluted and the pre-purified nitrogen through identical soap bubble flow meters (100 ml burets), mixing the two streams and passing the resultant mixture through a small trap to remove liquid water, then through a drying column, and finally into the IRA for measurement of the mixture concentration. The gas washing bottles inserted in the gas streams ahead of the flow meters are intended to pre-saturate the gas streams with water to prevent evaporation of the

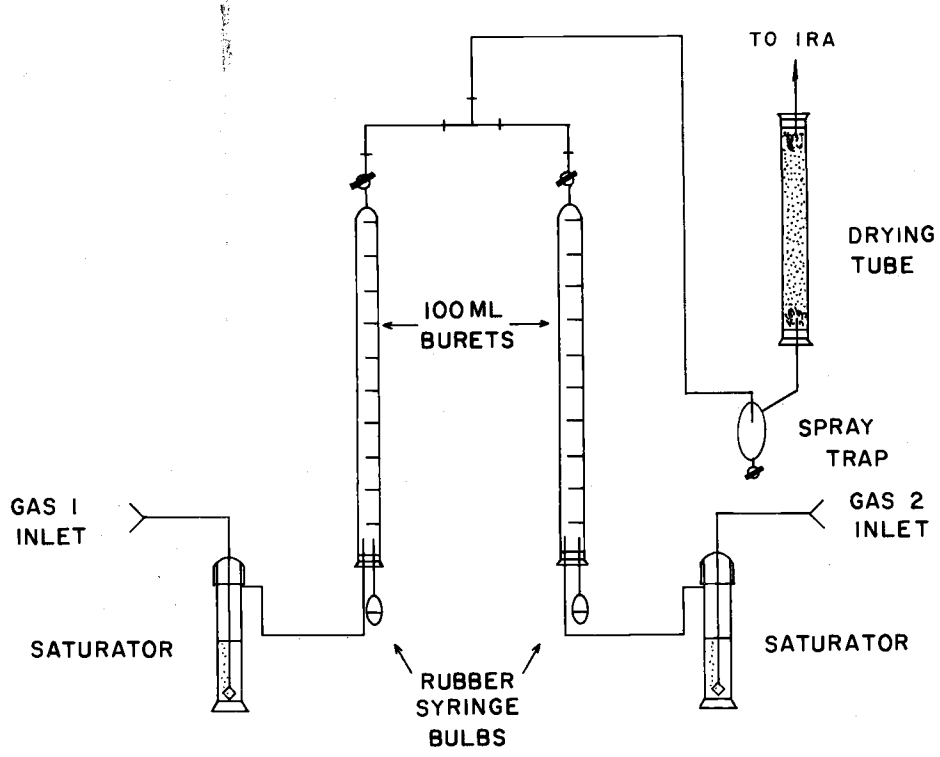

Fig. 2.7. The gas dilution apparatus. The components are interconnected by Tygon® tubing. The operation of the dilution apparatus is described in the text.

soap bubble film.

Error analysis for the gas dilutions. The errors estimated for the resultant gas concentrations amounted in the aggregate to approximately ± 1%. The volume calibrations of the flow meters introduced an error of ± 0.2%. The error in the volume measurements corresponding to starting and stopping a stopwatch amounted to approximately ± 0.5 ml or 0.5% of the reading, and it is this error rather than the buret calibration error which is taken as the volume error. (Human reaction time in starting and stopping the watch was on the order of

0.1 second. However this seemed to cancel out between the start and stop operations because the scatter in the calibrations is less than what an error of this magnitude would introduce.) Errors in reading the recorder trace amounted to ± 0.5% as a maximum. The observed precisions for the dilutions are ±0.3% (one standard deviation); this is less than the estimated aggregate precision for the dilutions.

Results of the 610 ppm calibration gas measurements. The nominal 610 ppm gas was analyzed on two successive days, exchanging the flow meters through which the two gases passed on the two days. This was done to detect and cancel out the effects of any possible differences between the two sides of the dilution system.

Simple linear proportionality is assumed in calculating the concentration of the resultant gas mixture. The concentration of the mixture is given by:

$$C_m = \frac{C_0 F_0 + C_{610} F_{610}}{F_0 + F_{610}} \qquad (2.12)$$

where:

C = concentration of CO_2 in ppm,

F = flow rate in ml/sec,

$= \frac{100 \text{ ml}}{t \text{ sec}}$,

t = time for the soap film to pass from the 100 ml mark to the 0 ml mark on the buret; the subscripts 0 and 610 refer to

the nominal concentrations of the gases; m refers to the mixture.

Since $C_0 = 0.0$,

$$C_m = \frac{C_{610} F_{610}}{F_0 + F_{610}} \tag{2.13}$$

Using the definition of F and rearranging,

$$C_{610} = C_m \cdot \frac{(t_{610} + t_0)}{t_0} \tag{2.14}$$

C_m was measured as described in the section on data reduction and C_{610} was calculated. This method of calibration is referred to in Table 2.4 as the "dilution" method of analysis.

Table 2.5 gives the results obtained from analyses of the 610 ppm OSU standard by this method. The data indicate a ± 4 ppm standard deviation for five analyses on the first day and ± 2 ppm standard deviation for the second day's five analyses. The difference between the average concentrations obtained on the two days is less than 1 ppm, indicating no significant difference between the two sides of the dilution system. The overall average of 654.9 ppm has been rounded to 655 ppm. The standard error of the mean concentration is 1.2 ppm.

A cylinder of compressed air which has a carbon dioxide concentration of approximately 1350 ppm was used as a span standard on

Table 2.5. Calibration data and results for 2-610 and 12-1350 OSU standard gases.

Date	IRA Standards Zero	IRA Standards Span	Dilution Gas	t_0 (sec)	t_x (sec)	C_m (ppm)	Calculated conc.[a] (ppm)	Daily Mean (ppm)	±1 SD[b] (ppm)	Grand Mean (ppm)	Std. Error of the Mean (ppm)
4 III 69	13-270	5-360	6-0	18.0	13.9	367.3	651.2				
				18.5	13.6	377.4	654.8				
				16.5	13.6	357.1	652.8				
				15.2	13.7	343.9	654.1				
				14.9	13.8	344.6	663.4	655.3	±4.1		
5 III 69	13-270	5-360	6-0	11.35	14.15	292.2	657.2				
				11.4	14.25	290.3	653.2				
				11.3	14.95	281.1	653.3				
				13.73	14.6	319.8	653.3				
				15.8	14.4	343.0	655.8	654.6	±2.0	654.9	±1.2
5 III 69	13-270	5-360	6-0	12.95	48.3	291.7	1379.7				
				10.30	44.9	258.4	1418.6				
				10.95	39.5	292.0	1346.1	1381.5	±31.0		
7 III 69	6-0	2-610	13-270	16.95	26.05	697.6	1363.6				
				12.33	20.85	686.3	1399.9				
				12.65	21.20	683.3	1385.5				
				13.20	22.90	672.9	1381.8				
				13.45	22.80	675.9	1373.6	1380.8	±12.3	1381.1	±6.6

[a] Calculated from Eq. (2.12) or (2.15) as appropriate.

[b] Approximated as 1.24 times the average deviation from the mean.

cruise Y6812A. This gas was calibrated by the dilution method and found to have a concentration of 1381 ppm with a standard error of 6.6 ppm. Three measurements were made on one day and five measurements two days later; the difference between the means of the measurements on the two days was less than 1 ppm. The data for this calibration are also given in Table 2.5.

In this case, Eq. (2.12) has been solved for C_{1350} using a non-zero dilution gas. The subscript, 610, has been replaced by 1350.

$$C_{1350} = C_m + (C_m + C_o)(t_{1350}/t_o) \qquad (2.15)$$

It may be seen that Eq. (2.15) reduces to Eq. (2.14) for the case $C_o = 0$.

In analyzing the 610 and 1350 ppm standards, the range of the IRA was kept small and the concentrations of the gas mixtures were adjusted such that the recorder traces for the mixtures fell close to either the zero or span gas traces. This minimized errors arising from the nonlinearity of the IRA.

Step 4. IRA nonlinearity. The next objective was the correction for the nonlinearity of the IRA. The response of all non-dispersive IRA's is more or less nonlinear. Therefore passing two calibration gases of known concentrations through the IRA, one near the low end and one near the high end of the range, does not serve to calibrate it completely. One could only interpret subsequent readings obtained for

unknown gas streams assuming the instrument to be linear and accept the magnitude of the nonlinearity errors for that particular instrument at the range to which it is adjusted.

The various manufacturers of these instruments generally supply calibration curves for one or more ranges of gas concentrations as specified by the purchaser. In the present case the IRA was calibrated for two ranges by the Mine Safety Appliances Company (MSA). These ranges were 0 to 600 ppm and 300 to 600 ppm of carbon dioxide, in dry nitrogen or dry air.

One could thus graphically correct for the nonlinearity of this instrument for these two concentration ranges. However additional concentration ranges were desirable as mentioned earlier and the nonlinearity corrections for these would be unknown. Further, to apply the nonlinearity corrections mathematically rather than graphically would be advantageous. The result would be an appreciable saving in time, particularly if digital computer data reduction were to be employed.

It was discovered in this work that the nonlinearity of this IRA could be approximated as a function of the difference between the known concentrations of the two reference gases used to adjust the low and high ends of its scale; that is, as a function of its range only. A formula was first derived for the maximum nonlinearity, at mid-range, as a function of the range. The two constants in the formula

were evaluated using the calibration data supplied by MSA for the 0-600 and 300-600 ppm ranges. Then the calibration curves supplied by MSA were approximated by a quadratic equation and tested for fit. Finally, the quadratic equation was tested by measuring gases of known concentration and using the equation to calculate their concentrations. This was done both for gases lying within and outside the range of the IRA calibration gas concentrations; that is, the equation was used both as an interpolation and extrapolation formula.

The maximum nonlinearity at mid-range observed by MSA for the two concentration ranges, 0 to 600 and 300-600 ppm, was fitted to an exponential equation of the form:

$$\Delta C_m = k R^A \qquad (2.16)$$

where ΔC_m = the maximum departure of the analyzer response from linearity, in ppm CO_2, at mid-range;

$R = C_s - C_z$, the difference between the CO_2 concentrations of the span and zero calibration gases (range).

k and A are the empirical constants to be found.

The nonlinearity data supplied by MSA furnished two sets of ΔC_m and R, allowing the formulation of two equations in k and A. The system of two equations was solved yielding $k = 2.36 \times 10^{-6}$ and $A = 2.585$. This treatment assumes that the departure from nonlinearity is a function of the range only and that the nonlinearity at

zero range is zero. The results calculated on the basis of these assumptions agreed well with known values, as will be shown later. The basis for selection of the form of this equation is that the nonlinearity is itself a nonlinear, increasing function of the range. Figure 2.8 illustrates this. The curve is calculated from Eq. (2.16). The two non-zero points plotted are those derived from the MSA calibration data for the instrument.

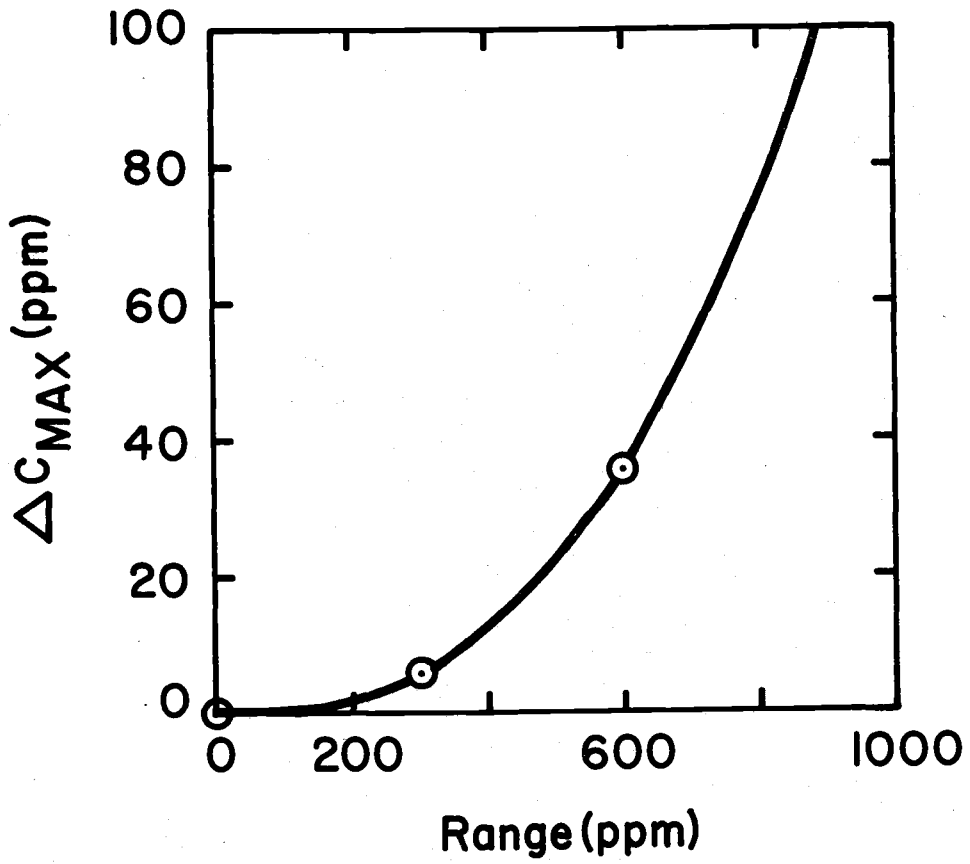

Fig. 2.8. The nonlinearity of the IRA as a function of the range for which it has been calibrated. The two circled points are the values for the nonlinearity of the analyzer as furnished by MSA. The curve is calculated from Eq. (2.16), using $k = 2.36 \times 10^{-6}$ and $A = 2.585$. R is the range to which the IRA has been set, that is the concentration of the span gas minus the concentration of the zero gas.

One may now derive a working formula for calculation of unknown gas concentrations from the IRA meter, or recorder, readings. Figure 2.9a shows, in schematic fashion, the response curve of the IRA. The unknown gas concentration, C_x, can be expressed in two parts, a linearly calculated part, C'_x, and a nonlinearity

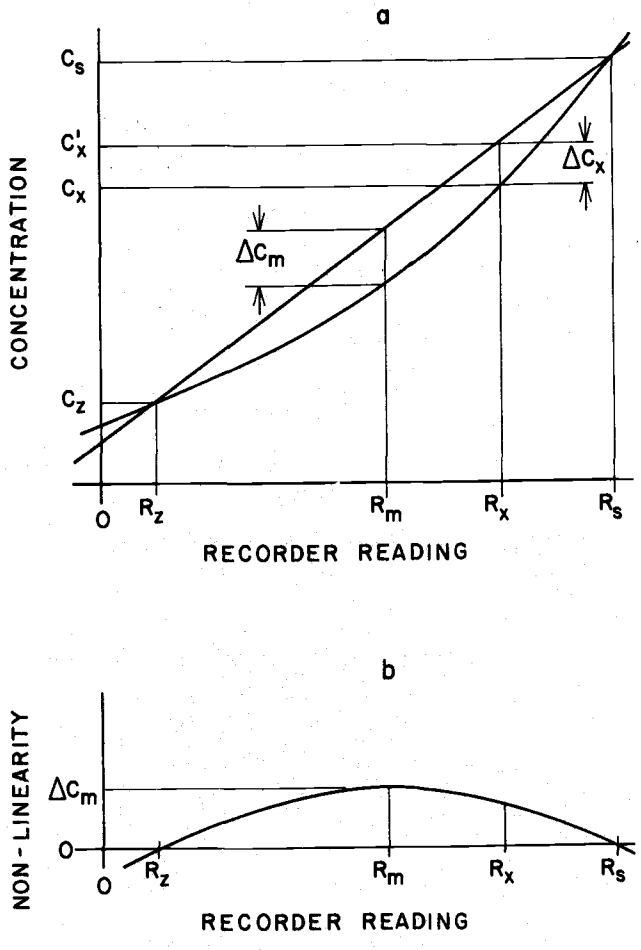

Fig. 2.9. The IRA nonlinearity. a) The nonlinear response curve. ΔC_m is the maximum nonlinearity error at mid scale, R_m; ΔC_x is the nonlinearity error at any other point on the scale. The curve is approximated by Eq. (2.22) in the corrections used in this work. R_m is calculated as the mean between R_S and R_Z, Eq. (2.23). b) The nonlinear part of the calibration curve. This is approximated as a quadratic in $(R_X - R_m)$, Eq. (2.21).

correction, ΔC_x:

$$C_x = C'_x - \Delta C_x \tag{2.17}$$

in which

$$C'_x = C_z + m(R_x - R_z) \tag{2.18}$$

where R_x and R_z are the recorder readings for the unknown and zero gases, respectively, and

$$m = (C_s - C_z)/(R_s - R_z) \tag{2.19}$$

R_s is the span gas recorder reading and C_s and C_z are the concentrations of the span and zero gases, respectively. From Eqs. (2.18) and (2.19),

$$C'_x = C_z + [(C_s - C_z)/(R_s - R_z)](R_x - R_z) \tag{2.20}$$

To obtain the nonlinearity correction, ΔC_x, refer to Fig. 2.9b which represents the nonlinearity correction as a function of the recorder reading. The nonlinearity data furnished by the manufacturer is approximated as a parabolic function:

$$\Delta C_x = \Delta C_m \left[1 - [(R_x - R_m)/(R_s - R_m)]^2\right] \tag{2.21}$$

and the final expression for C_x becomes, using Eqs. (2.17), (2.20), and (2.21):

$$C_x = C_z + \frac{C_s - C_z}{R_s - R_z}(R_x - R_z) - \Delta C_m \left\{ 1 - \left(\frac{R_x - R_m}{R_s - R_m} \right)^2 \right\} \quad (2.22)$$

In Eqs. (2.21) and (2.22), R_m is the point on the recorder chart midway between the readings of the zero gas, R_z, and the span gas, R_s,

$$R_m = (R_z + R_s)/2 \quad (2.23)$$

Step 5. To test the validity of the calibration formula the following procedure was used: 1) From the MSA calibration curves for the LIRA a set of meter readings and gas concentration pairs was read. 2) A set of concentrations from the meter readings using the derived calibration formula was calculated. 3) The difference between the calculated and original concentrations was plotted against the original concentrations. The results are given in Figs. 2.10a and 2.10b. For the range 300 to 600 ppm the discrepancy is less than or equal to 0.2% of the concentration. For the 0 to 600 ppm range the discrepancy is less than 1% of the concentration above 70 ppm, but is 2.7 ppm or 9% at the 30 ppm level. Examination of the calibration curve furnished by MSA for the 0 to 600 ppm range revealed a break in the curve which occurred just at 30 ppm. It is quite possible that our calibration formula is more accurate than the MSA calibration curve.

Then the possibility of using our calibration formula as an

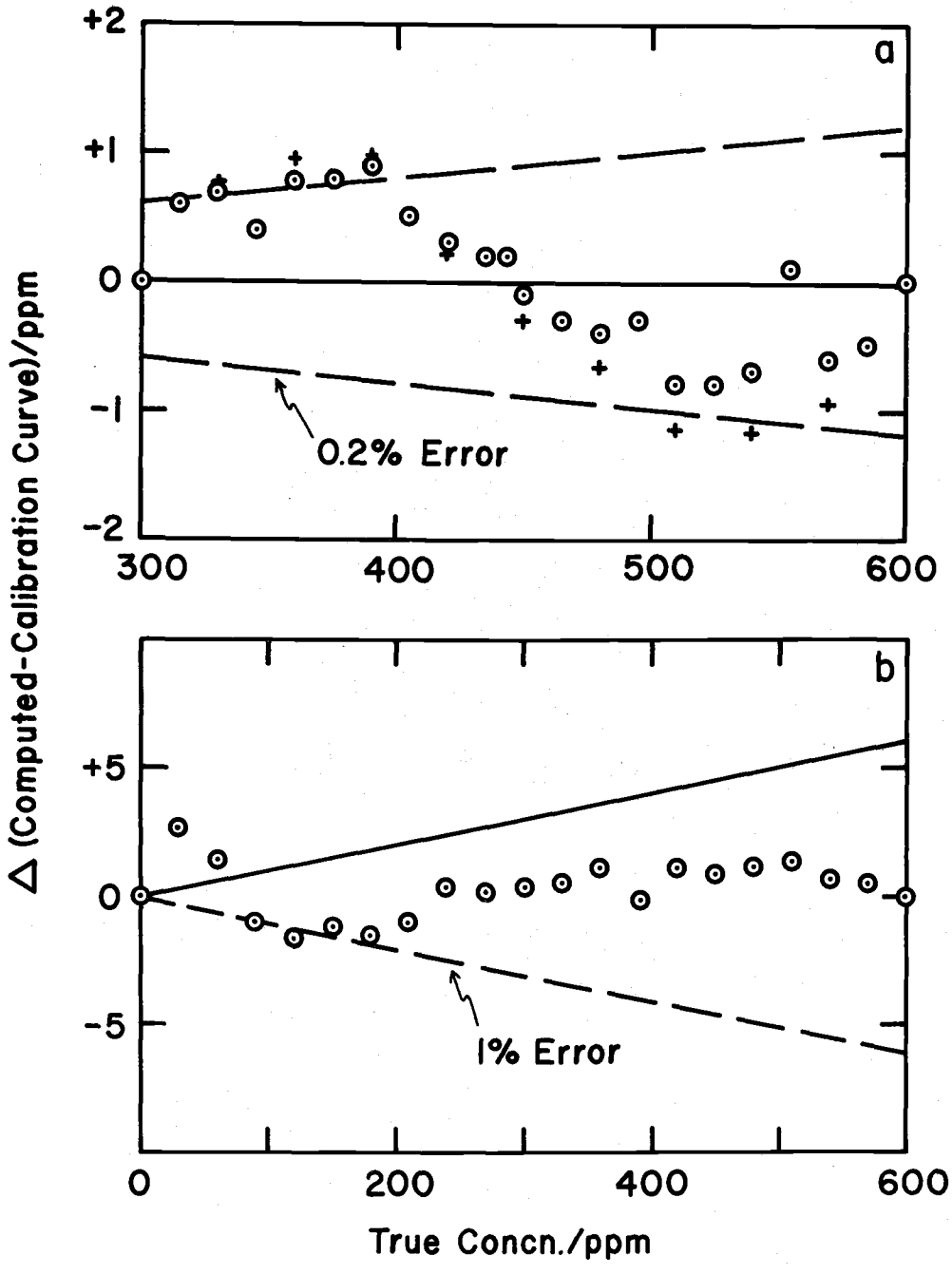

Fig. 2.10. Residual discrepancies between CO_2 concentrations calculated from the derived calibration formula and the MSA calibration data. a) For the concentration range 300 to 600 ppm. The points have a radius of 0.1 ppm on the scale of the ordinate. The dashed lines indicate the 0.2% error limits based on the concentration measured. b) The analogous plot for the 0 to 600 ppm range. Note that the points are drawn with a radius of 0.5 ppm and the dashed line now denotes the 1% error limits. The discrepancies below 70 ppm are discussed in the text.

extrapolation formula was tested for CO_2 concentrations beyond the range of our zero and span gases. It was immediately apparent that below the concentration of the zero gas the formula was very poor. However, above the concentration of the span gas the formula fits surprisingly well. The fit is shown in Fig. 2.11 for the range 600 to 1200 ppm. The figure was obtained by making a set of dilutions of the 1380 ppm OSU standard gas and measuring these with the LIRA set for

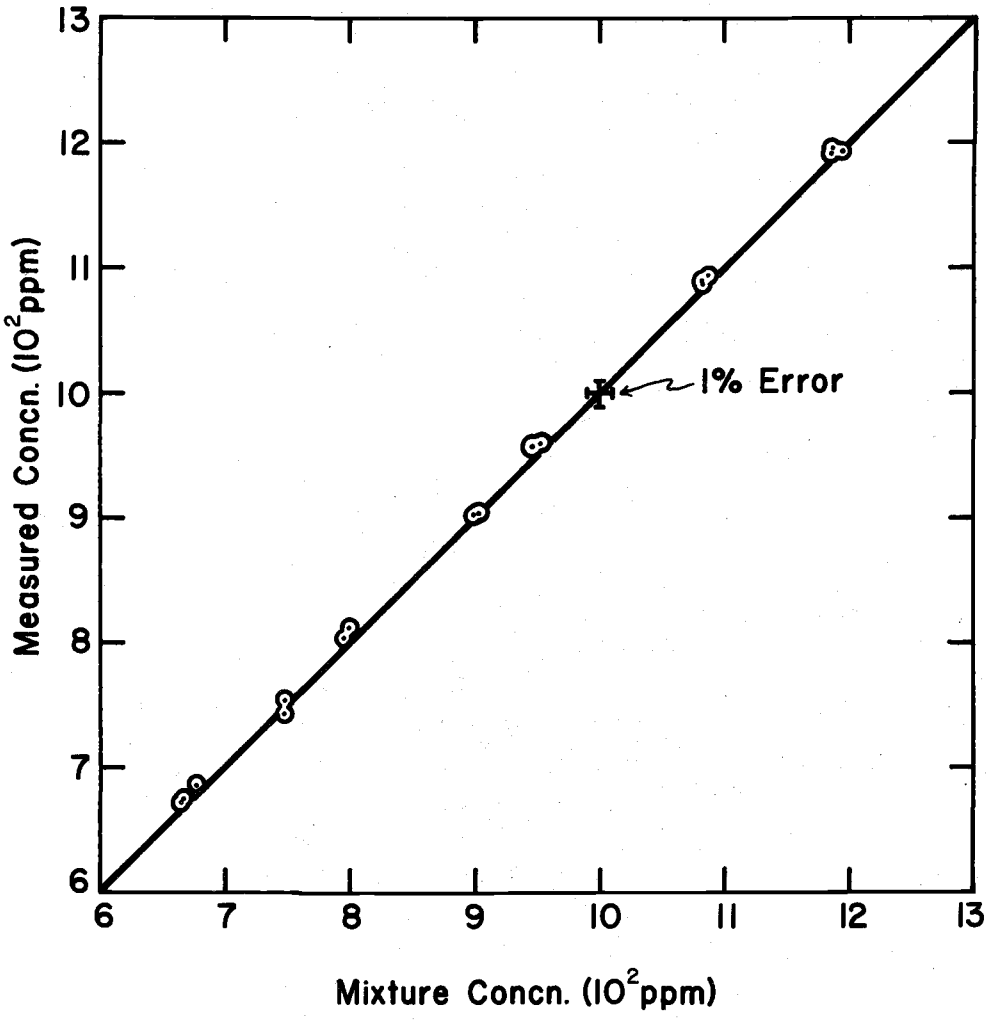

Fig. 2.11. Test of the nonlinear calibration formula for the LIRA as an extrapolation formula. The line is the 1:1 line indicating a perfect fit.

the range 0 to 600 ppm. The recorder gain was reduced to keep the trace on the scale. The measured concentrations, calculated from the calibration formula, were then plotted against the concentrations calculated from the dilution data, with the result shown.

Apparently the calibration formula may be used as an extrapolation formula over this concentration range with an error of less than 1%. This circumstance is very fortunate indeed. Much of the work in the coastal waters of Oregon and Washington has required the use of the concentration range 0 to 1200 ppm.

2.4 Correction for Pressure and Humidity Effects

Correction of the measured PCO_2 for pressure variation in the IRA. The IRA measures concentrations of carbon dioxide in its measuring cell. The concentration is proportional to the partial pressure of carbon dioxide in the cell. For the gases and pressures involved in this work, Dalton's Law is considered to be obeyed. In this system the total pressure in the measuring cell of the IRA is the same for the reference gases and for the mast air stream. Therefore, no pressure correction for the mast air PCO_2 is necessary. However, the pressure in the cell when the IRA is measuring the equilibrator air stream is considerably less than for the calibration gases and one must correct for this.

The form of the correction employed involves a normalization

to one atmosphere total pressure of both the reference and the equilibrator air streams. Let C' be the concentration at ambient atmospheric pressure P, and C_x be the observed concentration of carbon dioxide at pressure P plus ΔP. ΔP is the difference of the pressure in the cell from ambient atmospheric pressure. Then,

$$C' = C_x \cdot \frac{P}{(P + \Delta P)} \tag{2.24}$$

since an increase of total pressure in the cell increases the observed concentration. P and ΔP offer simplicity of measurement compared with measurement of the absolute pressure in the IRA cell. The methods of measurement of P and ΔP are discussed later.

But neither the reference gases nor the sample streams are measured exactly at P. We now subscript the ΔP's by "ref" and "eq" to denote the IRA cell ΔP for reference gases and equilibrator air streams, respectively. Assume P constant during the period of measurement. To correct an observed concentration, C_x, of CO_2 in the equilibrator air stream for $\Delta P_{ref} \neq \Delta P_{eq}$, and $\Delta P_{ref} \neq 0$, Eq. (2.24) becomes

$$C = C_x \cdot \frac{(P + \Delta P_{ref})}{(P + \Delta P_{eq})} \tag{2.25}$$

where C is the corrected concentration, and P, the atmospheric pressure, fluctuates about a mean of 1013 millibars (mb) or one

atmosphere at sea level.

To measure the atmospheric pressure a temperature compensated aneroid barometer was employed which can be calibrated by U. S. Weather Bureau personnel located at commercial airports. The accuracy of measurement was ± 1 mb, or less, in 1013 mb, contributing an insignificant error to the final PCO_2.

The differences, ΔP's, from atmospheric pressure in the IRA cell are measured by a water-filled manometer. This is connected as closely as possible to the outlet of the cell as indicated by M_{IRA} in Fig. 2.3. ΔP_{eq} usually amounts to 25-30 mb in this system. (A small dryer and water trap are interposed between the manometer and the analyzer cell to prevent the entry of liquid water or water vapor into the cell.) The ΔP's may easily be measured to within ±0.25 mb. However, the ΔP_{eq} fluctuates over a few minutes time up to ±1.5 mb, and drifts up to ±2.5 mb per day. By reading the ΔP_{eq} several times per day, and carefully monitoring and controlling air flows the uncertainty in ΔP_{eq} can be held to less than 1 mb. The resultant error in the final seawater PCO_2 is then less than 0.1%.

Correction of the measured PCO_2 for concentration changes caused by drying the air streams. The atmospheric and equilibrator air streams to be measured both contain more or less water vapor. Because the IRA is somewhat sensitive to water vapor as well as to carbon dioxide most of the water must be removed from the air

stream. This is done with Drierite®-filled drying tubes. When the water vapor is removed from the air stream, the concentrations of all the remaining gases are increased. The increase is proportional to the original water vapor pressure in the air stream. If one knows the water vapor pressure, he can calculate the PCO_2, the CO_2 concentration in the original undried air stream, by

$$AIRPCO_2 = C \cdot (P - AH)/P \qquad (2.26)$$

where C is the CO_2 concentration in the dried air stream, AH is the water vapor pressure, or absolute humidity, and P is the atmospheric pressure. AH is measured, using a sling psychrometer to determine wet and dry bulb temperatures, at two to six hour intervals at a suitable location on deck. The absolute humidity may then be found in psychrometric tables or calculated from (U. S. Weather Bureau, 1953; p. 4):

$$AH = P_{sv}(WBT) - 6.60E\text{-}4\ P(1 + 1.15E\text{-}3\ WBT)(DBT - WBT)\ mb \qquad (2.27)$$

WBT and DBT are the wet and dry bulb temperatures in degrees Celsius, respectively, P is the atmospheric pressure in mb, and $P_{sv}(WBT)$ is the saturated vapor pressure of water at the wet bulb temperature, in mb; E-4 means 10^{-4}.

The saturation vapor pressure relative to pure water at

temperature T, in degrees Kelvin, is given by:

$$P_{sv}(T) = 1013.246\ u^{5.02808}\ 10^{z}\ mb \qquad (2.28)$$

where: $u = 373.16/T$

$z = -7.920298\ w - 1.3816E\text{-}7\ 10^{x} + 8.1328E\text{-}3\ (10^{y}-1)$

$w = u - 1$

$x = 11.334(1 - 1/u) - 1$

and $y = -3.49149\ w$

Eq. (2.28) is from List (1966, p. 350).

The PCO_2 in the equilibrator air stream is corrected in the same manner as the PCO_2 in the outside air stream:

$$SEAPCO_2 = C[P - P_{sv\text{-}sw}(T_w)]/P \qquad (2.29)$$

where C and P have the same meaning as in Eq. (2.26) and $P_{sv\text{-}sw}(T_w)$ is the saturated vapor pressure of seawater in the equilibrator, in mb, calculated using:

$$P_{sv\text{-}sw}(T_w) = (1 - 0.000537\ S)\ P_{sv}(T_w) \qquad (2.30)$$

at the temperature, T_w, and salinity, S, of the seawater in the equilibrator (Sverdrup et al., 1942, p. 115).

The gas phase in the equilibrator is assumed to be saturated with respect to water vapor. This assumption is probably true to within a few percent of $P_{sv\text{-}sw}(T_w)$. Since the total correction

amounts to a maximum of 3% of P at normal, open-sea temperatures the final uncertainty from this cause is negligible.

2.5 The Units Employed for Expression of the PCO_2 Data

We express our CO_2 concentrations in gas mixtures (air, or in air equilibrated with seawater) as the volume mixing ratio,

$$\mu = PCO_2 / P \qquad (2.31)$$

where PCO_2 is the partial pressure of CO_2 and P is the total atmospheric pressure. If Dalton's Law is obeyed, this is identical to the concentration of CO_2 expressed as the volume fraction of CO_2 in the gas mixture or air. If the total pressure is one atmosphere, the mixing ratio is numerically equal to the partial pressure, expressed in atmospheres. The unit adopted here is the partial pressure of CO_2 in the air or seawater at one atmosphere total pressure expressed in 10^{-6} atmospheres, or ppm-atm (sometimes given as simply "ppm"). The values reported are the actual partial pressures of CO_2 in the air or in equilibrium with the seawater in the undried, or "wet," condition at one atmosphere total pressure. For a more complete discussion of this topic see Keeling et al. (1965, pp. 6088-6091). Our numerical values will differ slightly from theirs because they express their data in terms of what the PCO_2 would be if the water vapor were removed from the air, and the total pressure remained

at one atmosphere, i.e., on a "dry" basis. The water vapor pressure effect is small, usually amounting to 2 or 3% or less. The system used in this work permits direct comparison of atmospheric data with surface water data to determine the magnitude and direction of the PCO_2 air-sea gradient. For a direct comparison in fine detail of the present data with that of Keeling et al. (1965) the present data may be recalculated to a dry air basis. Included in the data listings are the necessary barometric pressure and humidity data to permit this treatment. This is readily accomplished by doing the inverse of the correction for the humidity effect which is discussed in Sect. 2.4.

2.6 Outline of the Calculation of PCO_2 from the Raw Data

A brief outline is presented here of how the data processing is done; manually, or by computer. The nomenclature follows that of the previous sections. First, the maximum nonlinearity correction ΔC_m is calculated from

$$\Delta C_m = k R^A \tag{2.16}$$

Next the concentration of the CO_2 in the IRA detector cell C_x is calculated from the reading R_x using

$$C_x = C_z + \frac{R_x - R_z}{R_s - R_z}(C_s - C_z) - \Delta C_m \left\{ 1 - \left(\frac{R_x - R_m}{R_s - R_m} \right)^2 \right\} \tag{2.22}$$

The midpoint of the range, R_m, is obtained by

$$R_m = (R_s + R_z)/2 \tag{2.23}$$

If the concentration of the CO_2 in an air sample is being calculated, it is corrected for humidity by

$$AIRPCO_2 = C_x(P - AH)/P \tag{2.26}$$

The concentration of CO_2 in a seawater-equilibrated air stream is corrected by combining Eqs. (2.25), (2.29), and (2.30).

$$SEAPCO_2 = C_x \frac{(P - \Delta P_{ref})}{(P - \Delta P_{eq})} \left(\frac{P - P_{sv}(T_w)(1 - 0.000537\,S)}{P} \right) \tag{2.32}$$

where $P_{sv}(T_w)$ is the saturation vapor pressure of pure water at the equilibrator temperature, T_w [see Eq. (2.28)].

Program PCO2 has been written in Fortran IV for reduction of the PCO_2 data using the OSU CDC3300 digital computer system. Input to the program is by punched cards and the output is in the form of printed tables, magnetic tape, stored files, and/or punched cards at the option of the user. All corrections except for that necessitated by the heating of the seawater stream (see Sect. 2.7) are performed by the program. A fully documented listing of this program is given by Gordon and Park (1972d).

2.7 Correction of PCO_2 Data for Heating of the Seawater Sample

In the methods for measuring the PCO_2 of seawater using IRA's, the seawater samples or sample streams suffer more or less warming from the sampling point to the point of measurement (Gordon and Park, 1972d; Keeling and Waterman, 1968; Kelley et al., 1971; Li et al., 1969; Miyake and Sugimura, 1969; Takahashi, 1961). This warming causes an increase in the measured PCO_2. The amount of warming must either be kept very low such that the resultant increase in PCO_2 is negligible or a correction to the measured PCO_2 must be made for this effect. Alternatively, the correction may be omitted and a moderate systematic error accepted in the data. However, sufficient information is not always reported with PCO_2 data to allow estimation and/or correction of this error.

Various authors have chosen among the several alternatives. Miyake and Sugimura (1969) kept the temperature increase below 0.5° C and thus held the error from the heating effect to a low value.

Kelley et al. (1971) whose temperature increases were also less than 0.5° C evaluated the resultant error based upon the data presented by Harvey (1955). They concluded that the error which arose was less than 2 ppm.

Keeling and Waterman (1968), using both the tables given by Harvey (1955) and Takahashi's (1961) data, established a value of the

increase of PCO_2 with increase of temperature ($\delta PCO_2 / \delta t$) which was nearly constant at 3% (of the value of PCO_2 /° C).

Li et al. (1969) calculated in situ hydrogen ion activities (a_{H+}) and alkalinity values for their samples from their measured PCO_2 and total CO_2 (TCO_2) values at the measurement temperatures. They employed Lyman's (1956) values for the apparent dissociation constants of carbonic and boric acids in seawater (K'_1, K'_2, and K'_B) and Buch's (1951) values for the solubility of carbon dioxide in seawater (α) to calculate a_{H+} from PCO_2 and TCO_2. They used:

$$a_{H+} = \alpha\, PCO_2\, K'_1\, [1 + (a_{H+}/K'_1) + (K'_2/a_{H+})]/TCO_2 \qquad (2.33)$$

(Li et al., 1969, p. 5507). After correcting the pH at the measurement temperature to the in situ temperature by

$$(pH)_{\text{in situ}} = (pH)_{meas.} + 0.011\,(t_{meas.} - t_{\text{in situ}}) \qquad (2.34)$$

(Li et al., 1969, p. 5508) they computed the corresponding PCO_2 at the in situ temperature and one bar total pressure, again using (2.33). The increase in PCO_2 per degree Celsius temperature increase ($\delta PCO_2 / \delta t$) they obtained was about 5% of PCO_2.

Kanwisher (1960) directly measured the $\delta PCO_2/\delta t$ for a natural seawater of salinity (S) of 31.5‰ and various values of TCO_2, over the temperature range of 10 to 24° C. He treated the case of constant S, total alkalinity (TA), and TCO_2 and concluded that the

increase was a rather uniform 4.5%/°C. This case is applicable to most of the PCO_2 measurement schemes in which a seawater sample or stream is equilibrated with air and the concentration of CO_2 is measured in the air. It is equivalent to requiring that the field sampling system deliver the seawater without gain or loss of water vapor or salt, acids or bases, or CO_2. He also pointed out that the increase of 1%/°C given by Harvey (1955, p. 5) is what the increase would be if the pH remained constant. As Kanwisher noted, the pH of seawater does not remain constant when the water is heated but decreases by about 0.01/°C temperature increase.

Takahashi (1961) also directly measured the $\delta PCO_2/\delta t$ in seawater. He did this both for his PCO_2 measurement system in which excess CO_2 could escape from the seawater to the gas phase and for an experimental system in which the TCO_2 of the seawater could be held constant. For the latter case, which approximates the present system, he gave the $\delta PCO_2/\delta t$ he found (but not the value of PCO_2 itself) as 8-12 ppm in the temperature and pH range where TCO_2 was constant. Assuming that his seawater sample had a specific alkalinity (total alkalinity/chlorinity) of 0.125 it is possible to calculate for his temperature, salinity, and pH values a range of PCO_2 of 200-900 ppm. For PCO_2 from 200-300 ppm his change in PCO_2 of 8-12 ppm would then correspond to a $\delta PCO_2/\delta t$ of 4%, in close agreement with Kanwisher's measured value of 4.5%/°C. If

Takahashi obtained 8-12 ppm/1° C at the high end of the PCO_2 range of 200-900 ppm, then the agreement is not good; Takahashi's value of $\delta PCO_2 / \delta t$ then becomes 1%/° C. However, TCO_2 would have been less likely to have remained constant at the higher values of PCO_2 and therefore the former figure of 4%/° C may be the more likely one.

Skirrow (1965, p. 276) in his comprehensive review of the marine chemistry of carbon dioxide discusses the effect of temperature on the PCO_2 of seawater. He does not explicitly state the restrictions on exchange of carbon dioxide between the seawater and the atmosphere (or gas phase of a measurement system) which may or may not have obtained in the work he reviewed. The point of view from which he reviewed was more general than this work.

Because there seemed to be little agreement between these authors and because of even more extreme $\delta PCO_2 / \delta t$ values published elsewhere (Revelle and Suess, 1957) the writer decided to attempt to derive $\delta PCO_2 / \delta t$ from the data of Lyman (1956) and Buch (1951). The objective was a simple correction formula which could be applied to measured PCO_2 values to correct for the heating of the seawater stream.

Method. The initial step was to create a numerical data file with each line of data in the file containing a salinity (S), a total alkalinity (TA), a temperature (t), and a pH. The values of the four parameters were chosen to include the full range of data found in the field work

which is described later. The salinity and alkalinity ranges and combinations chosen are shown in Table 2.6. Each of these sets of S and TA was combined with a temperature (ranging from 0° to 25° in 5° intervals) and a pH (ranging from 7.5 to 8.6 in 0.1 pH intervals) in all combinations of t and pH. Here total pressure is treated as constant at one atmosphere.

Table 2.6. The ranges and combinations (indicated by "X") of total alkalinity and salinity for which $(\delta PCO_2/\delta t)$ was computed.

Total Alkalinity (meq/l)	Salinity (‰)				
	28	30	32	34	36
1.8	X				
2.0	X	X	X	X	
2.1	X	X	X	X	
2.2	X	X	X	X	
2.3		X	X	X	X
2.4		X	X	X	X

For each line of data the corresponding total carbon dioxide (TCO_2) and partial pressure of carbon dioxide (PCO_2) were calculated using the OSU CDC3300 digital computer. The dissociation constants for carbonic acid were calculated from a least squares fit to Lyman's (1956) data, and the solubility coefficients for PCO_2 were calculated from a least squares fit to the data of Bohr (Buch, 1951) as reported by Harvey (1955) (see Appendix I).

From the resultant file of S, TA, t, pH, TCO_2 and PCO_2 all

lines of data with $PCO_2 \gtrsim 1200$ ppm were eliminated (leaving about 1200 data lines). Letting $t_1 = t - 0.5°$ and $t_2 = t + 0.5°$, two values of pH and their associated PCO_2's were determined for each remaining line of data at (S, TA, TCO_2, t_1) and (S, TA, TCO_2, t_2). The pH calculation was done by an iterative method adapted from those of Ben-Yaakov (1970) and Culberson (1972). The difference between the two calculated PCO_2's is $\delta PCO_2/\delta t$ for a set of t, S, TA, and TCO_2. Figure 2.12 shows the resultant $\delta PCO_2/\delta t$ as a function of PCO_2 for all the lines of data. From this figure it became apparent that a rather simple equation might be fitted to these points. This equation would express $\delta PCO_2/\delta t$ as a function of PCO_2 with only a relatively small residual error.

A program, SIPS (Statistics Instruction Programming System), in the OSU Computer Center Library, was used to fit a quadratic equation

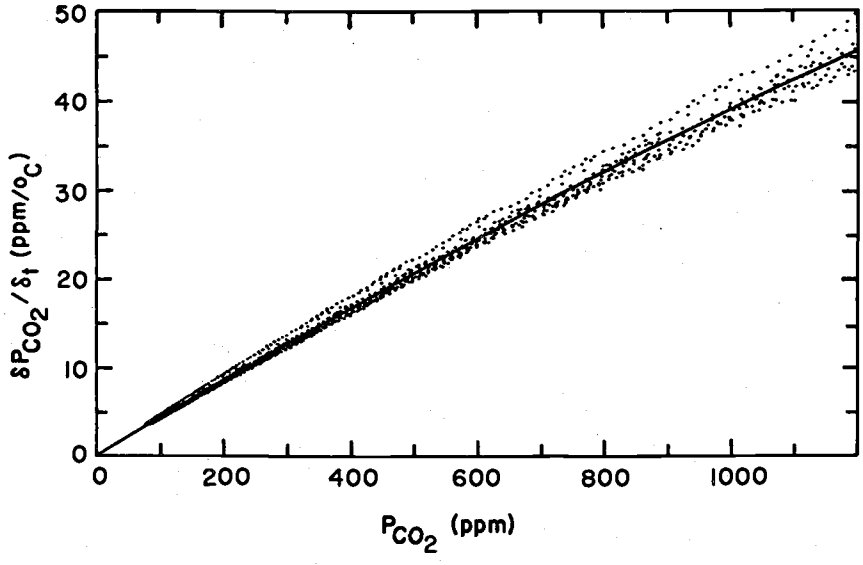

Fig. 2.12. Computed $\delta PCO_2/\delta t$ as a function of PCO_2. The solid line is a least squares fit to the points, Eq. 2.35.

to the values of $\delta PCO_2/\delta t$ vs. PCO_2 for all the lines of data. The resultant equation is

$$\delta PCO_2/\delta t = -1.966\ E\text{-}2 + 4.371\ E\text{-}2\ PCO_2 - 4.623\ E\text{-}6\ (PCO_2)^2\ (ppm\text{-}atm/^\circ C) \quad (2.35)$$

The curve defined by this equation passes along the center of the band of points and lies within ± 9% of all the calculated values of $\delta PCO_2/\delta t$.

One can use the above relationship to correct PCO_2 values at the measured temperature [$PCO_2\ (t+\Delta t)$] to <u>in situ</u> PCO_2 [$PCO_2\ (t)$]. Since the curvature of the line is slight, and in most work Δt is small, a linear correction of the form

$$PCO_2\ (t) = PCO_2\ (t+\Delta t) - \Delta t(\delta PCO_2/\delta t) \quad (2.36)$$

where $\delta PCO_2/\delta t$ is evaluated at $t+\Delta t$ will usually suffice.

The error in $\delta PCO_2/\delta t$ from using the fitted curve instead of the individual calculated values is never greater than 9%, and usually much less. The correction $\Delta t(\delta PCO_2/\delta t)$ is less than 5% of the PCO_2 value, so the maximum error resulting from the use of this fit to $\delta PCO_2/\delta t$ for a 1° C increase in temperature of a seawater sample is 0.4% of PCO_2.

<u>Discussion</u>. This derived $\delta PCO_2/\delta t$ is almost constant at 4.4%/° C. This is in excellent agreement with Kanwisher's (1960) measured

value of 4.5%/°C. In both cases the restrictions on the conditions were that salinity, total alkalinity, and total carbon dioxide of the seawater are conserved. The present treatment covers a wider range of temperature, salinity, and alkalinity than did Kanwisher's. The result is considerably less than Revelle and Suess' (1957) figure of 7%/°C.

The results of Takahashi (1961) and Li et al. (1969) are unaffected by this work. In the former case the temperature correction was measured for the particular apparatus and in the latter case, the correct set of restraints (S, TA, and TCO_2) was applied in calculating PCO_2 at the in situ temperature.

This magnitude of the heating effect on PCO_2 allows one to estimate the systematic errors present in some of the published seawater PCO_2 data. Thus, the data of Miyake and Sugimura (1969) will be at most 2.2% high because they held their seawater warming to less than 0.5°C. They considered the error negligible.

Kelley et al. (1971) measured PCO_2 values as high as 550 ppm. Taking the Δt they give as a maximum, 0.5°C, we find that their data will be at most 2.2% or 12 ppm high. Apparently they evaluated $\delta PCO_2 / \delta t$ for the restraints of constant pH, TA, and S, when they employed the data of Harvey (1955). This leads to a $\delta PCO_2 / \delta t$ of less than 1%/°C as Kanwisher (1960) points out and to an erroneous estimate of 2 ppm as their maximal error.

Keeling and Waterman (1968) have slightly underestimated their heating correction, having arrived at a value of 3%/°C. Thus their seawater data are somewhat undercorrected and contain a residual error of about +1%/°C.

The data presented in this dissertation have an estimated accuracy of ±5%. One of the principal sources of systematic error is this effect of the heating of the seawater stream. The correction for heating has not been applied and introduces an average error of +2% into all of the seawater data reported.

Summary and Conclusions. An equation has been derived which relates the increase of PCO_2 of seawater upon heating, to the temperature increase; that is $\delta PCO_2 / \delta t$. The restraints upon the heating process are that the salinity, total alkalinity, and total carbon dioxide of the seawater remain constant. This is the usual case for most of the systems which are employed for the measurement of PCO_2 by equilibrating air with the seawater and then measuring carbon dioxide concentrations in the air with an IRA. In these cases the measured PCO_2 can be corrected for heating of the seawater by a simple, quadratic formula which requires as input only the values of the measured PCO_2 and the temperature increase. This correction will be accurate to within ± 0.4% of the value of PCO_2. Some of the recently published seawater PCO_2 data as well as those contained herein contain small systematic errors arising from incorrectly

applying or not applying the heating correction.

2.8 Auxiliary Data

The methods employed for making the measurements of in situ temperature, salinity, dissolved oxygen, pH and alkalinity, total carbon dioxide, phosphate, nitrate, nitrite, and silicate are routine and are described by Wyatt et al. (1971), Wyatt et al. (1970), Barstow et al. (1969), and Atlas et al. (1971) and will not be repeated here.

Calculation of the apparent oxygen utilization. The apparent oxygen utilization (AOU) is the oxygen solubility (O_{sat}) at the temperature and salinity of the water minus the measured oxygen (O_{obs}) in ml/l,

$$AOU = O_{sat} - O_{obs} \tag{2.37}$$

The oxygen solubility is calculated from the chlorinity (Cl) and temperature (t) in °C by

$$O_{sat} = \sum_{I=1}^{10} \sum_{J=1}^{JN} A(I, J) Cl^{I-1} t^{J-1} \tag{2.38}$$

where JN = 11-I. Equation (2.38) and the values for the polynomial coefficients A(I, J) are from Gilbert et al. (1968), based upon Carpenter's (1966) oxygen solubility data. The chlorinity is computed

from the measured salinity (S) by

$$Cl = S/1.80655 \tag{2.39}$$

(Wooster et al., 1969). O_{obs} is the dissolved oxygen concentration in the water sample as measured by the Winkler method (Wyatt et al., 1971).

Calculation of relative humidity. The relative humidity (RH), in percent, is calculated from the absolute humidity (AH) and the saturation vapor pressure at the dry bulb temperature $P_{sv}(DBT)$,

$$RH = [AH/P_{sv}(DBT)]\,100 \tag{2.40}$$

Equation (2.40) is from U. S. Weather Bureau (1953, p. 3). Calculation of AH and $P_{sv}(T)$ was described in Sect. 2.4.

CHAPTER 3

CARBON DIOXIDE PARTIAL PRESSURES IN NORTH PACIFIC SURFACE WATERS - TIME VARIATIONS

3.1 Introduction

Many workers have observed that the partial pressure of carbon dioxide (PCO_2) in surface ocean waters is not in general equal to the PCO_2 in the atmosphere above (for instance, Takahashi, 1961; Keeling, 1968; Akiyama, 1969c; Kelley, 1970). Thus the atmosphere and oceans are not generally in equilibrium with respect to the carbon dioxide system, and there is more or less transport of carbon dioxide from the sea to the atmosphere or vice versa depending upon the direction of the gradient and its magnitude. Previous work including that cited earlier has delineated many of the features of the global distribution of carbon dioxide partial pressures in surface ocean waters particularly for summertime conditions. It is the purpose of this work to examine some of the variations in time of the PCO_2 in surface waters of the north Pacific Ocean.

The partial pressure of carbon dioxide in the surface layers of the oceans is determined by biological and physical oceanographic processes, as well as by the interactions of surface waters with the

atmosphere (Takahashi, 1961; Teal and Kanwisher, 1966; and Miyake and Sugimura, 1969). However, quantitative estimates of the relative influences of these various factors are few (Kanwisher, 1963; Eriksson, 1963). At Oregon State University a program has been in progress for some time to measure the variations in time of PCO_2, to evaluate rates of transfer of carbon dioxide between the atmosphere and the sea, and to further understand the processes which affect the distribution of dissolved CO_2 in the sea.

Data for the present study were collected in October, 1968, on the NOAAS SURVEYOR, and on the TRANSPAC expedition of the CNAV ENDEAVOUR. The SURVEYOR cruise occupied a grid of hydrographic stations between 40° and 46° N latitude and between 115° E and 180° longitude (Gordon et al., 1970). The principal objective was a hydrographic and chemical survey of the polar front in the northwestern Pacific Ocean. Hydrographic and STD casts were made at close intervals along 155°, 160°, and 165° E and along 180°. In addition to temperature and salinity, dissolved oxygen measurements were routinely performed. Samples were frozen and returned to Corvallis for nutrient analyses.

The TRANSPAC expedition of the CNAV ENDEAVOUR left Victoria, British Columbia, in the middle of March, 1969, and sailed essentially along the great circle route to Tokyo, Japan. After several days' stay in Tokyo, the ship proceeded north to Hakodate and

after a day there continued eastward, again on approximately the great circle route back to Victoria, British Columbia.

The principal objective of the ENDEAVOUR cruise was an early spring survey of phytoplankton production. A large variety of physical and biological measurements were made on the cruise (cf. Barraclough et al., 1969; Wickett, 1969; Parsons and Anderson, 1970; Seki, 1970; Stephens, 1970). These included measurement of productivity by the C^{14} uptake method, determination of extinction coefficients, measurement of total daily radiation, and plankton population and chlorophyll a studies. Measurements of nitrate, phosphate, and silicate were also made. Physical oceanographic observations included expendable BT, surface temperature, and salinity.

On both expeditions, measurements were made of PCO_2, pH, total alkalinity, and total inorganic carbon dioxide in addition to those outlined above.

3.2 Methods

PCO_2 was measured as described in Chapter 2.

On the SURVEYOR cruise discrete samples were taken from the equilibrator every two hours for the salinity, dissolved oxygen, alkalinity, total CO_2, pH, and plant nutrient measurements. The salinity samples were taken in bottles having pressure clamp stoppers with rubber gaskets and measured within one day using an inductive

salinometer. The dissolved oxygen samples were taken in 270 ml BOD bottles, pickled immediately and analyzed within 24 hours by Winkler titration. The procedure was essentially that described by Strickland and Parsons (1968). The pH and alkalinity samples were drawn in 100 ml high density polyethylene bottles and the pH was measured within two hours according to the procedure given in Strickland and Parsons (1968). Aliquots were taken for alkalinity and measured by the method of Anderson and Robinson (1946). Samples for total CO_2 were taken in 10 ml glass vials and analyzed within 24 hours by the gas chromatographic method described by Park et al. (1964) using two ml aliquots for injection into the chromatograph. Sulfuric acid rather than hydrochloric acid was used for the acidification of the seawater in the stripping chamber.

On the ENDEAVOUR cruise the same analyses of discrete samples were performed but quite different sampling and storage procedures were employed. Samples were taken from the equilibrator every 12 hours. The samples were drawn into aged salinity bottles, sealed, and stored in the dark for later analysis in the Corvallis laboratory. The analyses were performed within a week after arrival in Corvallis. The dissolved oxygen and nutrient analyses were performed primarily as indicators of changes in the samples on storage.

3.3 Results

The PCO_2 data obtained for the subarctic portion of the SURVEYOR cruise are shown in Fig. 3.1. The PCO_2 data have been contoured considering the distributions of the other chemical and physical variables that were measured, as well as the carbon dioxide data. The western and southern limits of the PCO_2 minimum of 263 ppm do not necessarily agree in reality with the limits shown. There is no way of knowing these limits from the limited track of this cruise. We

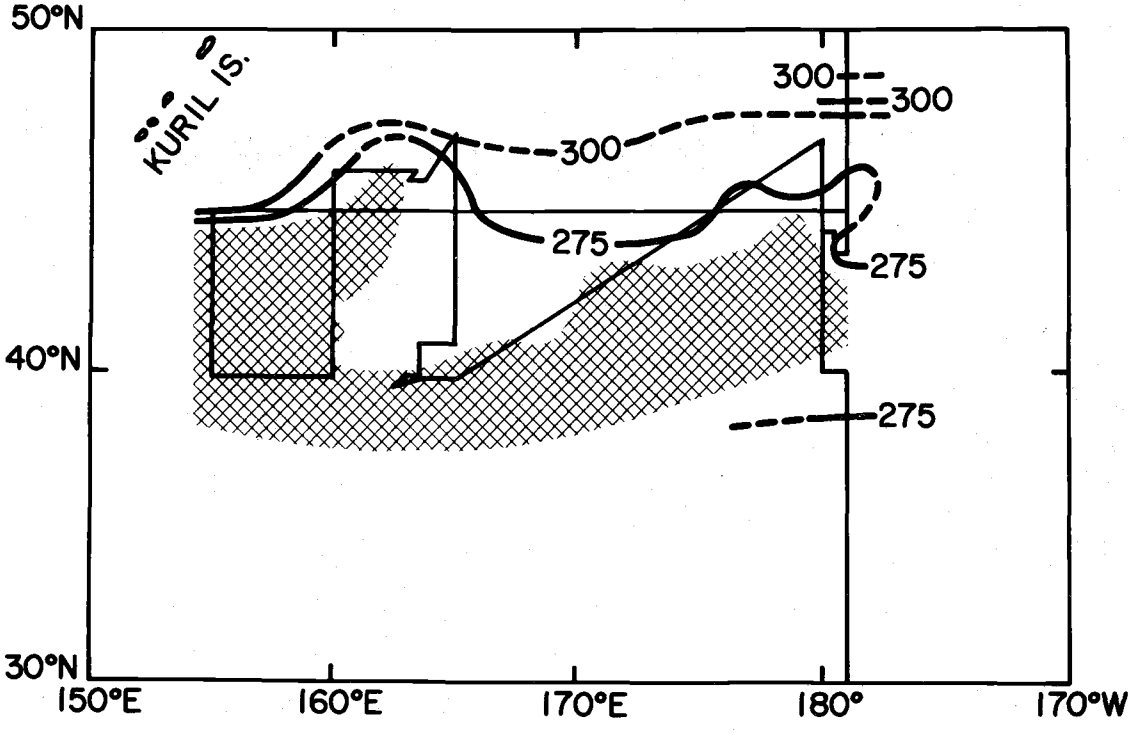

Fig. 3.1. Surface PCO_2 contours for the subarctic portion of the SURVEYOR cruise. The contour interval is 25 ppm. The shaded region represents a general minimum in PCO_2 of 266 ± 4 ppm whose western and southern limits are conjectural.

infer from the data of Keeling (1968) that the southern limit is probably in an east-west direction.

A summary of the observations on the westward track of the ENDEAVOUR cruise is given in Fig. 3.2. The dashed line is the atmospheric carbon dioxide partial pressure which varied slightly around 325 ppm and rose somewhat at the eastern- and westernmost

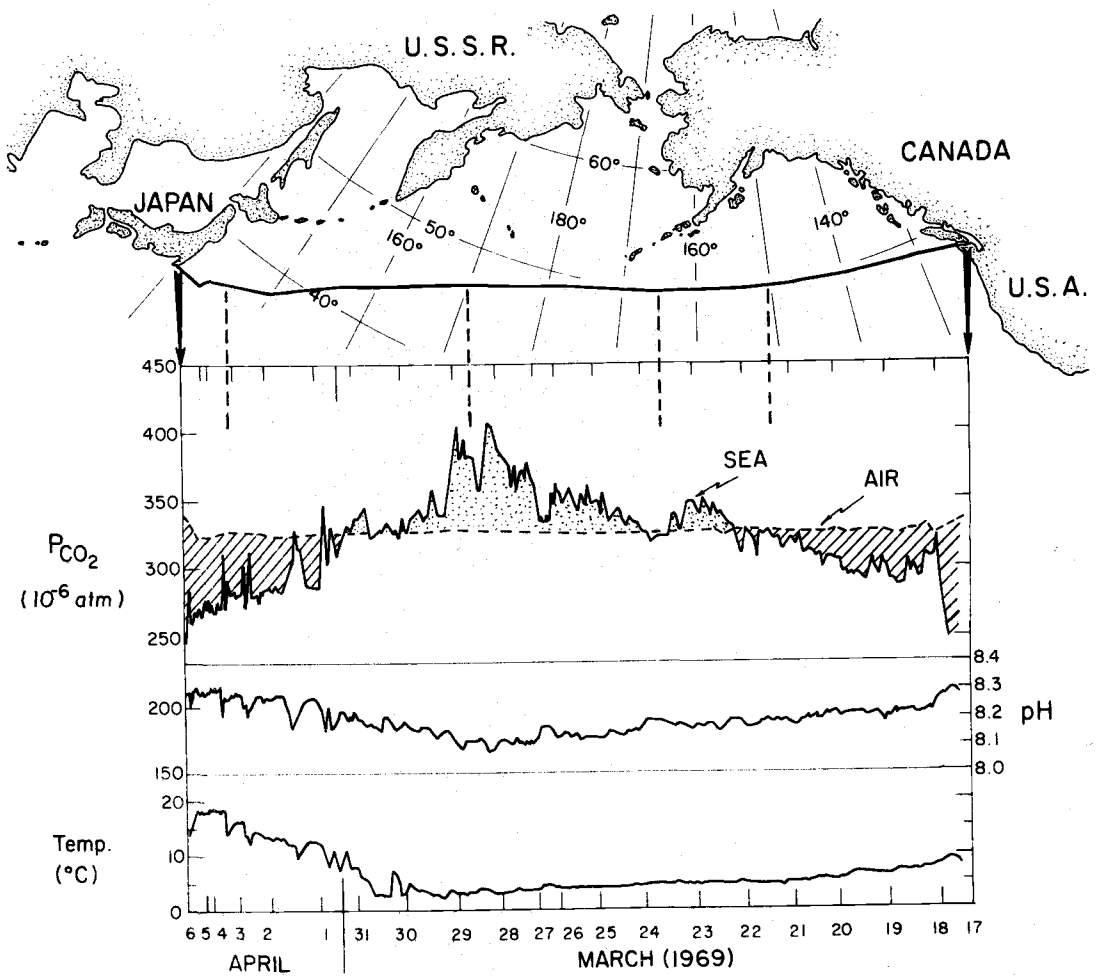

Fig. 3.2. Distribution of PCO_2 in the water and the atmosphere (dashed line), pH, and temperature on the westbound portion of the ENDEAVOUR cruise (17 March-6 April 1969). The dates and values of the observations are projected vertically downward from the track which is drawn at the top.

parts of the track where the activities of man became evident. The seawater PCO_2 displayed a wide area of supersaturation in the central and somewhat western North Pacific. That is, the surface seawater had a higher PCO_2 than did the atmosphere. The eastern and western parts were undersaturated by as much as 75 ppm. West of British Columbia the PCO_2 rose, became supersaturated, dropped back down to slightly undersaturated, and then increased again.

Data obtained on the return track of the ENDEAVOUR cruise, including the portion of the track from Tokyo to Hakodate, is shown in Fig. 3.3. If this is compared with Fig. 3.2, we see the same generalities hold: supersaturation in the north central part of the North Pacific and undersaturation predominating toward the continents. This holds even for details such as the little minimum and maximum at 160°W. Along the track between Tokyo and Hakodate there were wide fluctuations in the PCO_2 record.

The pH data and the temperature data, particularly along the western part of the cruise tracks, correlate very closely in fine detail with the PCO_2. The very high PCO_2 value of about 440 ppm coincided with the unusually low pH of 8.0. These are uniquely high, and low, respectively, mid-ocean observations at these latitudes.

The fine structure on the CO_2 traces has been deliberately retained and not smoothed so that the patchiness in the CO_2 distribution is clearly indicated. This is possibly related to the patchiness that

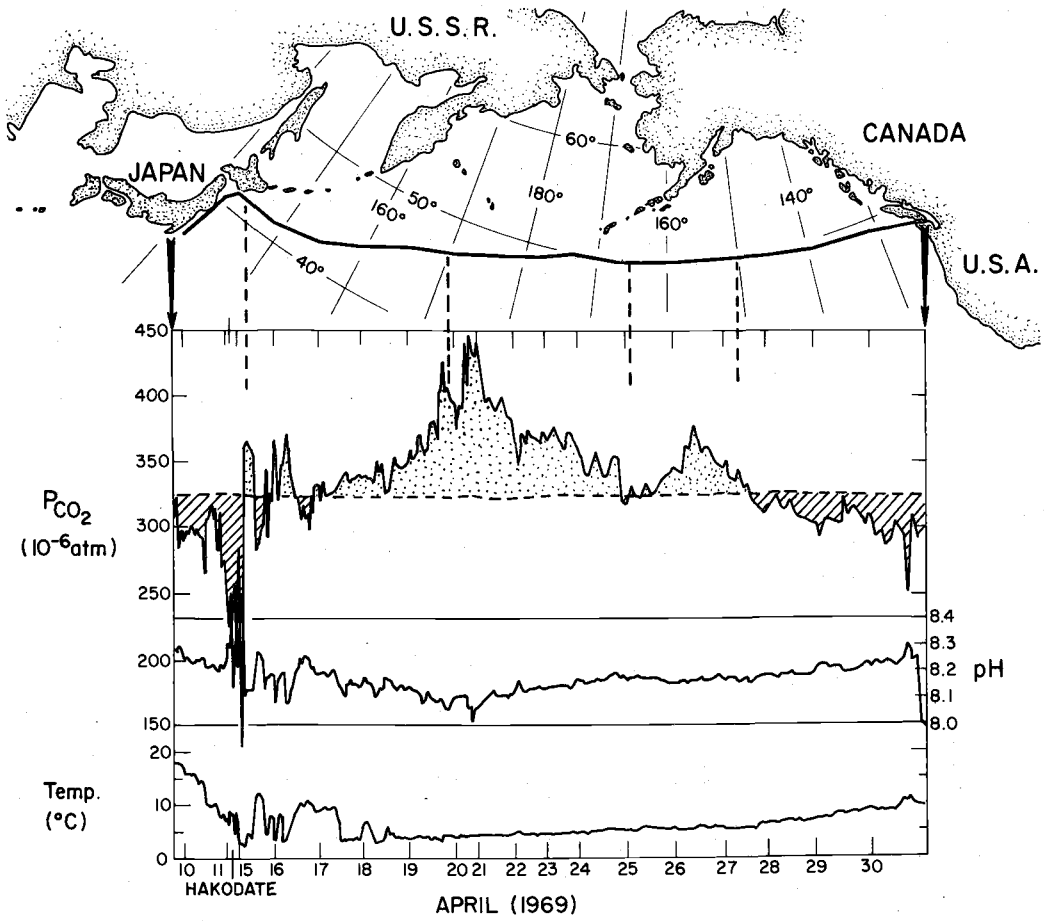

Fig. 3.3. Distribution of PCO_2 in the water and the atmosphere (dashed line), pH, and temperature on the Tokyo to Hakodate (10-11 April 1969) and eastbound (15-30 April 1969) portions of the ENDEAVOUR cruise. The lack of near-continent rises in atmospheric CO_2 could be due to air circulation at the time of measurement.

is observed in biological distributions.

Figure 3.4 presents a comparison of our measured PCO_2 values with PCO_2 calculated from the pH, titration alkalinity, temperature, and salinity. The physical-chemical constants necessary, α, the solubility coefficient of CO_2 in seawater, and the apparent

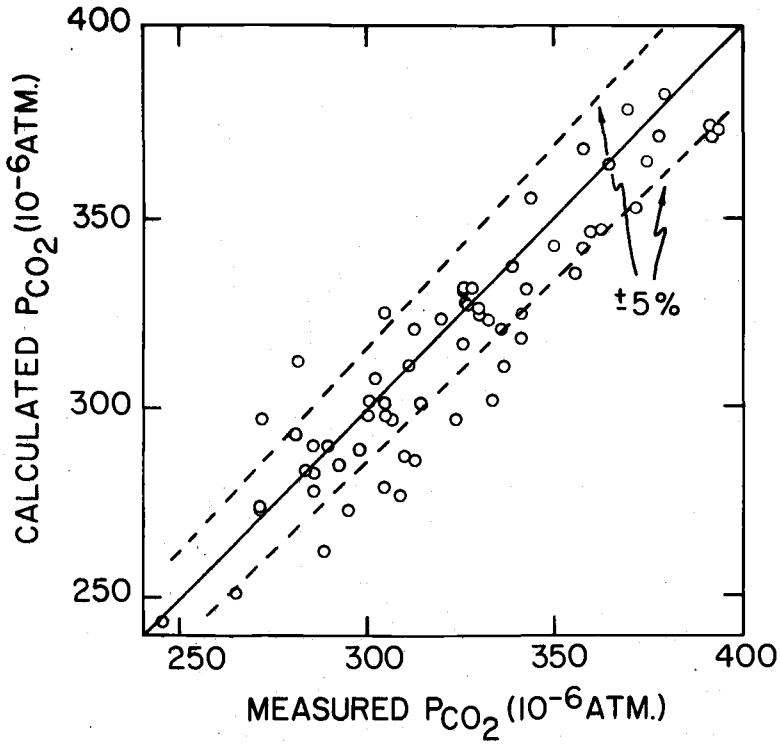

Fig. 3.4. Comparison of measured PCO_2 with PCO_2 calculated from pH and carbonate alkalinity by Eq. 1.18. The solid line indicates the 1:1 slope through the origin; the ideal case.

dissociation constants K'_1 and K'_2 of carbonic acid, and K'_B of boric acid are, of course, functions of temperature and salinity. Lyman's (1956) values for K'_1, K'_2, and K'_B and Buch's for α as quoted by Harvey (1955) were used. When this calculation is made, a relative, root-mean-square deviation of 4% is obtained between measured and calculated PCO_2. A least-squares linear fit to the data falls 2.3% below the 1:1 line. This gives a measure of the internal consistency between the various sets of data obtained in this study.

A comparison of the SURVEYOR and ENDEAVOUR data is presented in Fig. 3.5. The values from the points of the SURVEYOR

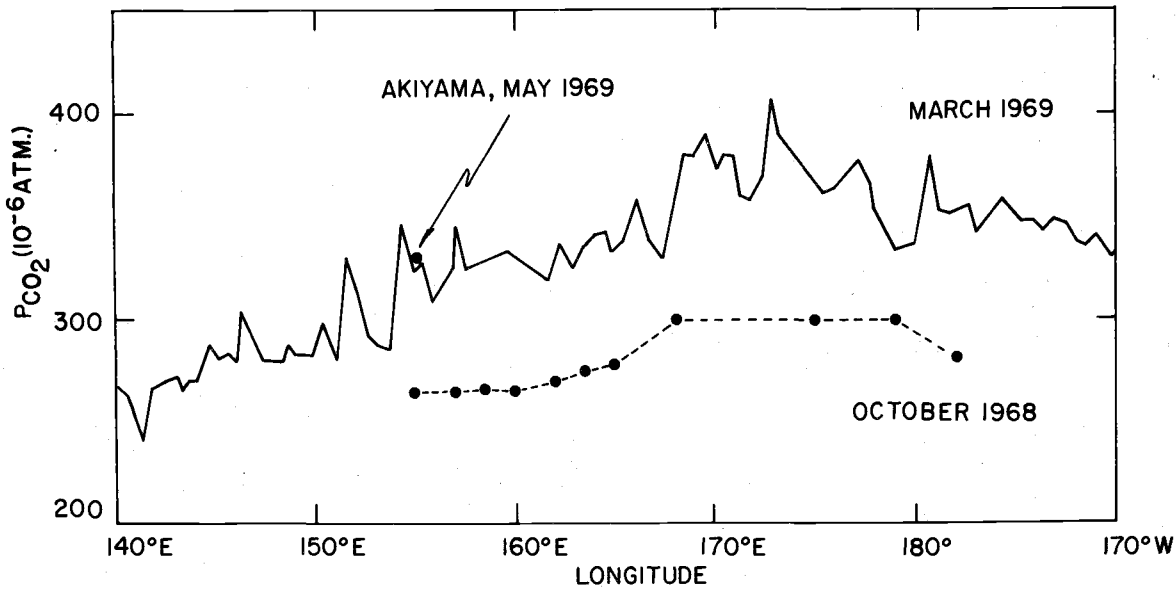

Fig. 3.5. Seasonal variation in PCO_2 as indicated by comparison of ENDEAVOUR data (solid line) and data of Akiyama (1969c) (one point) with SURVEYOR data (dashed line). The seasonal difference is about 60 ppm.

track crossed by the ENDEAVOUR track have been interpolated from Fig. 3.1, entered on this figure and joined by straight dashed lines. The figures show the March ENDEAVOUR results as a solid curve, as in Fig. 3.2, except that only a narrow longitude range has been selected. The SURVEYOR data appear smoother, having been interpolated from a smoothed contour chart. Note that the two curves are nearly parallel and that they are on the average 60 ppm apart.

One point, obtained by Akiyama (1969c) at the same location, in May 1969 is also plotted. This observation is identical to our May value, within experimental error.

A comparison of the PCO_2 and temperatures for the eastern-

most parts (150°W-125°W) of the ENDEAVOUR cruise tracks is given in Fig. 3.6. The time elapsed between successive occupations of the same position ranged from 37 to 44 days. Temperatures were higher over all of this region on the return trip. The PCO_2 were also generally higher.

3.4 Discussion

Processes which influence sea surface PCO_2 include exchange with the atmosphere, vertical mixing of high PCO_2 subsurface water with low PCO_2 surface water, upwelling of subsurface water,

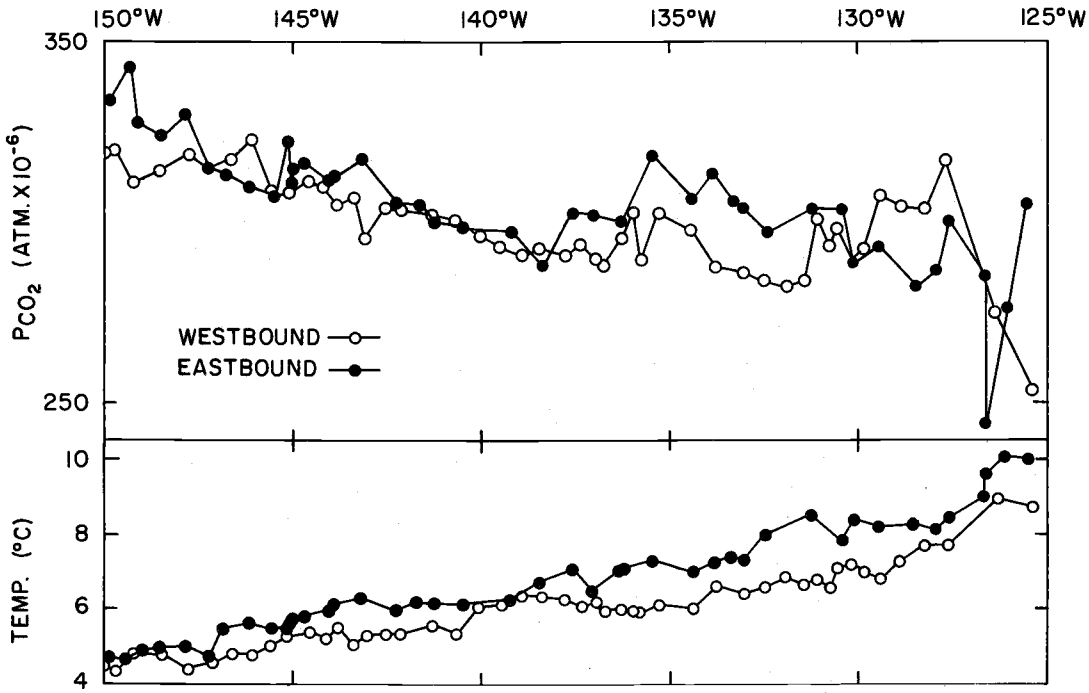

Fig. 3.6. Comparison of PCO_2 and temperatures from the westbound and eastbound legs of the ENDEAVOUR cruise. Only a small portion of the track (150°W to 125°W) is shown.

horizontal circulation and mixing, warming or cooling of surface water, respiration and uptake of CO_2 during photosynthesis. Air-sea exchange must be in general, comparable in rate, or slower than one or more of the other processes because the surface PCO_2 seldom equals the atmospheric PCO_2.

The magnitude and direction of air-sea exchange is partially determined by the magnitude and sign of the PCO_2 gradient between the sea surface and the atmosphere. In addition, the wind speed over the sea surface affects the rate of exchange of CO_2 (Kanwisher, 1963). A detailed evaluation of air-sea exchange rates will not be attempted in this dissertation. However, the direction of the flux of CO_2 in the North Pacific for March and April can be predicted from consideration of the seawater and atmospheric PCO_2 given in Figs. 3.2 and 3.3. Note that the North Pacific loses CO_2 to the atmosphere in the central region and gains CO_2 at its eastern and western margins at this time of year.

Horizontal circulation influences the observed PCO_2 distribution. Wickett (1969) has suggested that the TRANSPAC cruise encountered the following water masses: 125°W to 150°W - Alaskan Gyre; 150°W to 165°W - Eastern Subarctic; 165°W to 170°E - Western Subarctic; and 170°E to 145°E - Kuroshio Extension and Kuroshio. The boundaries between these water masses are given as vertical dashed lines on Figs. 3.2 and 3.3. It appears that the observed PCO_2

distribution may be related in part to the water masses encountered. In addition, the mixing of the Kuroshio and Oyashio, characterized by low PCO_2-high temperature and high PCO_2-low temperature respectively (Akiyama, 1969c), may have contributed considerable variability to the PCO_2 record in the western part of the return track.

Miyake and Sugimura (1969) have pointed out a correlation between the depth of the mixed layer and observed surface PCO_2 in the Indian Ocean. In Fig. 3.7 are plotted CO_2 saturations versus the depth of the top of the thermocline during the ENDEAVOUR cruise.

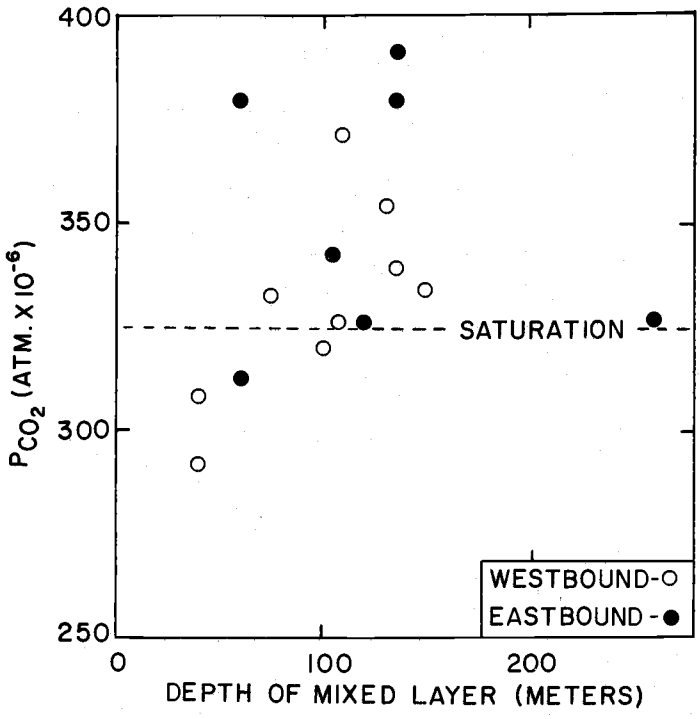

Fig. 3.7. Relationship between PCO_2 and depth of the mixed layer. The mixed layer depth was determined from expendable bathythermograph traces. Data include only those points for which production at the depth of sampling (3 m) was less than the mean production value (0.88 mg $C/m^3/hr$) at that depth.

The plot illustrates the extent of correlation we found. Although quite weak the correlation is sufficient to indicate a possible influence of vertical mixing upon the PCO_2 distribution during the period of this study.

Warming of seawater produces a rise in PCO_2 if exchange with the atmosphere is restricted (see Sect. 2.7). A rough calculation from the data of Fig. 3.6 seems to indicate a 2-3% /°C effect. For constant S, TCO_2, and TA, the effect would be 4.4%/°C as shown in Sect. 2.7.

Examined next is the relation between phytoplankton production as approximated by measured chlorophyll a concentrations and the PCO_2 in Fig. 3.8. The chlorophyll data are from Parsons and

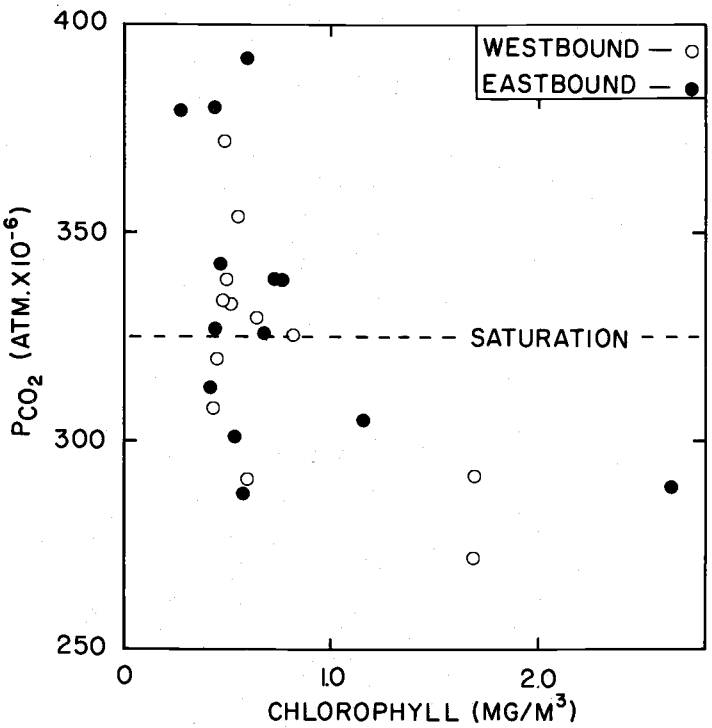

Fig. 3.8. Chlorophyll a concentration versus PCO_2 at the depth of the water intake (3 m) for the westbound and eastbound legs of the ENDEAVOUR cruise. Horizontal dashed line indicates the PCO_2 saturation value.

Anderson (1970). Interpolated chlorophyll a values at 3 meters have been plotted. Chlorophyll a concentration was chosen as the indicator of production because it perhaps represents a weighted average of what the production had been over the past few days. It was felt that this would better correlate with the PCO_2 which because of relatively slow exchange of CO_2 with the atmosphere also reflects the extent of production over the past few days or weeks. The figure indicates an inverse correlation of phytoplankton production with the observed PCO_2 distribution for the ENDEAVOUR cruise.

The correlation coefficient computed for all the data in Fig. 3.8 was -0.53. However the data might better be considered as falling not along one straight line for which this correlation coefficient was computed but along two; in one case, considering only PCO_2 values less than 350×10^{-6} atm and in the other case considering only chlorophyll a values less than 1.0 mg/m^3. For the latter case there would, of course, be a very poor correlation, because at very low chlorophyll a concentrations, other processes than production would become dominant in influencing the PCO_2 distribution. Considering the accuracy of the production data and the number of other processes than photosynthesis acting, the correlation is quite strong; this is particularly so in the eastern and central portions of the track.

Close to Japan, the correlation between PCO_2 and chlorophyll a concentrations becomes even weaker and the variation with distance

in the PCO_2 record increases. We attribute this variation to several causes, among them very intense and patchy phytoplankton activity along the coast of Honshu Island, and the result of mixing of Kuroshio Extension and Oyashio waters in this region. The track outward from Hakodate reflects the same influences and in addition the intense phytoplankton production in the strait between Honshu and Hokkaido.

The processes discussed above combine to produce the observed PCO_2 distributions. Any one or several of these processes may dominate at any given time and place. Certainly the process rates vary with time, and therefore, the end result also varies with time. The data from the two legs of the ENDEAVOUR cruise give an idea of variations on a time scale of one to two months.

Generally speaking, surface PCO_2 was higher on the eastbound leg of the ENDEAVOUR cruise (April) than on the westbound leg (March). This might be due to a difference in the conditions of the analysis, to surface warming, or to a non-steady-state condition of the processes in the system. The warming of the sample waters as they are pumped from the intake to the equilibrator was about 0.6° C on the trip over and 0.9° C on the return trip. The reason for this difference is not known. However, the 0.3° C difference can account for only one third of the observed rise in PCO_2. (See Sect. 2.7.)

Data presented in Fig. 3.6 indicate that surface warming may

have been the major factor contributing to the higher PCO_2 observed east of 150°W on the return trip. Production in this region was slightly increased on the eastbound leg, and the depth of the mixed layer was diminished. The rate of air-sea exchange cannot be directly evaluated, but is probably less in calmer weather, i.e., on the return trip. All of these changes except surface warming would favor lower PCO_2. Therefore we conclude that surface warming was the dominant process affecting the PCO_2 east of 150°W during this period.

Comparing SURVEYOR and ENDEAVOUR cruise results gives an idea of variations on a seasonal or half-year time scale. For the ENDEAVOUR track east of 150°W, the CO_2 system appeared to be in a non-steady-state condition with PCO_2 increasing from March to April. Data given by Parsons and Anderson (1970) indicate that production in this area increases in March and April but reaches its highest levels in May, June, and early July. Thus the ENDEAVOUR cruise probably observed the end of the winter buildup of CO_2 in the surface waters of the subarctic North Pacific.

The SURVEYOR cruise in October may have observed the annual PCO_2 minimum. Temperature and salinity data from the cruise indicate that the breakup of the summer thermocline had not yet progressed significantly. The early fall storms we encountered did not appear to affect surface PCO_2 values. In addition, chlorophyll

a measurements indicated that summer phytoplankton production had come to an end. The data of Parsons and Anderson (1970) also indicate that summer production has greatly diminished by late July.

By comparing the SURVEYOR data (late summer minimum) and the ENDEAVOUR data (early spring maximum), we obtain an indication of the seasonal variation of surface PCO_2 in the North Pacific Ocean. We see from Fig. 3.5 that the SURVEYOR values (dashed line) roughly parallel the ENDEAVOUR values (solid line) and that the difference averages about 60 ppm. This represents the annual range of PCO_2 for the central subarctic Pacific Ocean. It is probably a minimal estimate because there may have been some very early spring production prior to the ENDEAVOUR cruise and the SURVEYOR was perhaps a little late to observe the most intense effect of the summer production.

3.5 Conclusions

This work has provided a direct evaluation of the annual range of the partial pressure of carbon dioxide in surface waters of the subarctic Pacific Ocean.

The magnitude of this annual variation in surface waters re-emphasizes the relatively slow kinetics of air-sea exchange on an ocean-wide scale when compared to such processes as photosynthesis. This feature of the CO_2 system has important implications for

calculations of air-sea exchange of carbon dioxide on a global scale. This is particularly so because most of the data on air-sea PCO_2 gradients has been obtained during late spring, summer and early fall seasons. The present work has shown that not only the magnitude but also the direction of the atmosphere-sea exchange of carbon dioxide varies seasonally on an oceanic scale.

CHAPTER 4

CARBON DIOXIDE IN THE SURFACE WATERS OF THE BERING SEA AND NORTH PACIFIC OCEAN

4.1 Introduction

This work contributes to the task of charting the global distribution of carbon dioxide partial pressures (PCO_2) in surface ocean waters. Such charts are necessary for an understanding of the patterns of carbon dioxide exchange between the atmosphere and the sea on a regional and time-dependent basis. Keeling (1968) has summarized this work up to 1968 and constructed a chart of the surface PCO_2 distribution in the world oceans. All the available data were contoured without regard to season except that most were obtained during the respective local summers. He found equatorial waters to be supersaturated and subtropical waters in the central ocean basins to be undersaturated with respect to atmospheric CO_2. However no data were available in the Pacific Ocean north of approximately 37° N.

Recently the equilibrium partial pressure of carbon dioxide has been measured in the subarctic Pacific Ocean and in the Bering Sea (Kelley and Hood, 1971; Kelley et al., 1971; and Gordon et al., 1971). In this dissertation we present those data and extend Keeling's (1968)

global chart northward through the subarctic Pacific and into the Bering Sea.

4.2 Methods

All carbon dioxide concentrations in various air streams were measured using non-dispersive infrared gas analysis as described in Chapter 2. The equilibrators used for the seawater measurements by the University of Alaska group (see below) were an aspirator type (Kelley et al., 1971) and a shower head type (Kelley, 1970). All measurements were referenced against secondary standard gases calibrated in the Atmospheric Carbon Dioxide Project Laboratory of C. D. Keeling at the Scripps Institution of Oceanography.

The terms undersaturation, equilibrium, and supersaturation refer to sea-surface water PCO_2 values which are lower than, near, or above the average ambient PCO_2 of near surface tropospheric air.

4.3 Results

Bering Sea surface PCO_2 distribution. The data which are presented were obtained on two cruises in the Bering Sea and subarctic Pacific Ocean aboard the NOAAS OCEANOGRAPHER and SURVEYOR. Observations aboard OCEANOGRAPHER along a track from Dutch Harbor to Nome in mid-July and along the reverse track at the end of August, 1968, are shown in Fig. 4.1. Although there were systematic

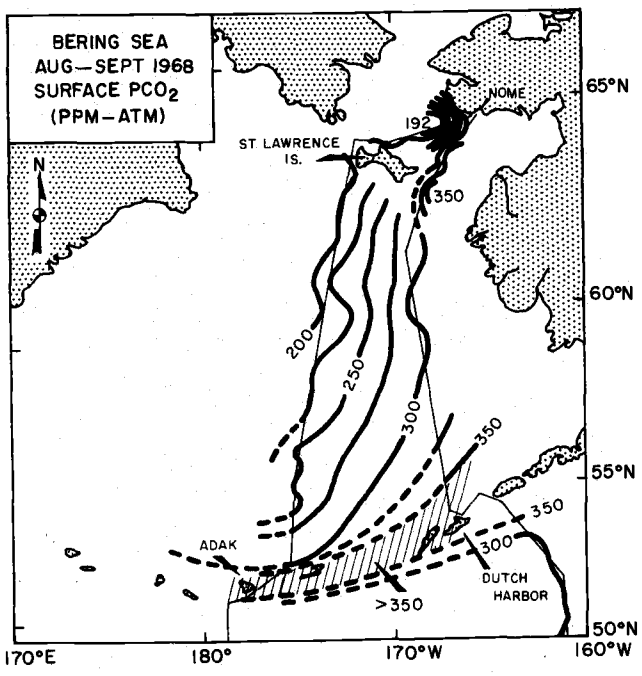

Fig. 4.1. Surface distribution of PCO_2 in the central Bering Sea. The numbers give the surface seawater PCO_2 in ppm. Dashed portions of the contours indicate conjectured positions of the contours. The lightweight lines made of straight-line segments indicate the approximate cruise tracks: SURVEYOR, to the west, in September; OCEANOGRAPHER, to the east, mid-August data only.

differences between the CO_2 partial pressures observed at the two periods the basic patterns remained the same. A group from Oregon State made the track shown from Nome to Adak from the 17th to 23rd of September 1968. The weather had remained quite stable in the region during the interval between the southward OCEANOGRAPHER cruise and the SURVEYOR cruise. For this reason and because zero chlorophyll a concentrations at two stations along the SURVEYOR track were found, one on, and one off the continental shelf, it is

justifiable to contour the two sets of data. The details of the contours may be somewhat in error but the main features are probably well represented.

The average atmospheric CO_2 partial pressure observed during the period 29-30 August was 311 ppm, during 17-23 September, 312 ppm. The difference is within the experimental error; 1 ppm is about one standard deviation for repetitive analyses of one cylinder of reference gas over a period of more than a year. (See Chapter 2.)

Western subarctic Pacific Ocean surface water PCO_2. SURVEYOR continued into the northwest subarctic Pacific Ocean on a study of the Polar Front by the Pacific Oceanographic Research Laboratory of NOAA (Reed and Laird, 1971; Gordon et al., 1971). The track and PCO_2 data were shown in Fig. 3.1. The track led south from Adak to 45° N and thence west to 45° N, 155° E. Three N-S lines of stations at 155° E, 160° E, and 165° E were then occupied between 40° N and 47° N. A diagonal course was then run from 40° N, 165° E to 47° N, 180° where a detailed set of stations in a 1° x 1° square was occupied and finally a line was run due south along 178° W to the latitude of Midway Island. The hatched area indicates a uniform undersaturated surface PCO_2 area of 263 to 264 ppm. Chlorophyll *a* concentrations were nil throughout the region.

Global distribution chart of sea surface PCO_2 anomaly. All of the data are combined in Fig. 4.2 with those of Keeling (1968) for the

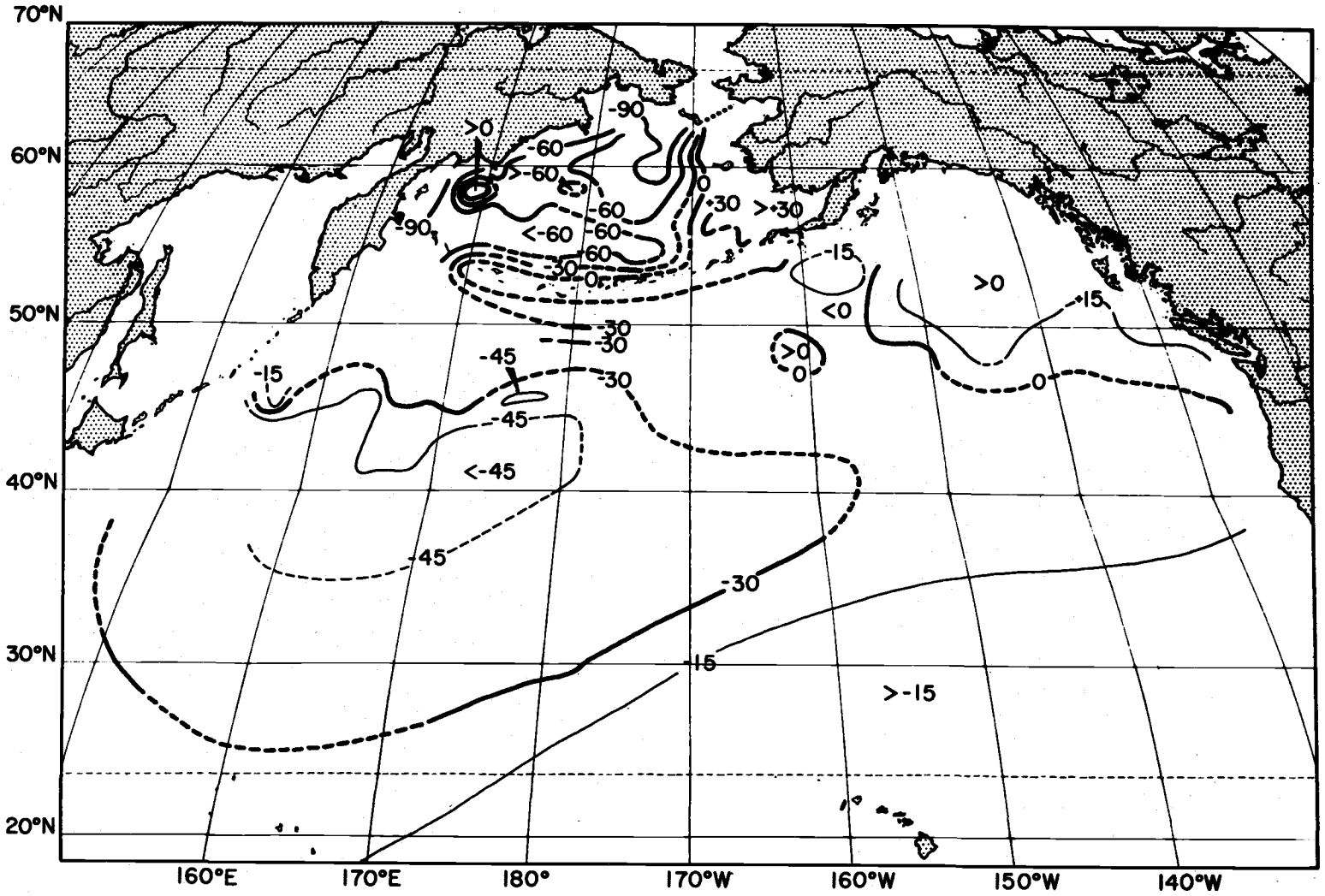

Fig. 4. 2. North Pacific and Bering Sea extension of the "Global Distribution" chart (Keeling, 1968) of surface seawater CO_2 saturation anomaly. Contoured on an interval of 30 ppm are values of the sea surface PCO_2 minus atmospheric PCO_2. The conjectural nature of some contours are indicated by the dashed lines.

Pacific Ocean north of Hawaii (ca. 20°N). Keeling's -15 and -30 ppm contours have been left intact. They agree well with the present data where the cruise tracks cross. Keeling's -45 and -60 contours which do not agree with these values at the track crossings have been deleted. This in no way implies that his figures are wrong. Both sets of data are undoubtedly valid and this point is discussed later. In Fig. 4.2 is shown the general pattern of the PCO_2 anomaly, or deviation of sea-surface PCO_2 from atmospheric PCO_2, and not a detailed, accurate, and synoptic picture.

For the western Bering Sea, data presented by Ivanenkov (1964, p. 102) based upon pH and alkalinity measurements in the early fall, 1951, have been utilized. These pH and alkalinity data might be discrepant from IRA PCO_2 measurements by 2.5% or more (Chapter 3), but the general pattern is no doubt meaningful.

The principal features of the PCO_2 anomalies in the Bering Sea are 1) an intense undersaturation of -100 ppm in the north central part, 2) the general undersaturation of about -60 ppm in the western part, and 3) supersaturation conditions indicated in the eastern part. The principal features of the subarctic Pacific are 1) a general undersaturation of as much as -45 ppm in the western North Pacific Ocean and an indication of a complicated structure in the region of the Subarctic Boundary, 2) near equilibrium in the Gulf of Alaska, and 3) a belt of near saturation water in the west ranging to supersaturation in

the east, between the Pacific Ocean and Bering Sea, along the Aleutian-Komandorskie Island Arc.

4.4 Discussion

Bering Sea surface PCO_2 distribution. The contours of PCO_2 run north-south, not quite parallel to the cruise tracks. Their trends change to northeast-southwest in the southeastern part of the Sea. Three important features are the two low PCO_2 (undersaturation) regions north of St. Lawrence Island and in the western part of the Sea, and the belt of very high PCO_2 (supersaturation) along the Aleutian Islands. The lows of less than 200 ppm are the result of active photosynthesis during the summer months. This CO_2 depletion in the surface water apparently is rapid compared to the rate of replenishment of CO_2 to the sea from the atmosphere and from deeper waters by vertical mixing or upwelling. The two chlorophyll determinations, one on the continental shelf and one over the basin, indicate that photosynthesis had already decreased to near zero at the time of the SURVEYOR cruise; therefore this is a residual effect. Note that the surface water partial pressures are more than 100 ppm-atm lower than the atmospheric partial pressures in the north central region SSW of St. Lawrence Island. This indicates an area of recent intense photosynthesis (see Chapter 2).

In the passes between the Aleutian Islands east of the Near

Islands (52° N, 172° E) there is little net inflow of water into the Bering Sea from the North Pacific. The major inflow is west of the Near Islands (Favorite, 1966). However, high velocity tidal currents occur in the passes between some of the islands and these promote intense vertical mixing of surface water with deep, high PCO_2 water resulting in conditions of local inertial upwelling (Kelley and Hood, 1971; Kelley et al., 1971). There is a resultant flux of CO_2 upward followed by a horizontal transport northward by horizontal eddy diffusion. There is an eastward flow along the north of the Aleutians from the Near Islands to the Andreanoff Islands (52° N, 175° W) where the flow splits. One branch trends northward toward the Gulf of Anadyr (65° N, 178° W) another eastward into Bristol Bay (57° N, 160° W). As the latter flow proceeds east it receives enroute more and more of the CO_2 introduced into the surface layers by vertical mixing and upwelling. This probably accounts for the higher values of PCO_2 to the east.

Another factor contributing to high PCO_2 in the eastern Bering Sea is river discharge, principally from the Yukon River but also from other rivers such as the Kuskokwim (Kelley et al., 1971). Very high PCO_2 values have been observed in river runoff, up to 900 ppm-atm for such Pacific Northwest waters as the Columbia River (Park et al., 1969b; cf. also, Figs. 5.2 and 5.4, this work) and the Strait of Juan de Fuca (Kelley and Hood, 1971; Gordon et al., 1971). Therefore the river inputs to the eastern Bering Sea may be in part causing the high

PCO_2 we see to the southeast.

Subarctic western Pacific surface PCO_2. Again the PCO_2 distribution appears to be dominated by photosynthesis and the surface circulation in the region. In this region also photosynthesis had come to a virtual halt by early autumn as shown by zero chlorophyll a values obtained throughout the SURVEYOR cruise track. The PCO_2 isograms are generally consistent with the surface circulation and water mass domain boundaries as deduced for previous years by several workers (Dodimead et al., 1963). The conclusion is reasonably clear that replenishment from the atmosphere of the CO_2 to reestablish an equilibrium surface PCO_2 distribution with respect to the atmosphere is slow relative to biological and physical processes.

The highly structured distribution of PCO_2 as shown by the northerly edge of the hatched area of Fig. 3.1 is in large part the result of the surface circulation, and mixing of waters from different domains (Dodimead et al., 1963). Each domain probably has its own characteristic PCO_2 signature. The PCO_2 isograms in this area correlate well with the dynamic height topography compiled for this cruise by Reed and Laird (1971). These facts indicate characteristic PCO_2 signatures of about 300 ppm for the Alaskan Stream Domian and 266 ppm for the Western Subarctic Domain at this season and year.

The southern edge of 266 ppm low PCO_2 region in the Western Subarctic Domain is only tentative and conjectural. From such

limited data one cannot do more. The present PCO_2 values for October are not the same as Keeling's (1968) values because of seasonal effects and also because of probable year-to-year variations. Gordon et al. (1971) (see Chapter 3) demonstrated that subarctic Pacific Ocean surface waters from autumn 1968 to spring 1969 underwent seasonal variations in PCO_2 on the order of 60 ppm, and that this estimate is possibly minimal. Therefore it is not surprising that Keeling's data, compiled for different seasons and years, should disagree with the present results.

Global distribution chart of the sea surface PCO_2 anomaly. Most of the main features in Fig. 4.2 have been discussed in the preceding sections in terms of the seawater PCO_2 itself; but there remains the large, nearly saturated region in the Gulf of Alaska. The correspondence here between PCO_2 or PCO_2 saturation anomaly and the upper zone domains of Dodimead et al. (1963) are not so clear because of the paucity of data. There are some hints of correspondence between the PCO_2 saturation anomaly and the Alaskan Stream Domain, Central Subarctic Domain, and the Coastal Domain in parts of the area. A more detailed survey is necessary to test for this correspondence.

Marked seasonal variations in surface PCO_2 values must be considered in the construction of an ultimate set of global distribution charts. Indeed, there will probably be a set of seasonal charts,

based upon synoptic, multi-ship surveys, and not one final chart for all seasons.

CHAPTER 5

STUDIES OF PCO_2 IN THE OREGON COASTAL UPWELLING REGION

5.1 Introduction

The summer upwelling which takes place along the Oregon coast is a feature of both practical and theoretical interest. The water which arrives at the surface brings with it abundant plant nutrients and carbon dioxide, stimulating intense biological production and therefore vigorous fisheries. In addition the upwelling stimulates intense scientific curiosity. Several groups at Oregon State University have been studying the various aspects of the phenomenon (Park et al., 1962; Pattullo and Denner, 1965; Ball, 1970; Pak et al., 1970ab; Pillsbury, 1972; Mooers et al., 1972).

Coastal upwelling arises from wind-driven transport of surface water offshore. Deeper water must then rise from below to replace it. This takes place along the eastern boundaries of the oceans whenever the wind blows equatorward for a sufficient time and intensity (Smith, 1968). The upwelling waters typically come from a depth of from 50 to 200 meters and are colder and often more saline than the regional surface waters. Owing to biological respiration and decay processes at depth these upwelled waters

contain less oxygen and more carbon dioxide and plant nutrients than the regional surface waters they replace.

This chapter presents results from multi-disciplinary cruises in 1968, 1969, and 1970. It will confine itself mainly to chemical observations. Of these, observations in the carbon dioxide system will be emphasized. Until this work, measurements in the carbon dioxide system by chemical oceanographers at Oregon State University were restricted to pH, alkalinity, and total inorganic carbon dioxide. But research for this dissertation employed for the first time the continuous measurement of PCO_2, the carbon dioxide partial pressure, in the waters where upwelling occurs off the Oregon coast.

The value of measuring PCO_2 lay in the relative ease with which it could be measured accurately and continuously by existing technologies. PCO_2 measurements seemed particularly suited for studies involving the exchange of molecular CO_2 between the atmosphere and the sea. In this case, the driving force for the exchange is the gradient in PCO_2 between the atmosphere and the sea. It would seem advisable to make as direct a measurement of this gradient as possible. In contrast, the classical method for establishing the gradient had been to measure the pH and alkalinity of the sea surface waters and to calculate PCO_2. Then this was compared with an assumed atmospheric PCO_2 corresponding to the average atmospheric composition.

There are several points to be made in this chapter. The first is that the direct and continuous measurement of PCO_2 can serve as a convenient and rapid indicator of upwelling and its associated processes. A comparison will be made of the use of PCO_2 with the use of temperature, salinity, sigma-t, pH, AOU, and dissolved oxygen concentration for this purpose.

The second point to be made in this chapter stems from the fact that PCO_2 may be theoretically related to pH and AOU. But systematic errors appear to be present in the relationships as understood at the present time. The errors are small in the case of the pH-PCO_2 observed data relationship and much larger and accompanied by greater scatter in the case of the AOU-PCO_2 relation. For this reason, it is advisable to directly measure PCO_2 where this is the fundamentally significant variable for a given study.

The next points concern the use of frequently repeated vertical sections of PCO_2 and density (or sigma-t). These will be used to demonstrate two features. The first and for some purposes more profound is that the comparison of PCO_2 distributions with density distributions indicates the possible presence of a carbon trap on the continental shelf off Oregon. This is located approximately under the upwelling frontal system. It results in an important source of CO_2 to the water column from the sediments during much of the year. The second type of information which comes out of examination of

frequently repeated vertical distributions of PCO_2 is a notion of the time scales of the variations of the distributions of the chemical variables in the coastal upwelling regime, and the use of PCO_2 as an indicator variable for these time scales.

In this chapter only those features will be presented and discussed which will illustrate the above listed points. The discussion of necessity will have to resemble the much overused term, "the tip of the iceberg," wherein the part which shows is but a small fraction of the work which has been done in the total effort. The sheer bulk of data which has been accumulated during this period of study by our chemical oceanography group is far too great to present in this dissertation. It is for this reason that the writer will confine himself to making these few, rather simple points.

5.2 Results

The first cruise on which PCO_2 data were obtained took place in June, 1968, aboard R/V YAQUINA. It was conducted in collaboration with physical and biological oceanographers and aimed at a multidisciplined attack on the nature of the upwelling process and a survey of the Columbia River plume. On this cruise the PCO_2 data were surface water observations only.

The next observations were made during the summer upwelling season of 1969, again in collaboration with the physical and biological

oceanographers. By this time, capability to obtain subsurface measurements by pumping the seawater to the surface had been developed. Cruises of from ten days to three weeks were made in June, August and October.

During the following winter a very brief opportunity was available to make observations in January, 1970. In May and June of 1970, as well as in March and June of 1971, additional data were obtained. However, this dissertation will treat only data obtained from June 1968 through May 1970. Table 5.1 summarizes the cruise numbers and dates.

Table 5.1. Dates during which Oregon coastal PCO_2 data were acquired.

Cruise	Overall Cruise Dates	Individual Sections Line	Inclusive Times & Dates	Stations and Their Order of Occupation
Y6806C	23 June-3 July 1968	1DB	1930, 23-1800, 24 June	1, 3, 5, 7, 10, 15, 20, 25, 30, 40
		2DB	0400 -2300, 28 June	1, 3, 5, 7, 10, 15, 20, 25, 30, 40
		3DB	0100 -2630, 2 July	1, 3, 5, 7, 10, 15, 20, 25, 30, 40
Y6906C (COOC-4)	18 June-3 July 1969	DB*	2020, 18-0400, 20 June	5, 10, 15, 25, 40
		NH	0700, 27-0700, 28 June	3, 5, 10, 15, 25, 35, 45
Y6908A (COOC-6)	31 July-12 August 1969	1DB	0700 -1600, 31 July	5, 15, 30
		2DB	0500 -1300, 5 August	20, 10, 5, 3
		3DB	0430 -1900, 7 August	10, 5, 1, 3, 15, 25, 30
		4DB	0830 -1600, 12 August	20, 15, 10, 5, 1
		1NH	1600 -2100, 5 August	3, 5, 15
		2NH	1900, 8-1800, 9 August	25, 10, 3, 5, 15, 35, 45
Y6910E (COOC-10)	22-31 October 1969	DB	0630, 28-1000, 29 October	45, 35, 25, 3, 5, 10, 15
		NH	1430, 22-2130, 23 October	3, 5, 15, 10, 25, 35, 45
Y7001A	2-10 January 1970	DB	0730 -1200, 9 January	25, 10, 5, 3
Y7005A	4-10 May 1970	1DB	1400, 4-0400, 5 May	1, 3, 5, 7, 10, 15, 25
		2DB	0330 -1500, 8 May	25, 15, 10, 7, 5, 3, 1
		NH	0600, 5-0700, 6 May	25, 10, 5, 1, 3, 7, 15, 35, 45

*Surface PCO_2 data only.

The cruise tracks for these cruises are shown in Fig. 5.1. Cruise tracks are not shown for Y7001A and Y7005A because only data obtained on the Depoe Bay and Newport hydrographic lines will

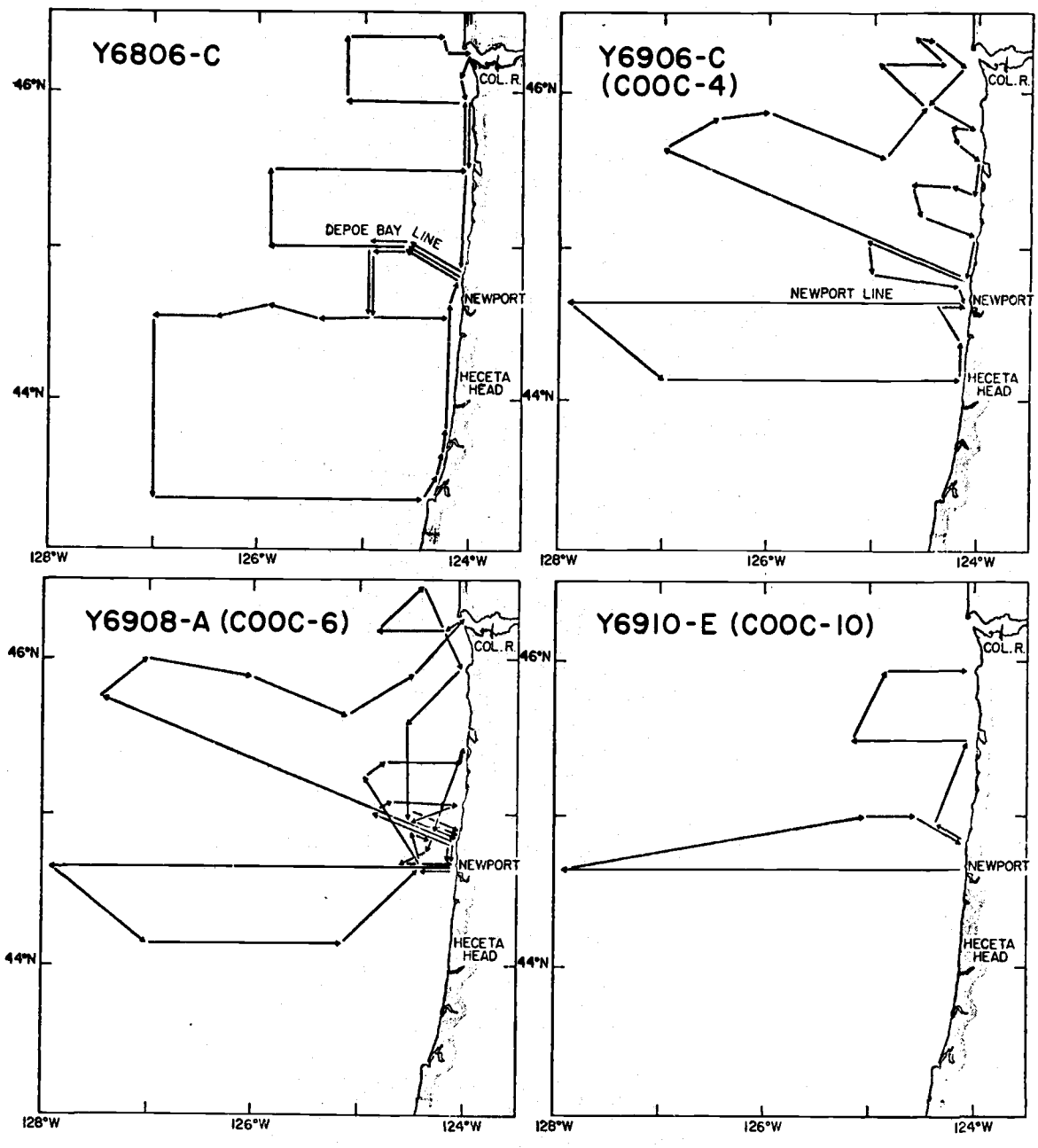

Fig. 5.1. Tracks of the cruises on which upwelling region data were obtained. For cruises Y7001A and Y7005A only the data obtained on the Newport and Depoe Bay hydrographic lines will be presented in this work.

be treated in this dissertation. Therefore, the remaining portions of the cruise tracks are irrelevant.

Complete hydrographic and chemical data listings for these cruises have been published by Barstow et al. (1969) and Wyatt et al. (1970, 1971). A discussion of the optical properties observed during Y6806C has been published by Pak (1970ab). Biological as well as some of the hydrographic and chemical data for the COOC series of cruises in 1969 have been discussed in the M. S. thesis of Schonzeit (1973). None of these publications treated the PCO_2 data obtained on the cruises.

The PCO_2 data for 1968 and 1969 have been submitted to the National Oceanographic Data Center (NODC). PCO_2 data for the years 1970 and 1971 will also be sent to NODC shortly after publication of this dissertation.

A brief overview of the regional surface hydrography and dissolved oxygen and PCO_2 distributions will now be presented. This will be followed by a comparison of PCO_2 with pH and AOU observations. Then, vertical sections of sigma-t and PCO_2 on the Depoe Bay and Newport hydrographic lines will be examined.

5.2.1 Regional Surface Hydrography and Dissolved Gas Distributions. The surface temperature, salinity, dissolved oxygen, and PCO_2 distributions for cruises Y6806C, COOC-4, -6, and -10 are shown in

Figs. 5.2 through 5.5. Note that the Depoe Bay and Newport lines were usually occupied several times during each cruise. To construct Figs. 5.2 through 5.4 the one or two sets of data from these lines intermediate in time between the remaining data to the north and south were used. Thus, if the Depoe Bay line were run once at the very beginning and at the very end of a cruise, as well as once more during a north-south sweep from the Columbia River mouth to Heceta Head for the large picture, then the data from the intermediate occupation of the Depoe Bay line would have been used for construction of the figure for that cruise. Because of the very wide spacing of the lines of the cruise tracks, particularly at the greater distances from shore, many of the contours can only be regarded as indicating general patterns. However, close inshore where the measurements are more detailed and where the upwelling is manifest, several interesting features do become apparent.

The first such interesting feature is seen in Fig. 5.2 which shows the data obtained on cruise Y6806C. Although the temperature and salinity indicate a rather smooth and continuous longshore hydrography, the non-conservative variables, oxygen and carbon dioxide, show a much more inhomogeneous longshore distribution. The inhomogeneous or "patchy" features showed characteristic dimensions of as little as 10-20 kilometers. Contouring at smaller intervals of temperature and salinity would show more inhomogeneity than is

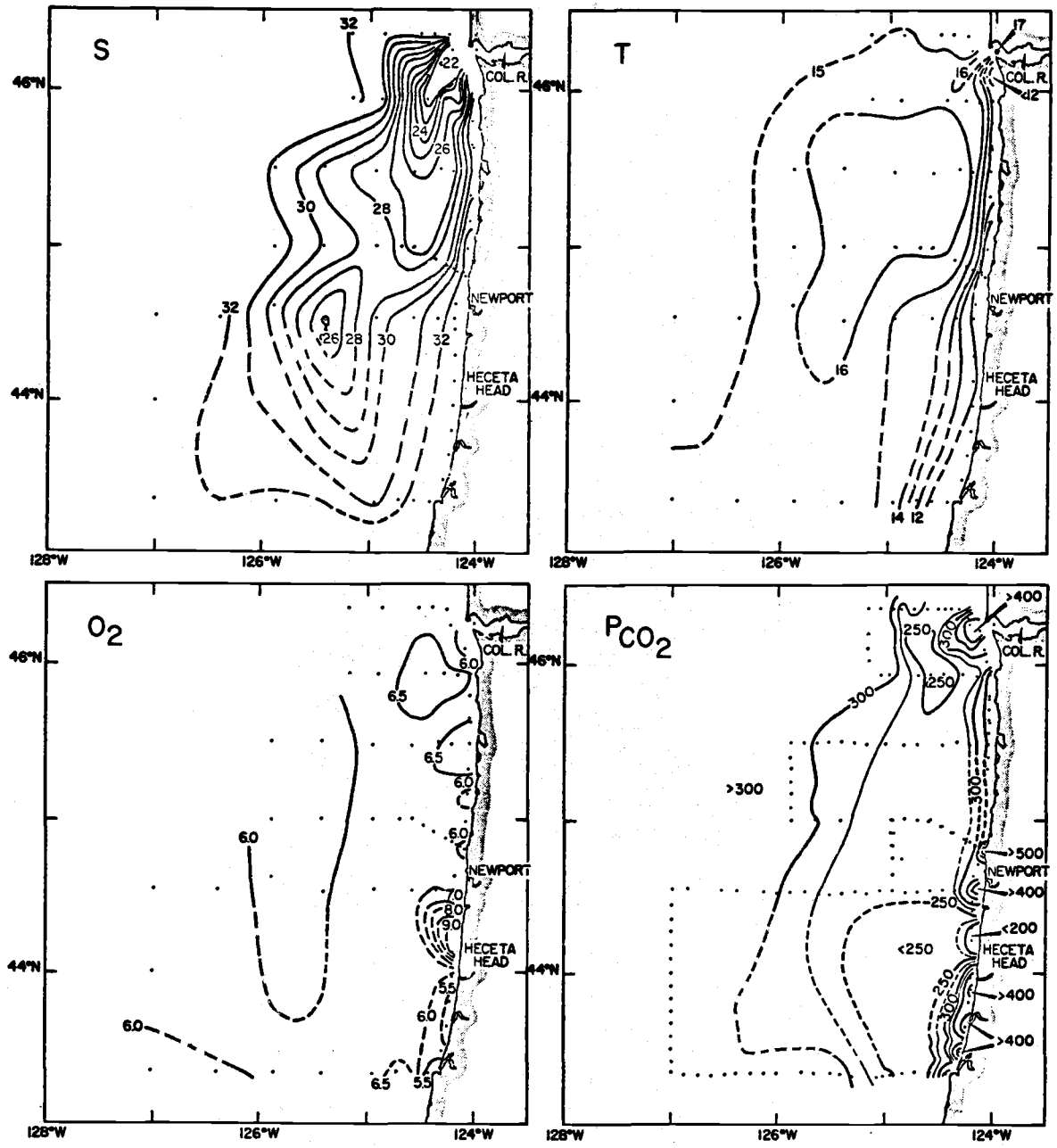

Fig. 5.2. Horizontal distributions of temperature, salinity, dissolved oxygen, and PCO_2 in the surface waters off northern Oregon, 23 June to 3 July 1968. Temperature is given in °C; the contour interval is 1°C. Salinity is in ‰; the contour interval is 1‰. Dissolved oxygen concentration is in ml/l; the contour interval is 0.5 ml/l. PCO_2 is in ppm-atm and the contour interval varies. Between 200 and 300 ppm it is 25 ppm. For PCO_2 greater than 300 ppm it is 50 ppm. Contours indicated by dashed lines are uncertain because of insufficient sampling detail.

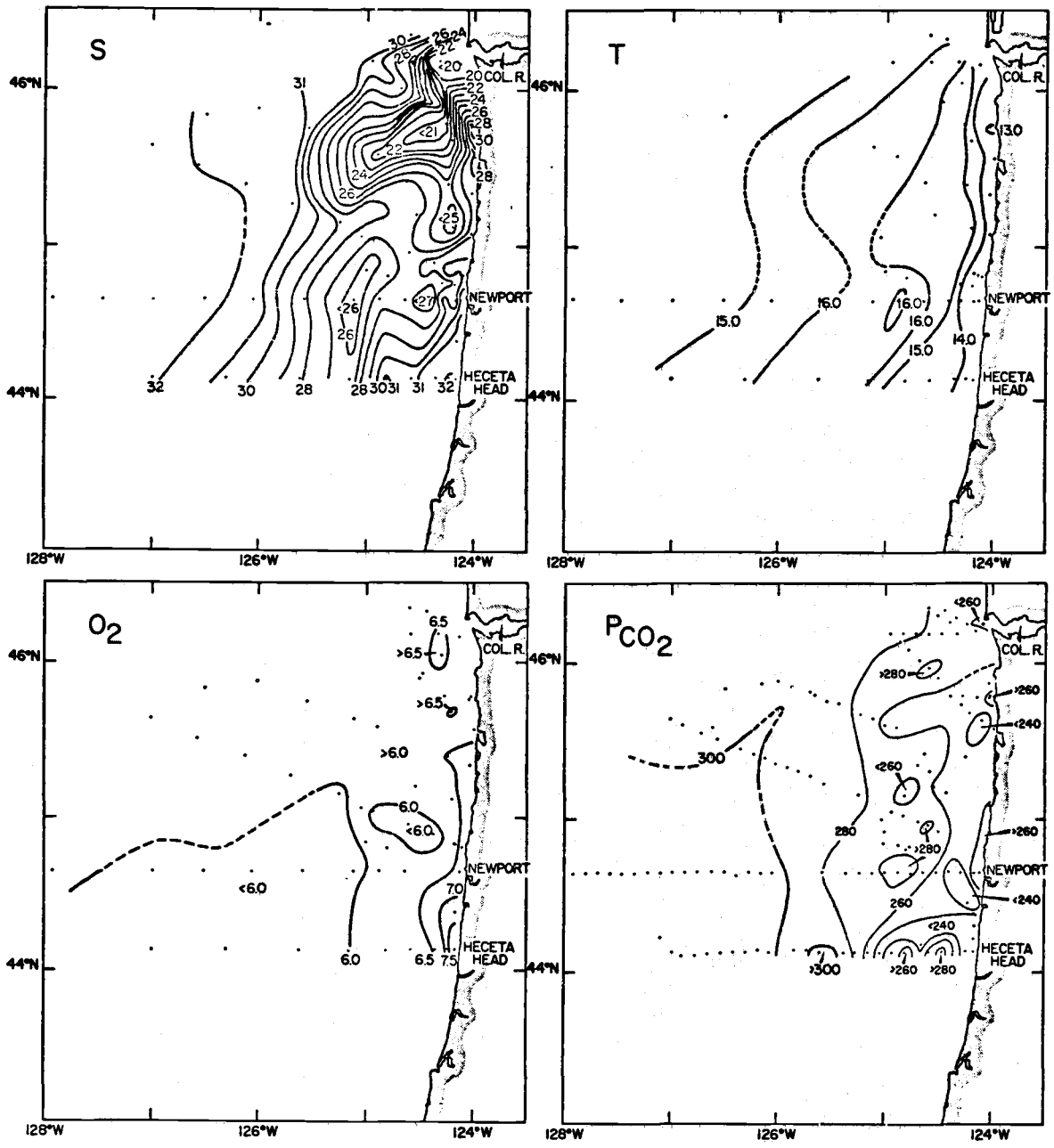

Fig. 5.3. Horizontal distributions of temperature, salinity, dissolved oxygen, and PCO_2 in the surface waters off northern Oregon, 18 June to 3 July 1969. The units and contours are as given in Fig. 5.2 with the exception of PCO_2. In this case the contour interval is 20 ppm.

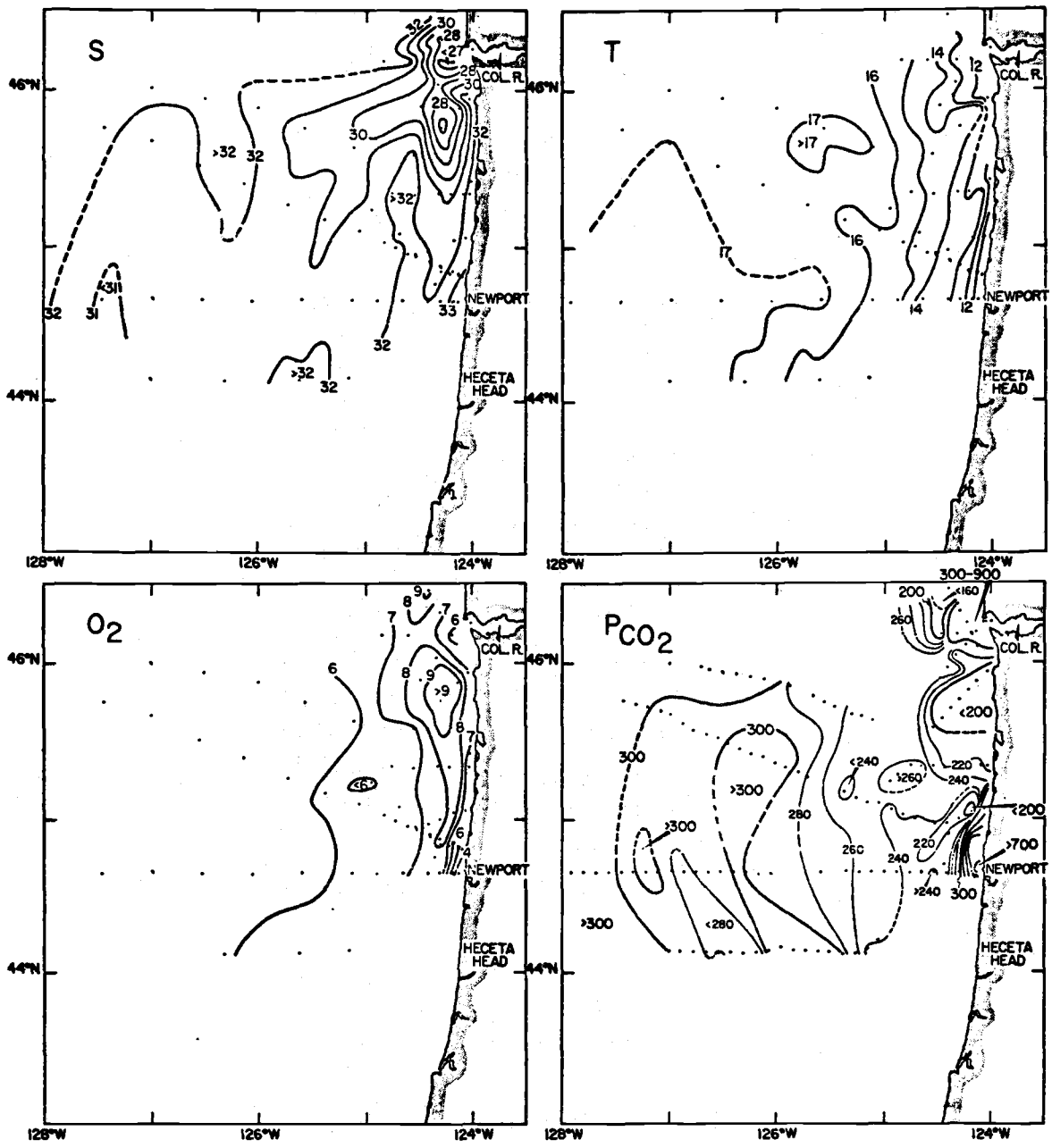

Fig. 5.4. Horizontal distributions of temperature, salinity, dissolved oxygen, and PCO_2 in the surface waters of northern Oregon, 31 July to 12 August 1969. The units and contour intervals are as given for Fig. 5.2 with the exceptions of dissolved oxygen and PCO_2. The oxygen contour interval is 1 ml/l. Between 200 and 300 ppm the PCO_2 contour interval is 20 ppm. Above 300 ppm it is 100 ppm.

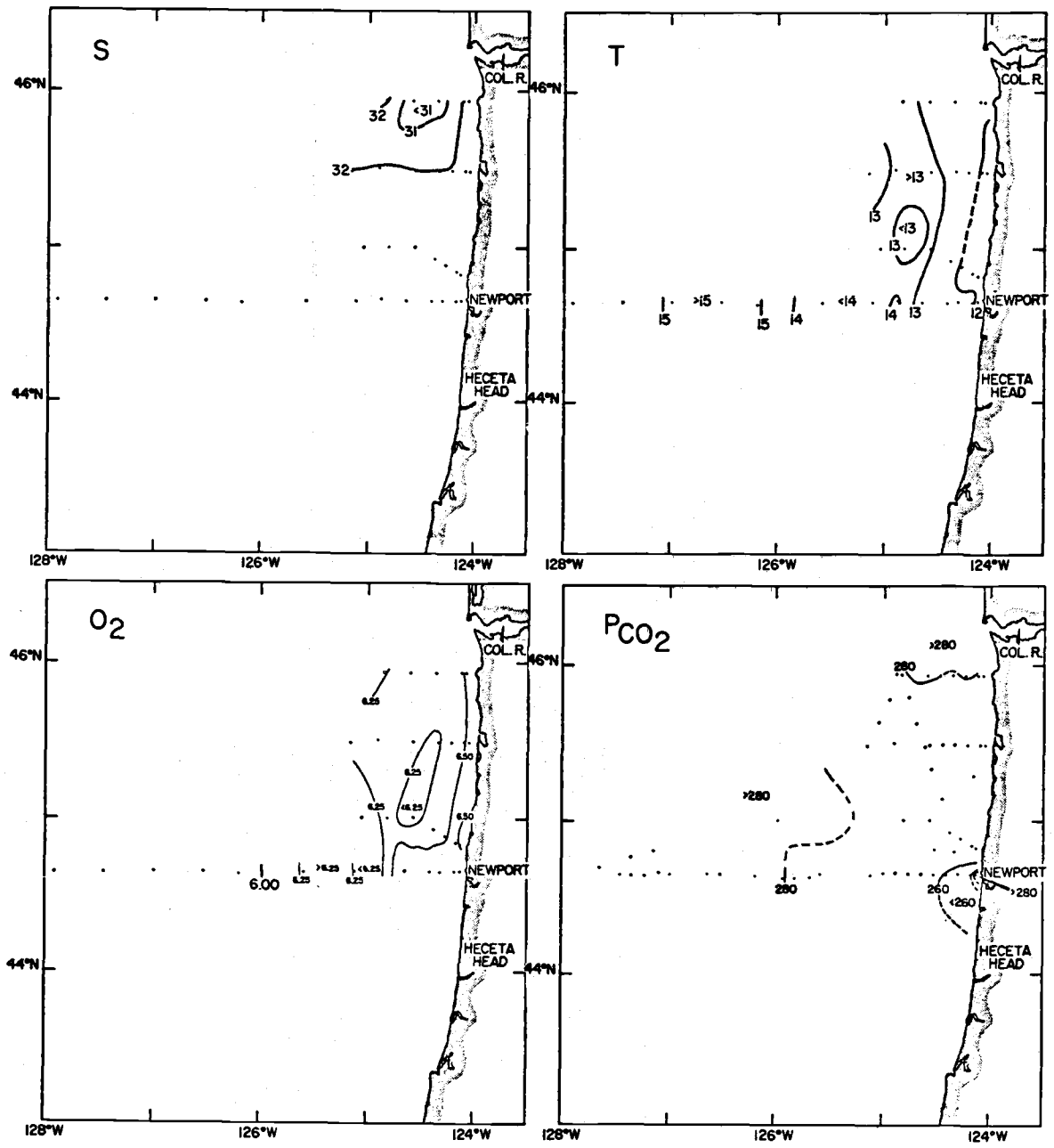

Fig. 5.5. Horizontal distributions of temperature, salinity, dissolved oxygen, and PCO_2 in the surface waters off northern Oregon, 22-31 October 1969. The units and contouring are as given for Fig. 5.2 except that the contour interval for dissolved oxygen is 0.25 ml/l here and the PCO_2 contour interval is 20 ppm.

evident in these figures but the biologically involved constitutents would probably still be more "patchy."

High PCO_2 correlated with low dissolved oxygen concentrations. The highest PCO_2 was 530 ppm found just off Depoe Bay. The lowest PCO_2 and highest dissolved oxygen concentration observed lay close inshore, just north of Heceta Head. There, PCO_2 was only 190 ppm. A high PCO_2 of 475 ppm was found five kilometers off the mouth of the Columbia River.

Figure 5.3 shows the results from the COOC-4 cruise in June of the following year. At this time the salinity and temperature distributions were more complicated than in the previous year, but the oxygen and carbon dioxide distributions were actually somewhat simpler. The very small scale longshore variations were absent. Again, there was a low PCO_2, high dissolved oxygen region located just north of Heceta Head. A high PCO_2 of 355 ppm was found just at the Columbia River mouth, almost at the entrance jetty.

The paucity of data in the region offshore and to the north and offshore of Heceta Head precludes a detailed contouring of oxygen and carbon dioxide there. The oxygen data are particularly sparse and show relatively less systematic variation than the PCO_2. The lack of correlation between oxygen distribution and the other three variables is thus to a certain extent probably an artifact. During the cruise the carbon dioxide was undersaturated with respect to the

atmosphere throughout the region.

In both this cruise and the one in August 1969 for which the surface data are shown in Fig. 5.4, the Columbia River plume had a distinct bifurcated shape. In both cruises there was one lobe of the plume located close inshore. There appeared to be a closer coherence between the dissolved oxygen distribution and the salinity than between PCO_2 and salinity. The PCO_2 did not seem to correlate with the salinity distribution to any great extent in this region.

During the August cruise in the inshore region around the Newport and Depoe Bay lines, there was an even stronger than usual inverse correlation between dissolved oxygen and carbon dioxide. Close inshore on the Newport line, the dissolved oxygen had fallen to values lower than 4.0 ml/l while PCO_2's of 730 ppm were observed. Very high PCO_2 values were encountered in and near the Columbia River mouth. Twenty kilometers off the jetty a high of 935 ppm was found.

By October 1969, as shown in Fig. 5.5, the situation had simplified considerably. All four distributions were much more uniform and the dissolved gases were much closer to equilibrium with respect to the atmosphere. Even so, in the nearshore areas around Newport, Oregon, as well as near the Columbia River mouth, carbon dioxide was appreciably undersaturated with respect to the atmosphere.

5.2.2 The observed relationship between pH and PCO_2. In Fig. 5.6 are plotted pH versus PCO_2 data for cruise Y6806C in June, 1968. It may be seen that the two variables appear to have a functional relationship with each other and this, or course, is theoretically predictable (see Eq. 1.18). The indicated curves have been calculated from Eq. 1.18 and will be discussed later.

Several other features should be indicated at this time. First, saturation of carbon dioxide with respect to the atmosphere would have dictated a PCO_2 of approximately 310 ppm. Note that, in general, the surface waters were not in equilibrium with the atmosphere; PCO_2 values ranged as high as 550 ppm and as low as 150 ppm. The highest PCO_2, lowest pH values occurred around station Depoe Bay 1, that is, two kilometers offshore of Depoe Bay, Oregon. The lowest PCO_2 values occurred at pH's as high as approximately 8.5. There is a dense clustering of points around pH 8.2 to 8.3 and PCO_2 around 250-270 ppm. This cluster of points was observed in the open-sea water a hundred or more kilometers offshore.

The points in this diagram are rather highly scattered and undoubtedly reflect the rather poor precision and accuracy obtained with the method for pH on this cruise. The samples were taken as discrete samples from the equilibrator for later analysis. An old and possibly malfunctioning pH meter was employed.

Another interesting feature to note is the location of the

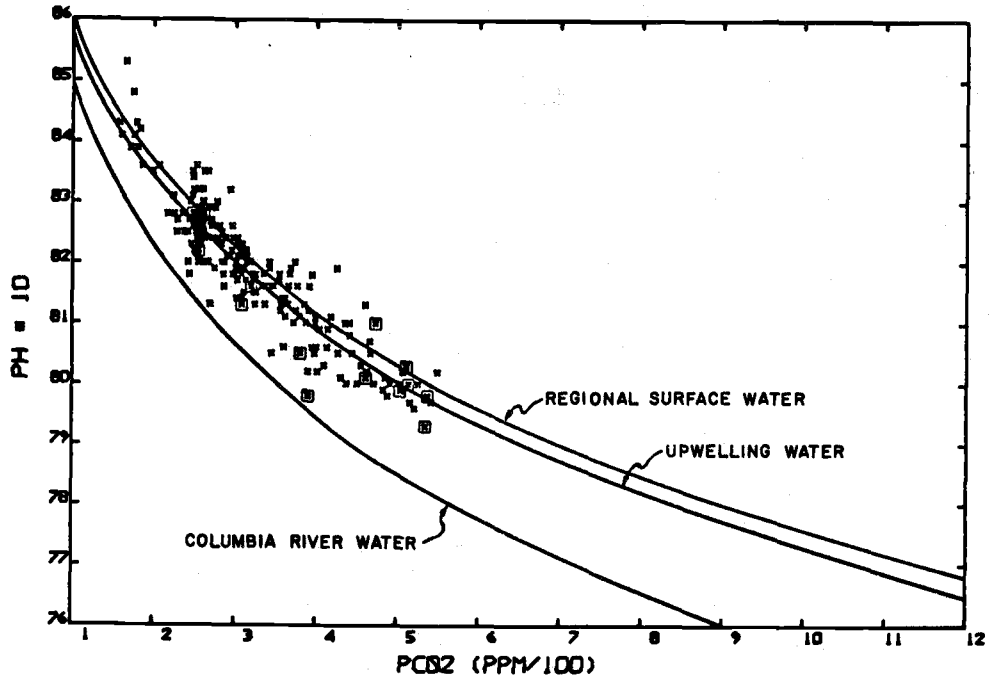

Fig. 5.6. The relation of measured pH to measured PCO_2, 23 June to 3 July 1968. The calculated curves are discussed in Sect. 5.3.2.

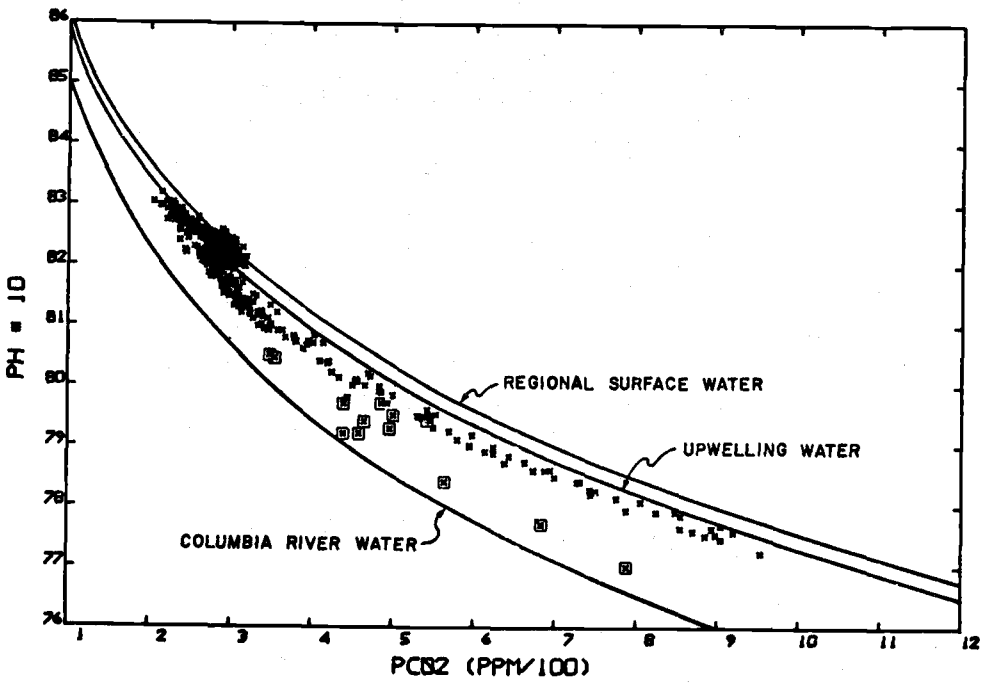

Fig. 5.7. The relation of measured pH to measured PCO_2, 18 June to 3 July 1969. cf. Fig. 5.4. The calculated curves are discussed in Sect. 5.3.2.

Columbia River points. These all lie some distance below, that is to say, at a lower pH for a given PCO_2, than the trend of most of the points. This also will be discussed in a later section.

The accuracy, or at least precision, of the pH measurements had greatly improved in the following year as evidenced in Fig. 5.7. These data were taken in June of 1969, and pH's were measured with the electrodes placed directly within the equilibrator and with a new pH meter (see Gordon and Park, 1972d, p. 32-35). Again, there occurred a wide range of PCO_2 and pH values, in this case because of the pumping from waters as deep as 55 meters. The data are more conherent than for the previous years.

Much lower pH's were found, down to pH 7.7, with correspondingly high PCO_2's, up to 950 ppm. These values reflect more accurately the source of upwelling water than would the purely surface data of Fig. 5.6. In 1969 such low PCO_2 values were not observed; only as low as 200 ppm. pH's were lower also, only 8.3, maximum. We did, however, see a similar clustering of points around 300 ppm and pH 8.2 to 8.25. The pH's in the 1969 dense cluster were somewhat lower than the previous year, by 0.05 units; however, one cannot be certain whether this resulted from the change in the method of measuring pH or was real.

In August, a month and a half later in the upwelling season, the picture shown in Fig. 5.8 was obtained. The highest pH's were

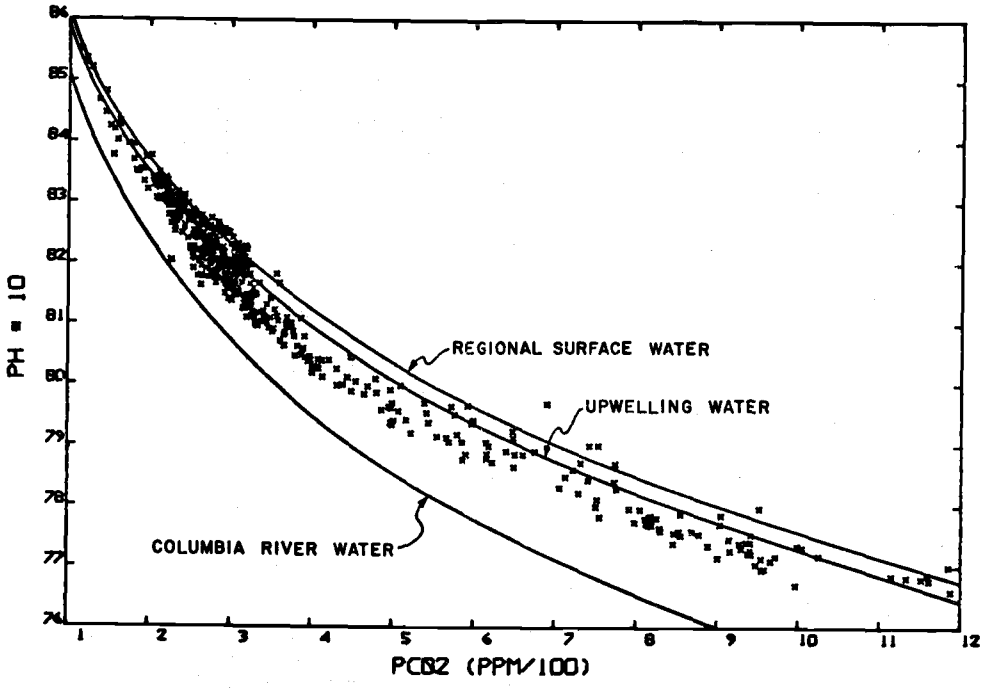

Fig. 5.8. The relation of measured pH to measured PCO_2, 31 July to 12 August 1969. cf. Fig. 5.4. The calculated curves are discussed in Sect. 5.3.2.

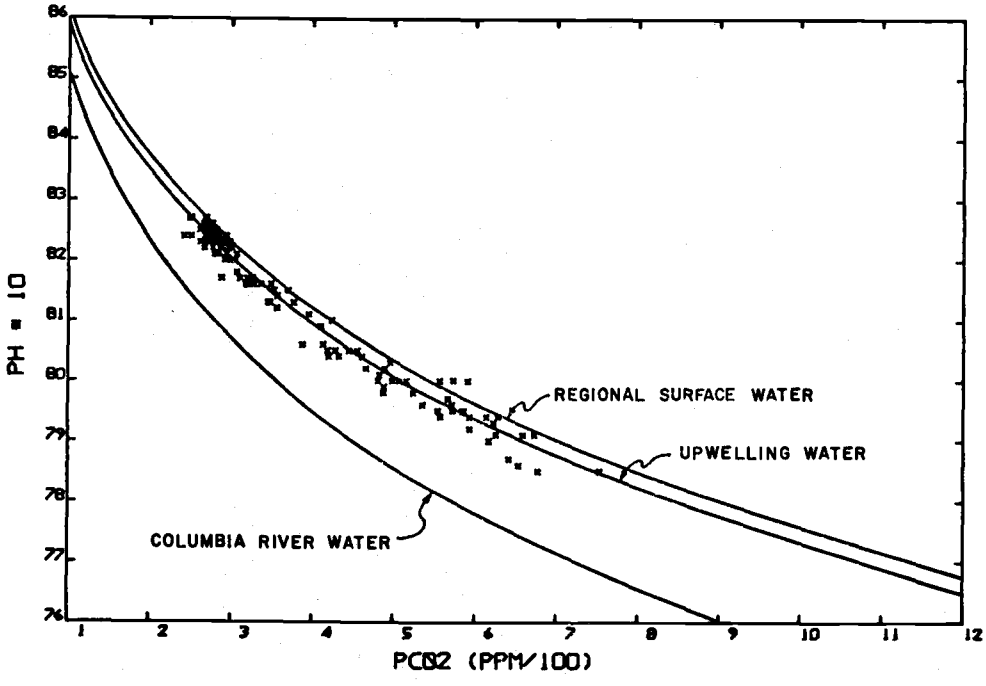

Fig. 5.9. The relation of measured pH to measured PCO_2, 22-31 October 1969. cf. Fig. 5.4. The calculated curves are discussed in Sect. 5.3.2.

up to 8.55 at very low PCO_2's of 115 ppm. The highest PCO_2's recorded were 1200 ppm at the very low pH's of 7.65. The cluster of most of the values observed lies between pH 8.15 and 8.3 corresponding to PCO_2's of 310 down to 200 ppm, respectively.

The October cruise displayed a much narrower range of both PCO_2 and pH values than the previous cruises (Fig. 5.9). The surface pH values were much more tightly clustered between pH 8.2 and 8.3 and PCO_2 250 to 300 ppm. These also represented the approximate maximum pH's and minimum PCO_2's. The minimum pH observed in all of the deep waters was but 7.85 corresponding to a maximum PCO_2 of 750 ppm.

5.2.3 The observed relationships between AOU and PCO_2 changes. In Figs. 5.10-5.13 the relation of AOU to PCO_2 changes in 1968 and 1969 are examined.

As in the case of the pH/PCO_2 relationship there may be derived a theoretical relationship between AOU changes and PCO_2 changes. This and the derived curves shown in these figures will be discussed in the Discussion section of this chapter. Figure 5.10 displays this relationship for the June, 1968, cruise for the surface waters only. AOU was calculated as outlined in Sect. 2.8. Large negative AOU's occurred (that is, supersaturation of the surface waters with respect to the atmosphere) amounting to as much as

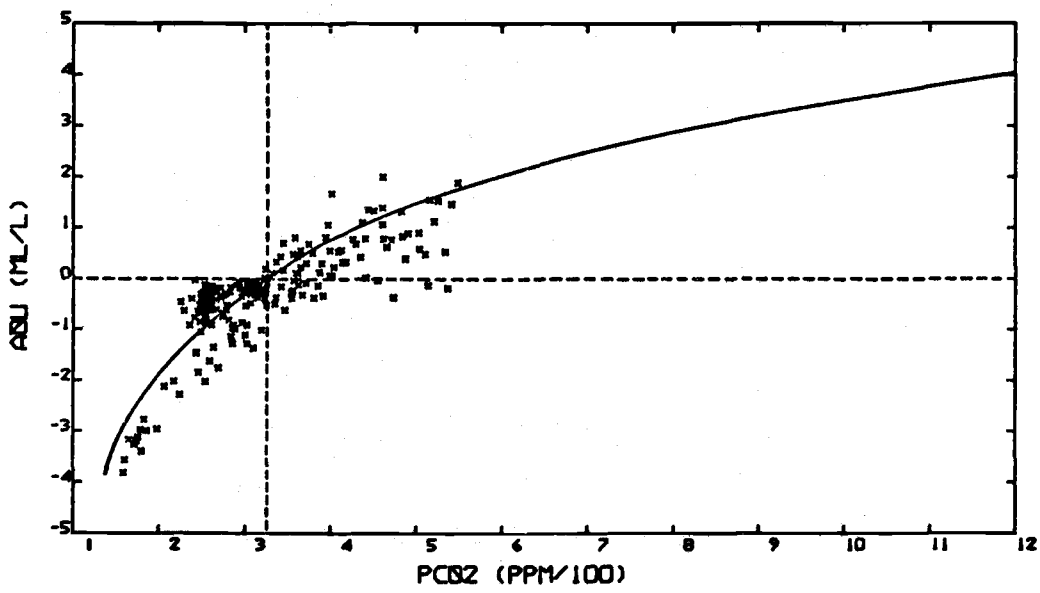

Fig. 5.10. The relation of AOU to PCO_2, 23 June to 3 July 1968. Indicated super- and undersaturations are with respect to the atmosphere. The calculated curve is discussed in Sect. 5.3.3.

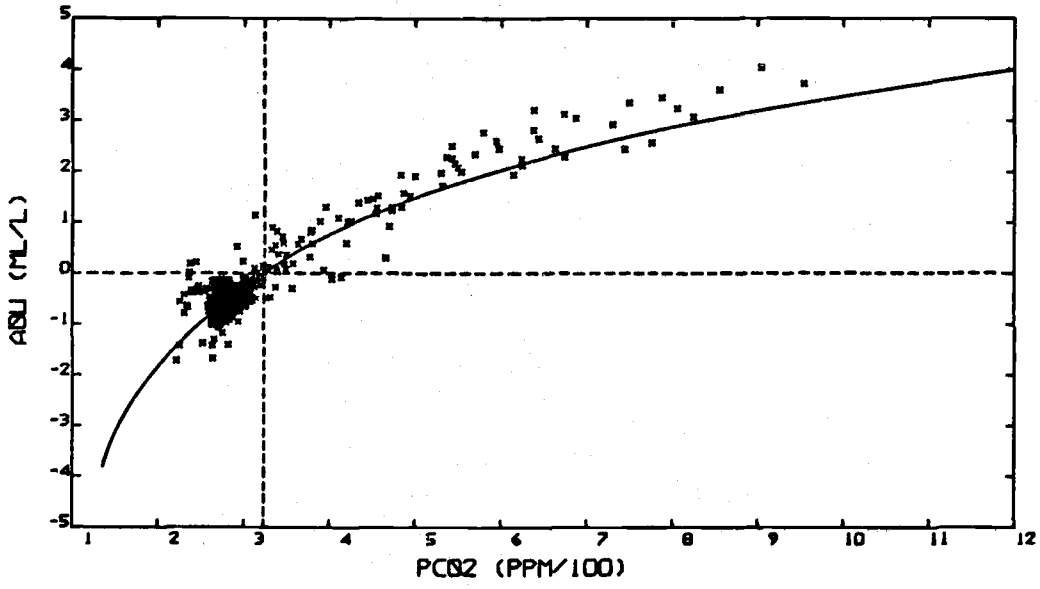

Fig. 5.11. The relation of AOU to PCO_2, 18 June to 3 July 1969. The calculated curve is discussed in Sect. 5.3.3.

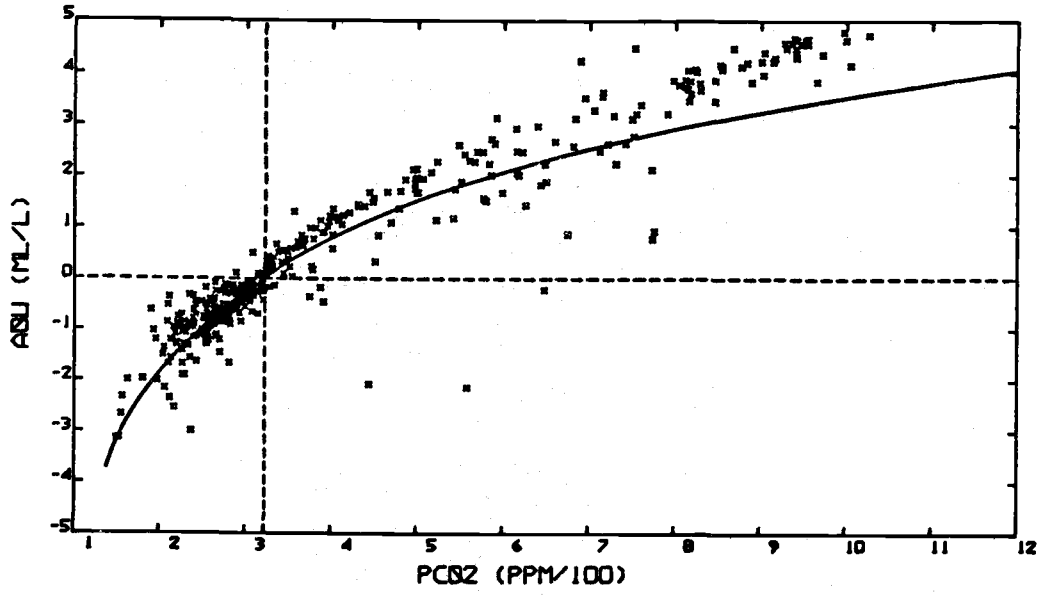

Fig. 5.12. The relation of AOU to PCO_2, 31 July to 12 August 1969. The calculated curve is discussed in Sect. 5.3.3.

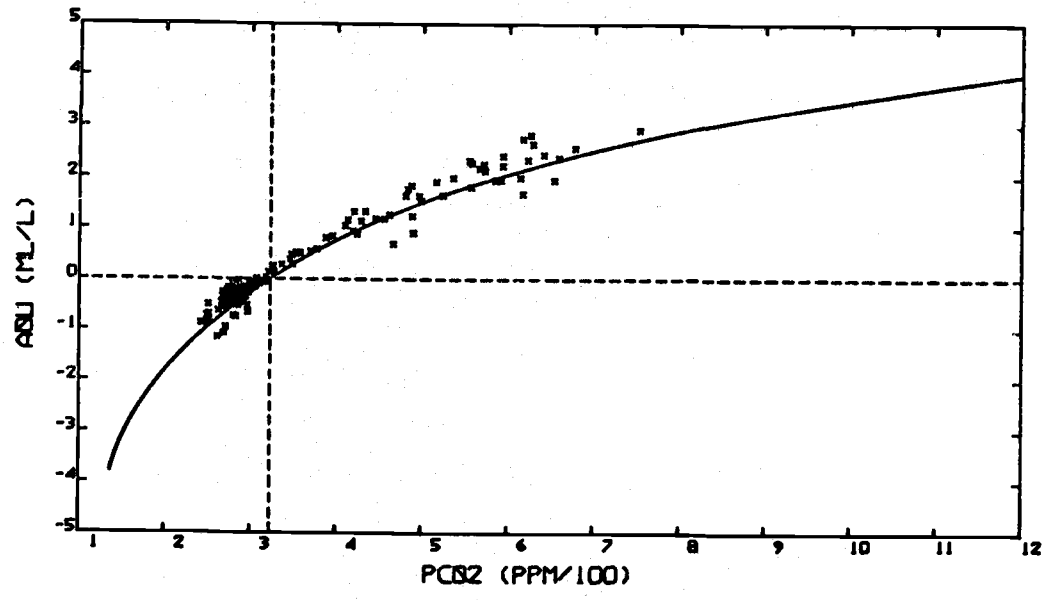

Fig. 5.13. The relation of AOU to PCO_2, 22-31 October 1969. The calculated curve is discussed in Sect. 5.3.3.

-4 ml/l, corresponding to PCO_2's of 150 ppm. At the other extreme were found AOU's of +2 ml/l corresponding to PCO_2's of somewhat more than 500 ppm and as in the case of the PCO_2 to pH relationships there was a dense clustering of a large number of the data points, in this case in the region of AOU = -0.5 and PCO_2 = 250 to 300 ppm.

Figure 5.11 displays the results for the June, 1969, cruise, and in this case, the lowest AOU's observed were but -1.8 ml/l occurring at PCO_2's of 225 ppm. However, we observed because of sampling to depths of 55 meters, rather high AOU's, amounting to +4 ml/l. These corresponded to the PCO_2 points having values in excess of 900 ppm.

By August of 1969 we observed the pattern displayed in Fig. 5.12. The very low PCO_2 values, down to 130 ppm, had corresponding AOU's as low as -4.5 ml/l. The high PCO_2's, more than 1000 ppm, corresponded to AOU's of almost +5 ml/l.

By October the picture (Fig. 5.13) became, as in all previous distributions shown for the October cruise, a much simpler one. The lowest AOU's observed were only -1 ml/l at the PCO_2 values of 250 ppm and the highest AOU's observed, once more by virtue of the deeper sampling, amounted to +3 ml/l corresponding to a maximum PCO_2 of 750 ppm.

5.2.4 Vertical sections of density and PCO_2 on the Depoe Bay and Newport hydrographic lines. There now follows a presentation of the results of 16 occupations of the Depoe Bay and Newport hydrographic lines from June 1968 through May 1970. For the locations of these lines, see Fig. 5.1. Only a few of the sections will be discussed in detail. For the remaining sections a small number of the most important features will be noted in order to illustrate one or more points.

In the case of the first three sections, Figs. 5.14, 5.15, and 5.16, the PCO_2 data have been calculated from measurements of pH and alkalinity upon discrete samples drawn from the PCO_2 equilibrator. The PCO_2 data displayed in the remaining figures resulted from direct observation upon water pumped from depth.

Figure 5.14 portrays the vertical sections of sigma-t and PCO_2 observed on the Depoe Bay hydrographic line during 23-24 June 1968. This section will be discussed in a rather detailed fashion in contrast to more superficial treatment of the remaining sections. The bottom of the seasonal pycnocline denoted by sigma-t 25.0 lay at about 30 meters, 25 kilometers offshore. Inshore of that distance it began to rise, breaking the surface abruptly, eight kilometers offshore. If we denote the top of the permanent pycnocline by sigma-t 25.5, in this case it seemed to occur at about 50 meters depth, at 45 kilometers offshore. Inshore of this it inclined upward, merging with the bottom of the seasonal pycnocline at 30 meters, 28 kilometers offshore and

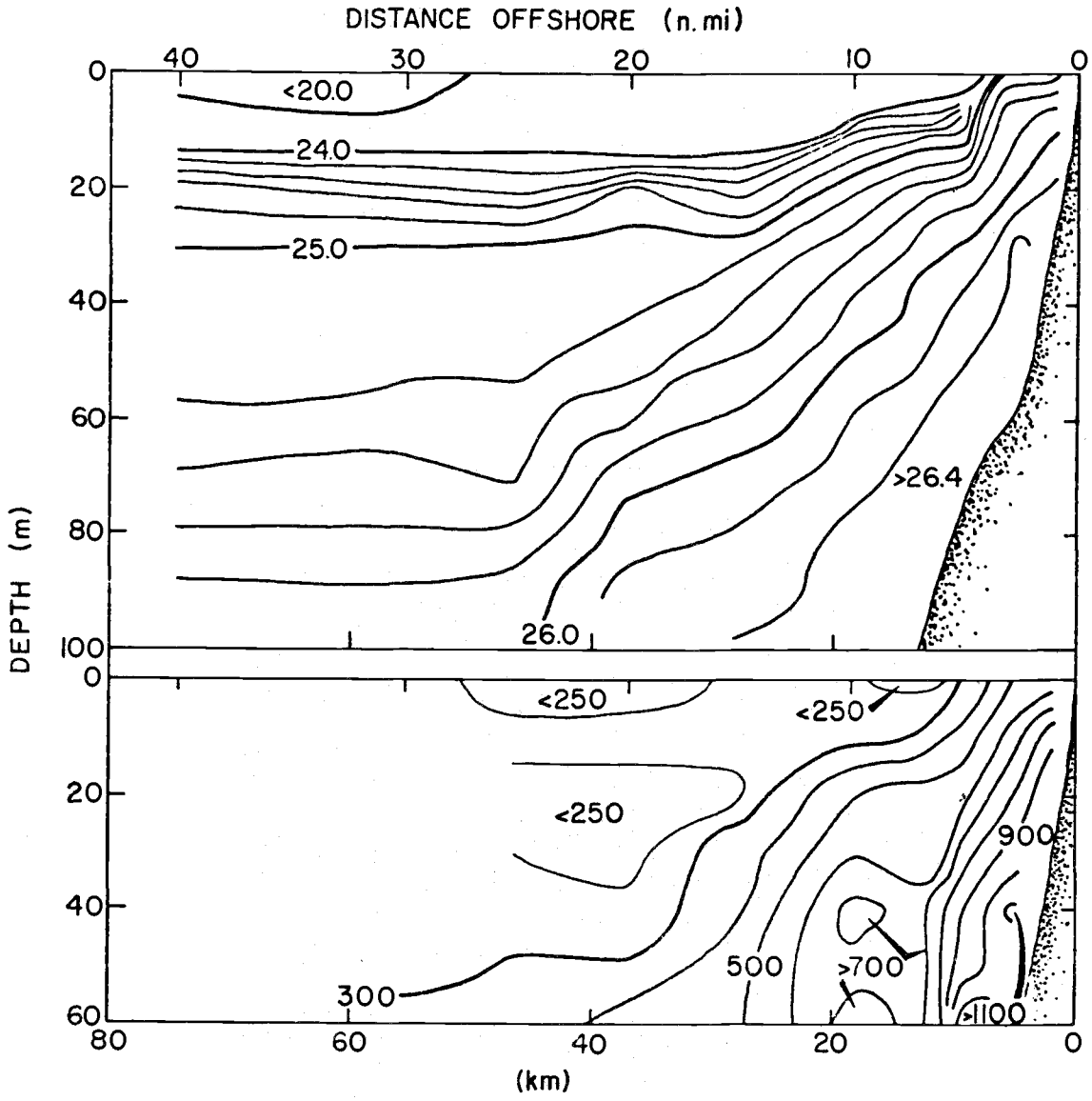

Fig. 5.14. Vertical distribution of density and PCO_2 on the Depoe Bay hydrographic line, 23-24 June 1968. Distance from the coast is plotted on the abscissa. PCO_2 was calculated from pH and alkalinity. The contour interval for sigma-t is 0.2 for sigma-t greater than 24; 4.0 below that density. The contour interval for PCO_2 is 100 ppm for PCO_2 greater than 300 ppm; 50 ppm below that.

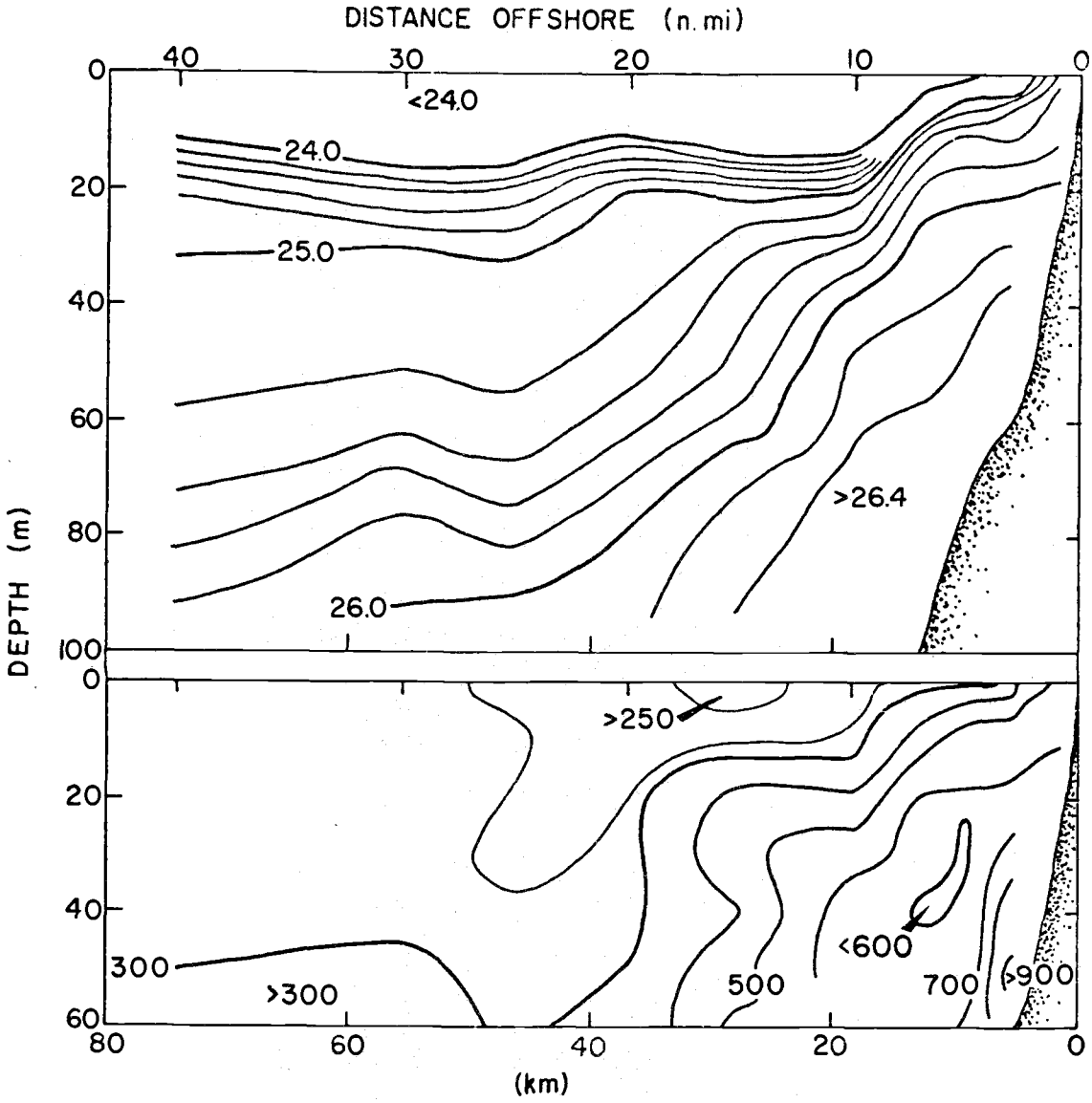

Fig. 5.15. Vertical distribution of density and PCO_2 on the Depoe Bay hydrographic line, 28 June 1968. cf. Fig. 5.14.

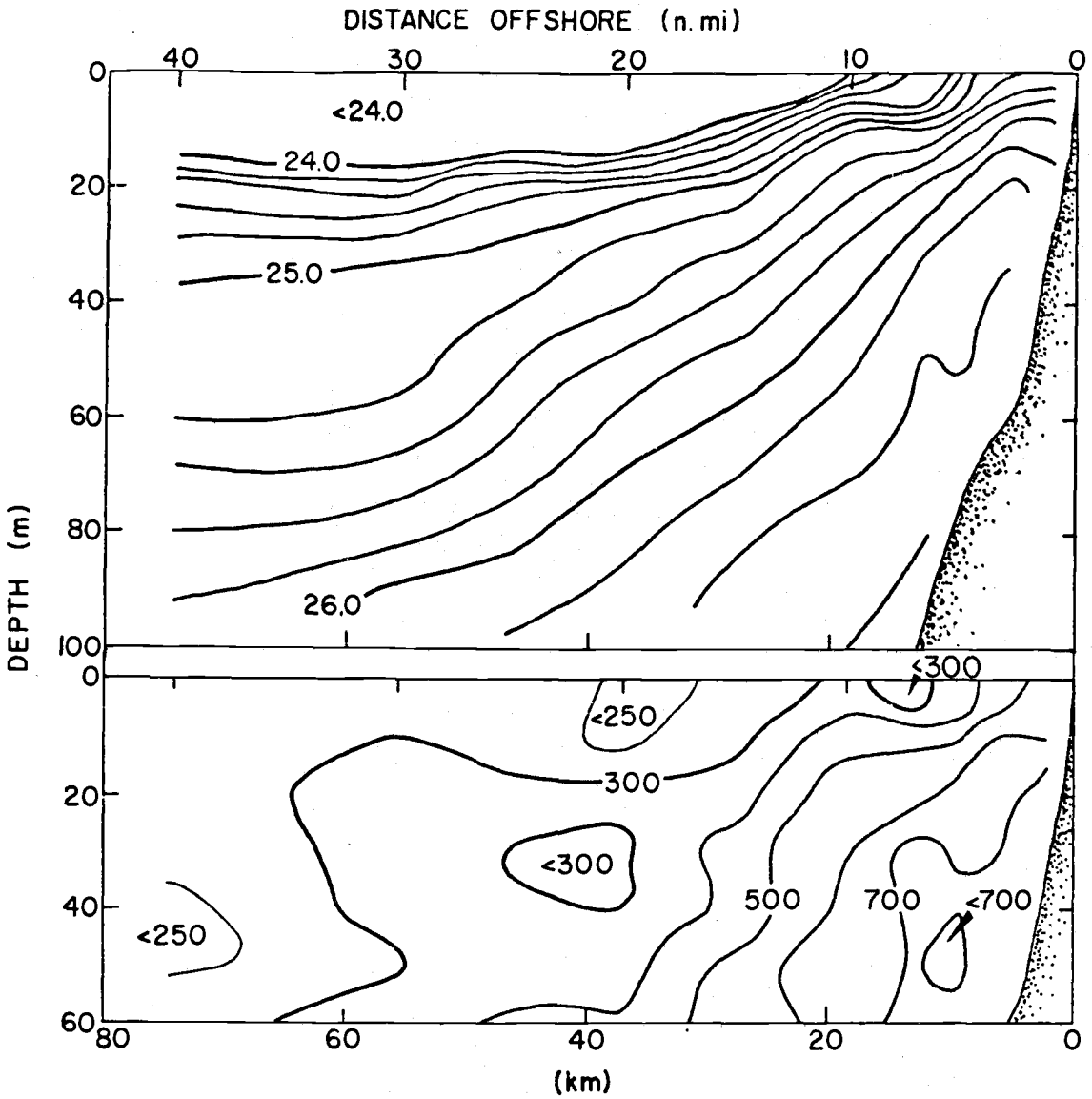

Fig. 5.16. Vertical distribution of density and PCO_2 on the Depoe Bay hydrographic line, 2 July 1968. cf. Fig. 5.14.

surfaced in the front seven kilometers offshore.

The lowest PCO_2 observed was 200 ppm at the surface four kilometers offshore of the front; the latter lay between six and nine kilometers offshore and essentially represented the surfacing of the seasonal pycnocline. This was characterized by the 24-25.0 sigma-t surfaces. A local surface low of 230 ppm PCO_2 was observed 36 kilometers offshore. Between these two lows the surface PCO_2 reached 265 ppm, 19 kilometers offshore.

The highest PCO_2 observed, 1180 ppm, was at 60 meters depth (20 meters off the bottom), nine kilometers offshore. The corresponding sigma-t was 26.6; this was also the highest density observed in this section. The highest surface PCO_2 observed was 530 ppm, two kilometers offshore.

Thirty-seven kilometers offshore at the bottom of the seasonal pycnocline denoted by the 25.0 sigma-t surface there was a local low in PCO_2. The value was 230 ppm, almost as low as the lowest surface value observed. Local high PCO_2 values of approximately 730 ppm occurred at 40 and 60 meters depth, 19 kilometers offshore. Another local high PCO_2 occurred at 40 meters, six kilometers offshore.

The isopycnals and PCO_2 isograms were roughly parallel in the section between 10 and 25 kilometers offshore below 20 meters. The 26.2 sigma-t surface, approximately the bottom of the permanent

pycnocline, lay roughly parallel to the 700 and 900 ppm contours inshore of ten kilometers as all of these contours rose to the surface.

Figure 5.15 shows the picture four days later. The density structure remained generally the same as before. However, the lowest surface sigma-t water of 18.1 had moved out of the section and the least dense surface water now present was 20.0. The surface PCO_2 pattern had also moved offshore but retained approximately the same maximum and minimum values. The maximum PCO_2 observed in the deep waters of the section had dropped from 1180 ppm to 910 ppm in nearshore near-bottom locations. The maximum density observed in the inshore surface waters at this time was slightly higher than previously, 25.5 compared to 25.36. The overall PCO_2-sigma-t coherence seems to be somewhat diminished compared to the last section.

Figure 5.16 shows the results obtained four days later on the same section. There was the same general density structure but small details had changed. There seemed to be a continued offshore movement of low density water. The front had moved from eight kilometers to 12 kilometers offshore. The maximum surface sigma-t observed at two kilometers offshore had dropped from 25.5 to 25.1.

There was almost no water of PCO_2 less than 250 ppm left. There was an increase, which was probably significant, in the maximum surface PCO_2, beginning with 530 ppm on the first section, going

to 538 ppm on the second section, and 453 ppm on the third section at the two kilometer-offshore station. The maximum, near-bottom, nearshore PCO_2 had fallen to 770 ppm from the 910 ppm four days earlier.

There seemed to be even less coherence between sigma-t and PCO_2 in the overall section. One interesting, small feature is that there seemed to be some evidence of turbulence, or an eddy forming, 14 kilometers offshore in the depth zone of 30-50 meters.

The next pair of sigma-t and PCO_2 sections (Fig. 5.17) portrays the distributions observed on the Newport hydrographic line on the 27th and 29th of June, 1969 (cf. Fig. 5.1). In the region more than 30 kilometers offshore, both PCO_2 and the density distributions roughly resembled those previously shown for the Depoe Bay hydrographic line in June of 1968. However, inshore of 35 kilometers it is immediately apparent that there was less upward sloping of the isopycnals towards shore. The PCO_2 distribution was somewhat smoother than in the previous figures. This possibly resulted from the fact that, beginning with 1969 and this data, the PCO_2 was directly measured by pumping subsurface water to the laboratory aboard ship.

Unfortunately, in this case data are not available for stations closer to the coast than six kilometers, and it was not possible to obtain very close inshore surface PCO_2 observations to compare with previous sections. The maximum observed PCO_2 of 900 ppm at 40 meters

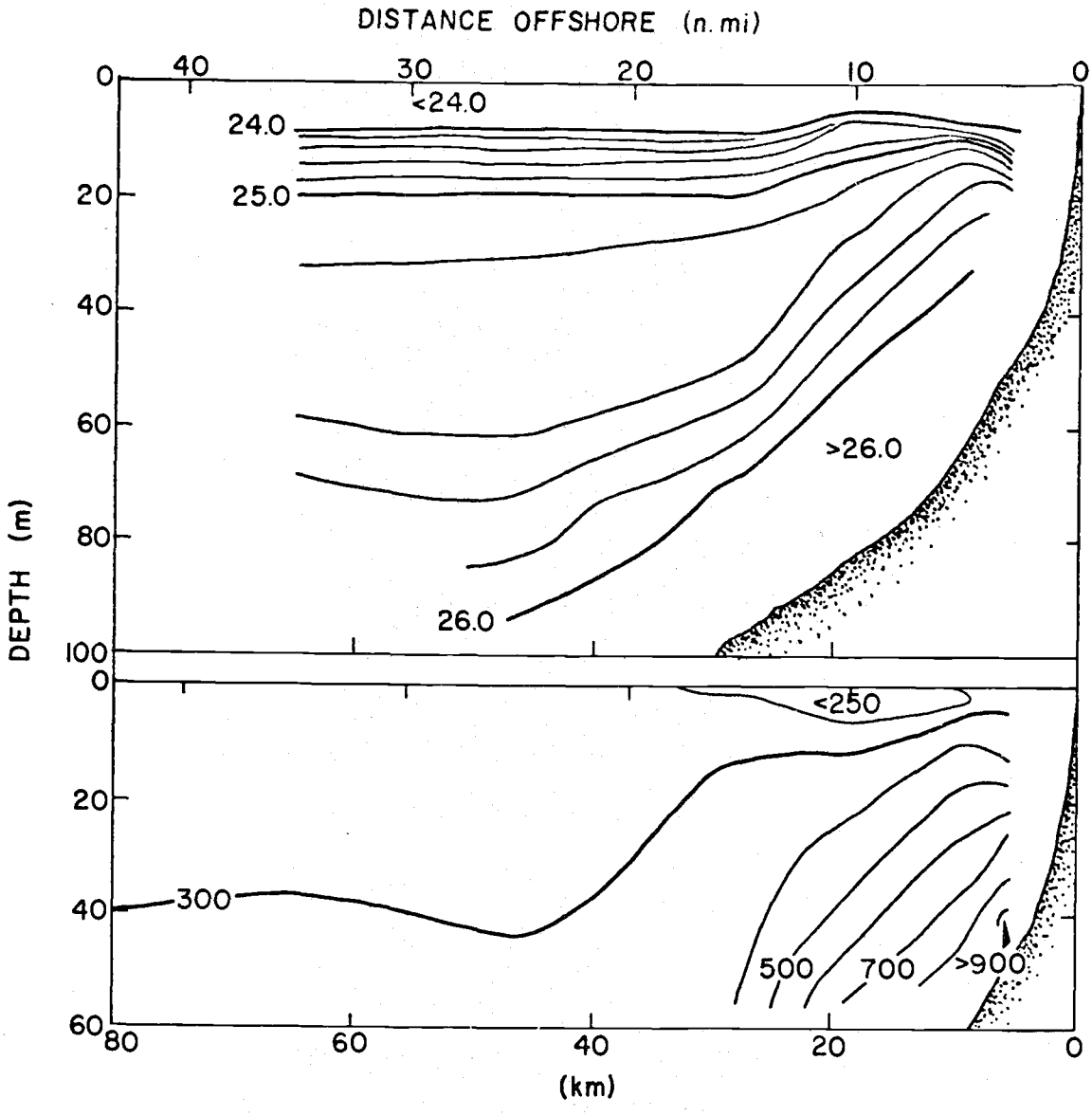

Fig. 5.17. Vertical distribution of density and PCO_2 on the Newport hydrographic line, 27-28 June 1969. cf. Fig. 5.14.

depth, seven kilometers offshore, is comparable to the data of the previous year and in depth on the Depoe Bay line, 28 June. Although the density and PCO_2 distributions were apparently quite coherent, there is one important feature to notice: the isolines of PCO_2 in the deeper waters 20-30 kilometers offshore sloped upward toward shore significantly more steeply than did the isopycnals. This point will be discussed in the Discussion section of this chapter.

The first pair of vertical sections (Fig. 5.18) obtained on the Depoe Bay line on 31 July 1969 are drawn from only three stations. However, the broad features represented are very interesting. The first of these is the very different density structure in the surface layers inshore of 50 kilometers. The front had moved well offshore and the isopycnals broke the surface much more steeply than in any of the previous figures. The most dense water arriving at the surface ten kilometers offshore had a sigma-t of 25.6. Another, very striking, feature is that the PCO_2 contours sloped much more steeply than the isopycnals between 10 and 50 meters depth, 20-25 kilometers offshore. In addition, the near-bottom isolines of PCO_2, namely the 700 ppm contour, sloped much more steeply than the 26.4 isopycnal appearing in the same depth vicinity. Thus, the usual, very general coherence between PCO_2 and sigma-t was still present to an extent, but was more systematically disturbed than in previous sections. Notice the PCO_2 inversion at the station 28 kilometers offshore in the depths

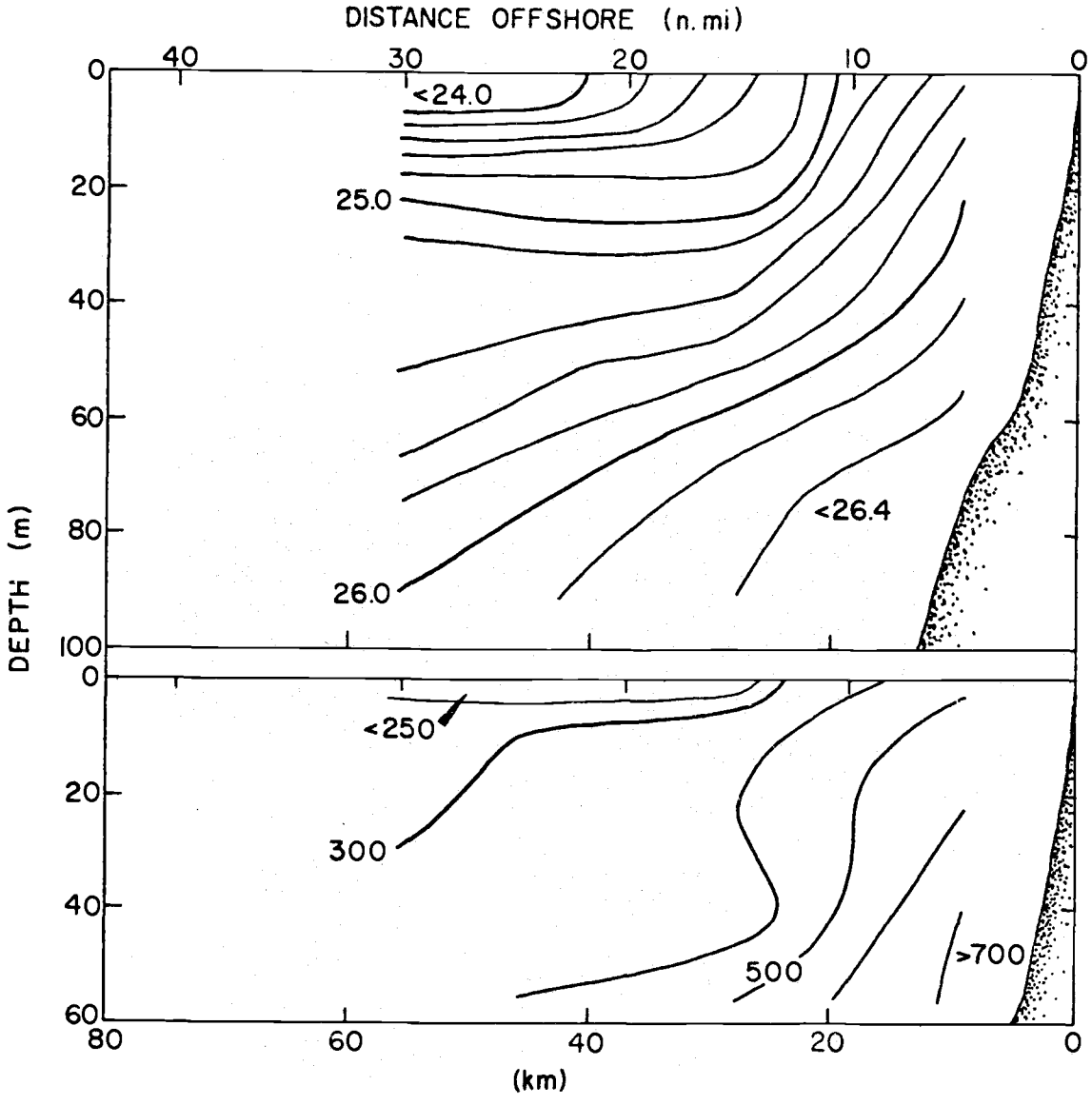

Fig. 5.18. Vertical distribution of density and PCO_2 on the Depoe Bay hydrographic line, 31 July 1969. cf. Fig. 5.14.

between 20 and 40 meters.

Five days later the density and PCO_2 distributions had the configuration shown in Fig. 5.19. There was by this time much more intense vertical stratification in both PCO_2 and sigma-t. No water of sigma-t greater than 23.7 appeared at the surface five kilometers offshore. PCO_2 had fallen to slightly less than 200 ppm, 15 kilometers offshore, in the very shallow surface layers. No water of PCO_2 greater than 216 ppm appeared at the surface between 5 and 35 kilometers offshore. The PCO_2 contours and the isopycnals were approximately parallel throughout the section, although, near the bottom, five kilometers offshore, the PCO_2 contours were slightly more steeply inclined than were the isopycnals. The PCO_2 contour was more inclined between 5 and 20 meters, five kilometers offshore.

Two days later, on the 7th of August, the picture had changed dramatically (Fig. 5.20). Sigma-t 23.7 water had moved about 55 kilometers offshore and the sigma-t 25.8 contour broke the surface five kilometers offshore. There was a very strong seasonal pycnocline, 24.0-25.0 sigma-t, seaward from about ten meters at 10-25 kilometers, to 20 meters at 65 kilometers. A very sharp surface density gradient of 25.8 to 24.8 lay between two and six kilometers offshore, respectively. A surface low PCO_2 was encountered 25 kilometers offshore, the value being 218 ppm. In this case, too, the PCO_2 contours were more steeply inclined than the isopycnals between five and ten kilometers

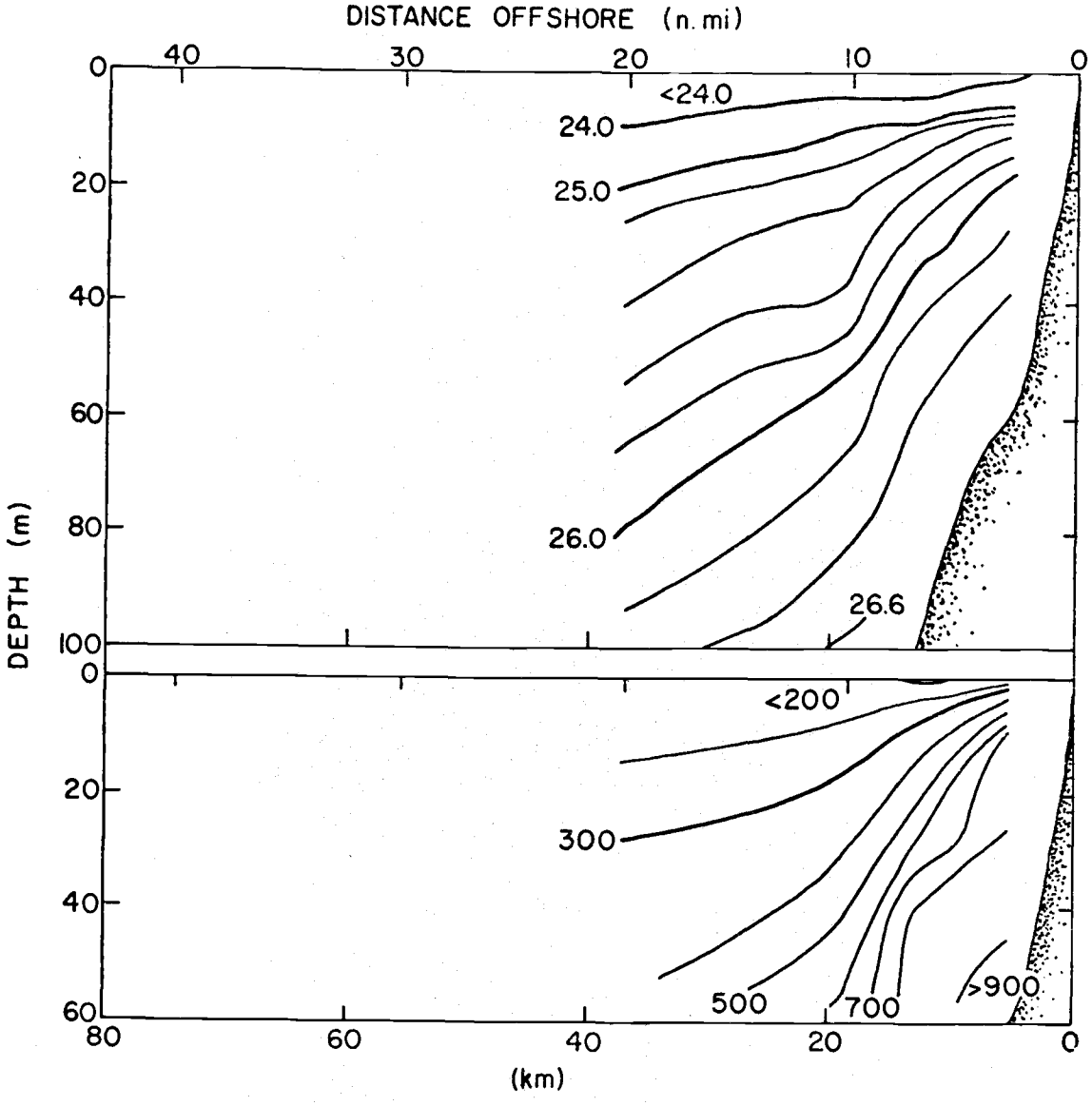

Fig. 5.19. Vertical distribution of density and PCO_2 on the Depoe Bay hydrographic line, 5 August 1969. cf. Fig. 5.14.

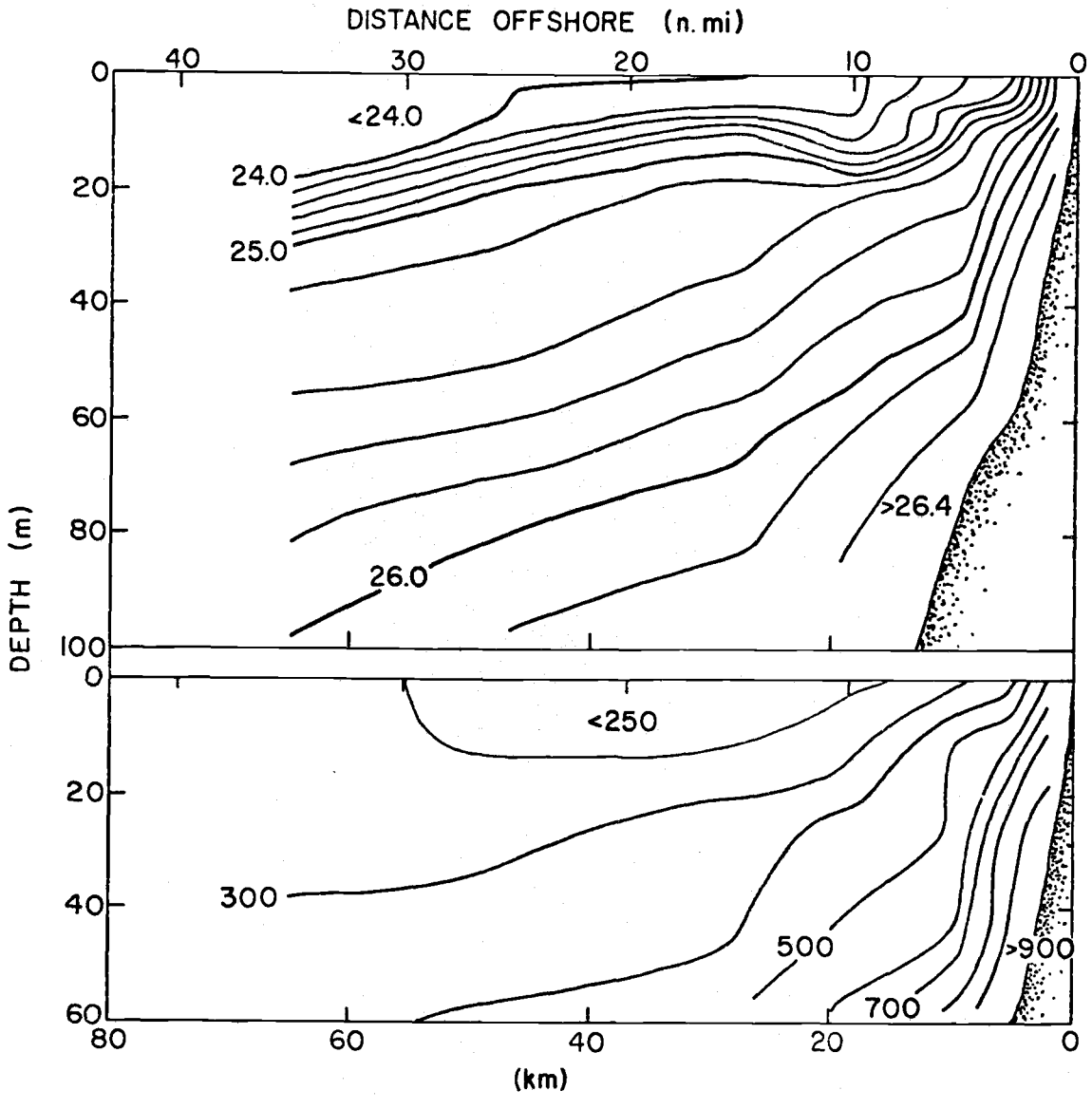

Fig. 5.20. Vertical distribution of density and PCO_2 on the Depoe Bay hydrographic line, 7 August 1969. cf. Fig. 5.14.

offshore from 10 to 50 meters deep. The maximum PCO_2 encountered lay seven kilometers offshore near the bottom at 55 meters depth. There was an unusual sinking of the isopycnals between 10 and 20 kilometers offshore at depths of 5-20 meters.

The latter feature had disappeared the next time the Depoe Bay line was occupied, five days later, on the 12th of August (Fig. 5.21). In addition, the isograms of both density and PCO_2 no longer broke the surface at near vertical angles close inshore.

Two dramatic changes had taken place in the PCO_2 structure: 1) The broad region of greater than 900 ppm, up to 965 ppm, close inshore and near the bottom, had become much more localized. The maximum value observed in this PCO_2 high fell to 930 ppm and the horizontal extent of the greater-than-900 ppm region was reduced to only two or three kilometers. The PCO_2 -density coherence was drastically diminished. The PCO_2 contours were almost vertical between 10 and 25 kilometers offshore at depths from 10 meters to 60 meters whereas the isopycnals retained their more usual slope of approximately 45°. 2) The PCO_2 isograms above 30 meters and within 20 kilometers of the coast became remarkably horizontal. In the same region the isopycnals had decreased in slope but were still markedly more inclined than the PCO_2 isograms.

The Newport hydrographic line was occupied on 5 August 1969 (Fig. 5.22) only a few hours after the Depoe Bay line had been

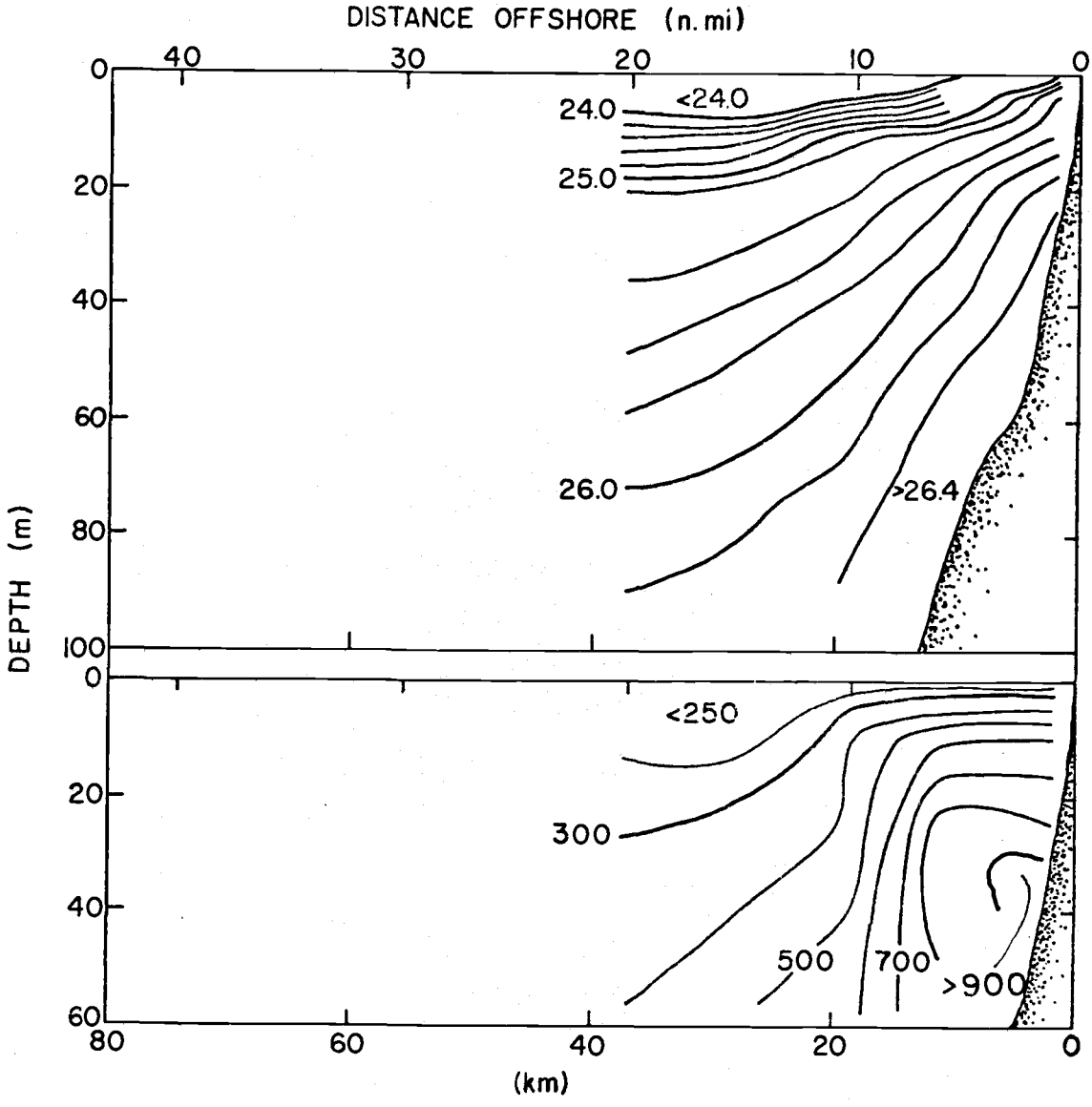

Fig. 5.21. Vertical distribution of density and PCO_2 on the Depoe Bay hydrographic line, 12 August 1969. cf. Fig. 5.14.

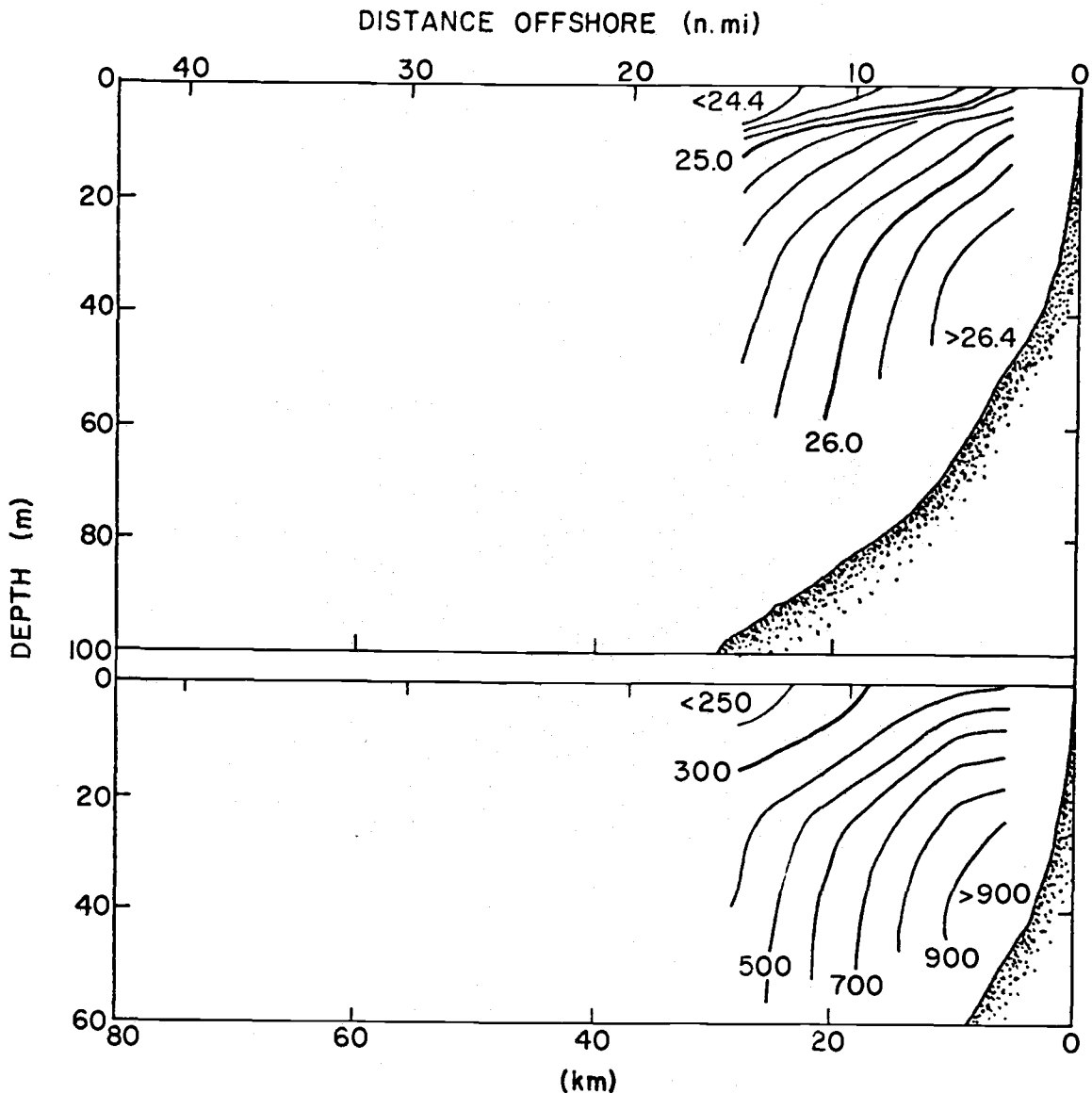

Fig. 5.22. Vertical distribution of density and PCO_2 on the Newport hydrographic line, 5 August 1969. cf. Fig. 5.14.

occupied on that date. It is interesting to compare the two lines, which are only a few kilometers apart. The feature which immediately becomes apparent in these two vertical sections is the much more intensely convex-upward nature of the contours for both density and PCO_2 on the Newport line compared to the Depoe Bay line. In this case the water column also seems to be much more highly stratified with a very marked seasonal pycnocline evident at about ten meters depth. More dense water of sigma-t 24.8 had broken the surface at a point six kilometers offshore. Approximately the same ranges of density and PCO_2 were observed in the two cases with slightly more dense water having appeared on the Depoe Bay line in the deeper waters. However, on the Newport line the sampling was not carried to as great a depth and could have missed the 26.6 sigma-t water found on the Depoe Bay line. PCO_2's of 940 ppm were found on the Newport line at 35 meters depth six kilometers offshore. On the Depoe Bay line the maximum PCO_2 was approximately 936 ppm and occurred at a depth of 55 meters, six kilometers offshore.

Four days later on the 9th of August, the Newport line was again occupied (Fig. 5.23). Compared to the previous occupation of the Newport line a singular feature was evident. This is the tongue of higher PCO_2 water which appears to perhaps be moving offshore at a depth of around 15 meters, 20 kilometers offshore. The region of high PCO_2 water, with values as much as 960 ppm, at 50 meters

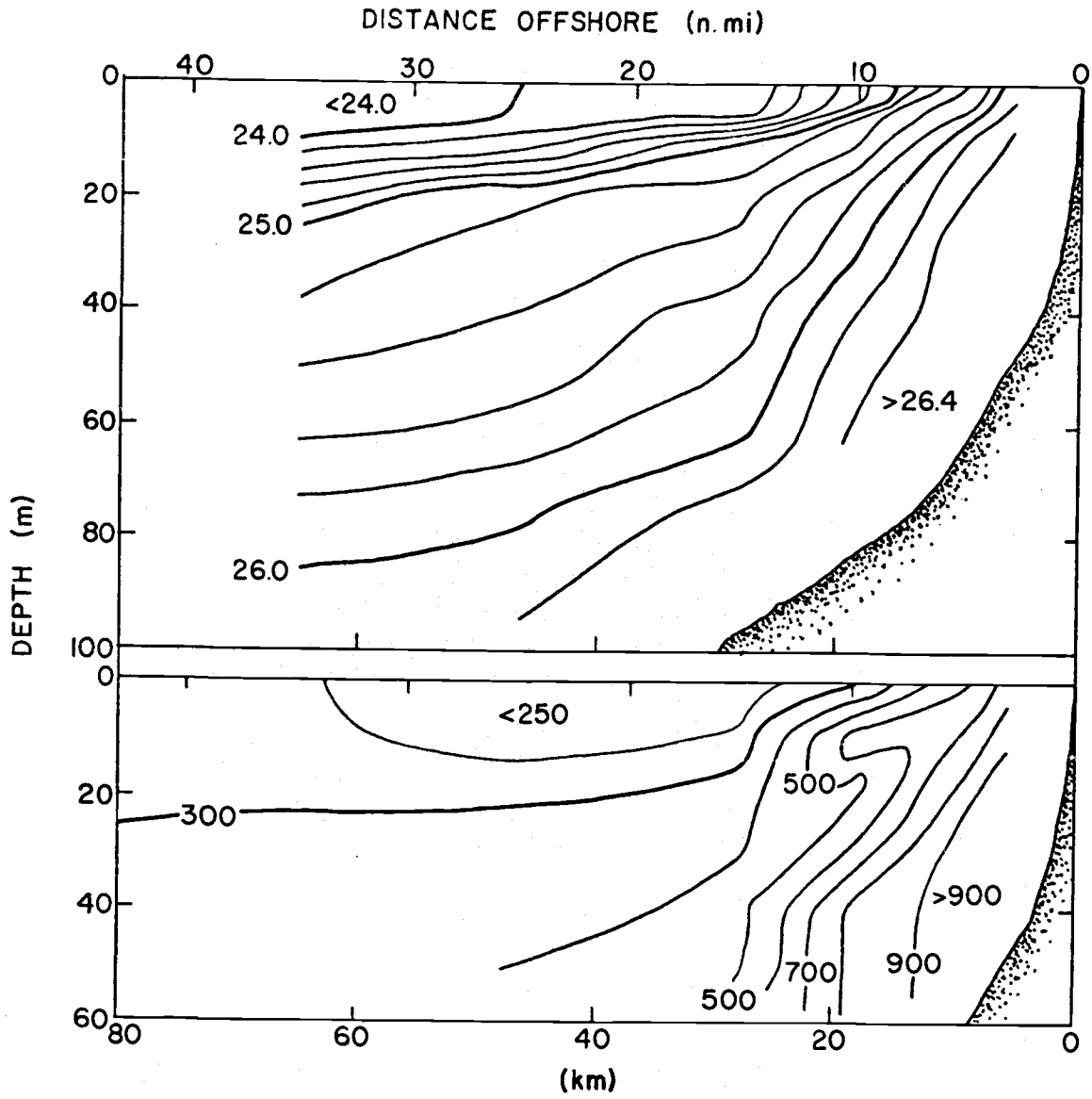

Fig. 5.23. Vertical distribution of density and PCO_2 on the Newport hydrographic line, 9 August 1969. cf. Fig. 5.14.

depth and nine kilometers offshore is even broader in extent on this section.

Once again one sees in the deeper contours of both PCO_2 and sigma-t inshore of 30 kilometers that the PCO_2 contours are significantly steeper than the isopycnals.

The tongue of high PCO_2 water sinking seaward corresponded to relatively warm temperature. This was the only such clear cut correspondence of a PCO_2 inversion with a temperature inversion observed on the Newport or Depoe Bay lines in this study.

The last cruise in 1969 took place in October. Figure 5.24 shows the density and PCO_2 distributions on the Depoe Bay hydrographic line. Several features are apparent which are consistent with this being close to the end of the upwelling season. The seasonal pycnocline was still present but no longer breaks the surface and is found no shallower than ten meters. The seasonal and permanent pycnoclines were more horizontal than earlier in the season. The seasonal pycnocline was almost exactly horizontal. If one excludes the observations six kilometers offshore, the most intense vertical PCO_2 gradient was located at 30 meters between 10 and 20 kilometers offshore. This location coincided with the merging of the permanent and seasonal pycnoclines and intense density gradient at this same place.

Surface waters were everywhere undersaturated with CO_2, the

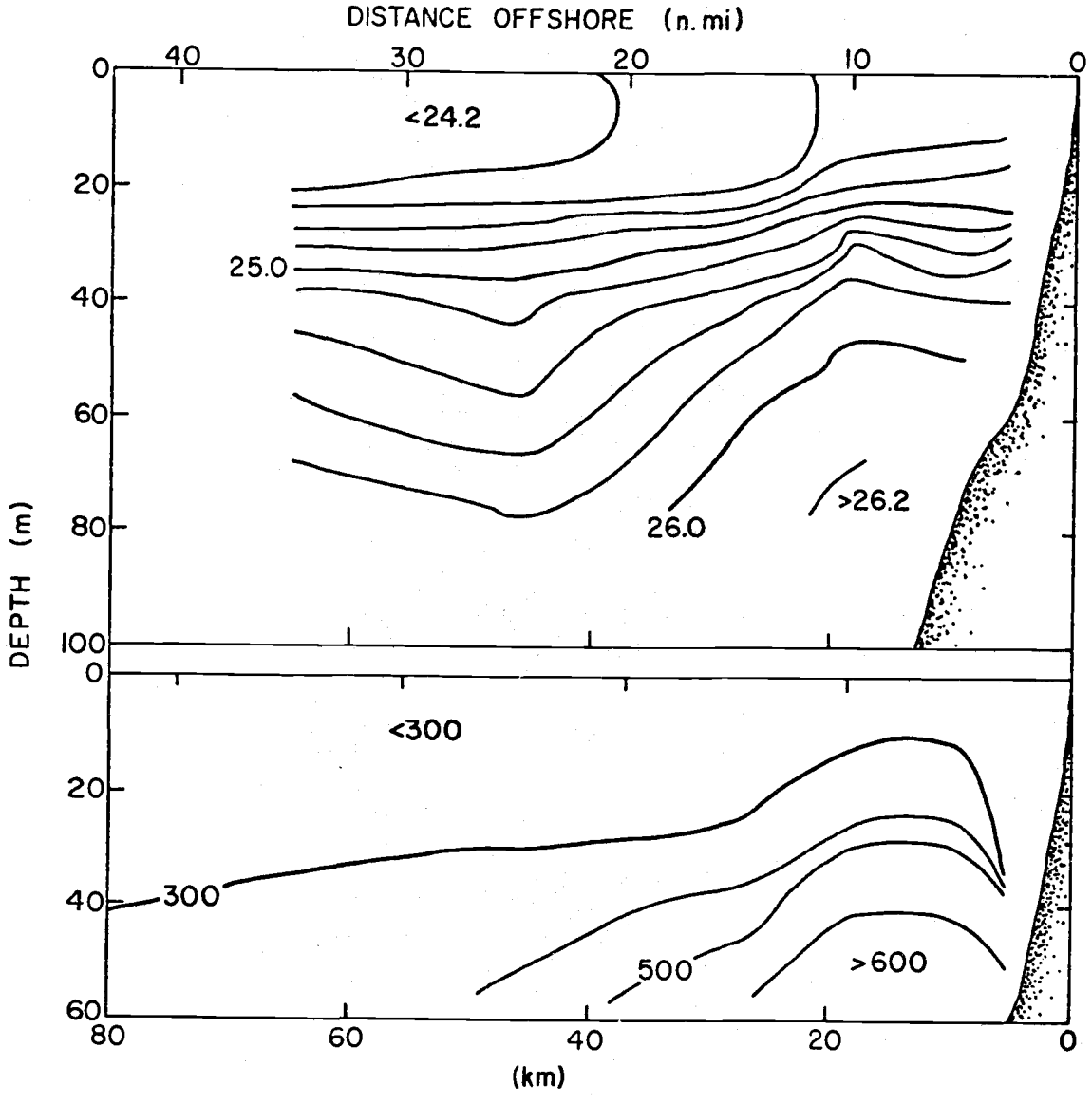

Fig. 5.24. Vertical distribution of density and PCO_2 on the Depoe Bay hydrographic line, 29 October 1969. cf. Fig. 5.14.

lowest values occurred 10 meters deep, 25 kilometers offshore, and the value there was 270 ppm. Inshore of 6 kilometers the PCO_2 again fell to 280 ppm, almost homogeneously, to a depth of 35 meters. The reason for the lack of coherence between PCO_2 and sigma-t at this station is not clear. Other than at this location there was a general close coherence between PCO_2 and density.

The Newport hydrographic line had been occupied almost a week earlier than this Depoe Bay section. Figure 5.25 shows the results for the Newport line obtained on 23 October 1969. At that time there was somewhat more inclination of the pycnoclines and PCO_2 isolines. As on the Depoe Bay line there was a general correspondence between the PCO_2 contours and the isopycnals. Again the location of the maximum vertical gradient in PCO_2 between 10 and 25 kilometers offshore coincided with the merging of the permanent and seasonal pycnoclines and the most intense vertical gradient in density.

The surface waters were, in this case also, everywhere undersaturated with respect to the atmosphere. The lowest value observed was 245 ppm, 10 kilometers offshore. The maximum PCO_2 observed was 755 ppm, 20 kilometers offshore and 57 meters deep.

It was possible to make one section on the Depoe Bay line consisting of four stations on 9 January 1970 (Fig. 5.26). Rudimentary as it was, this section permitted a very valuable set of winter observations to be made, and as of the date of this writing, is the only

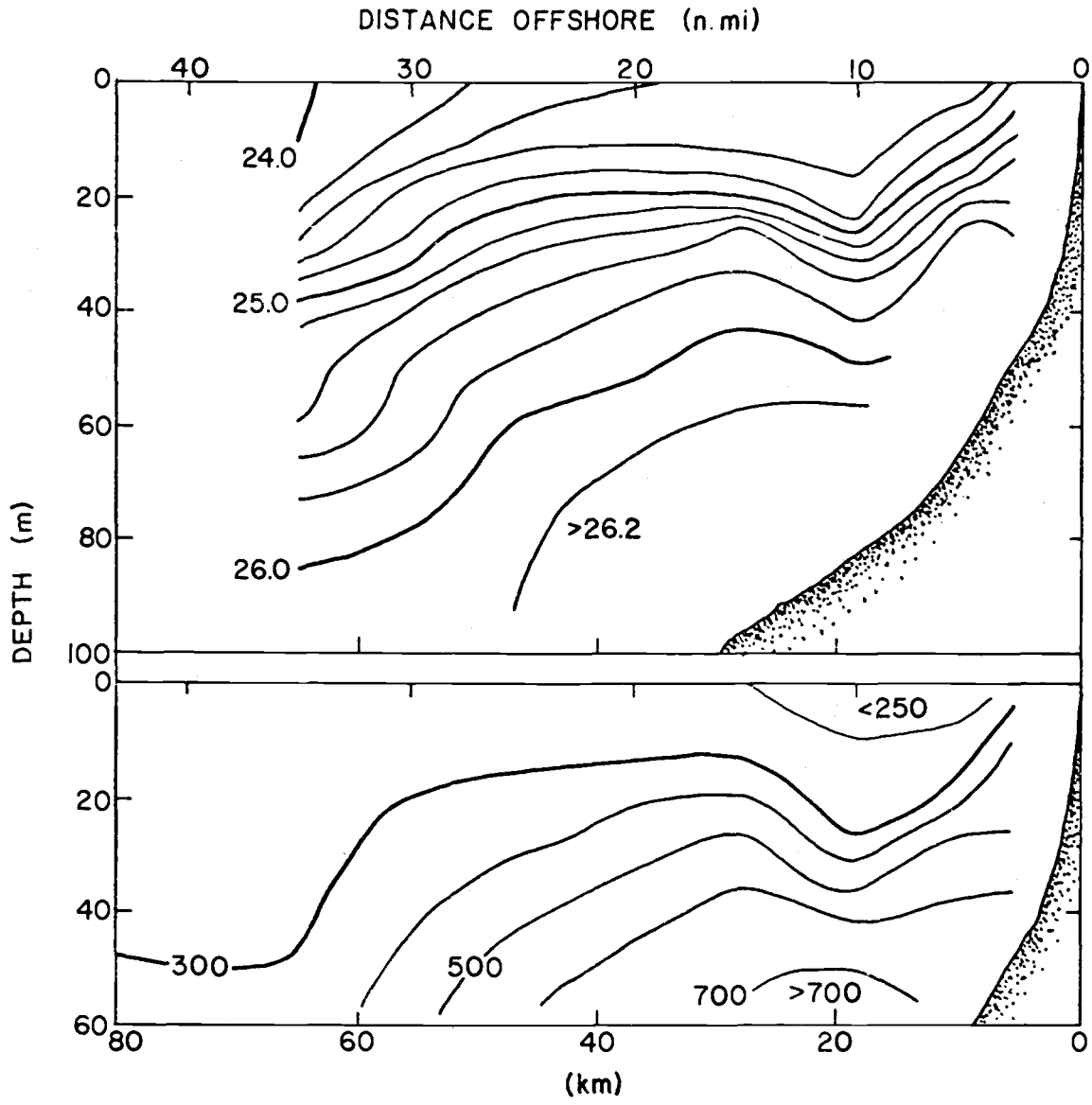

Fig. 5.25. Vertical distribution of density and PCO_2 on the Newport hydrographic line, 23 October 1969. cf. Fig. 5.14.

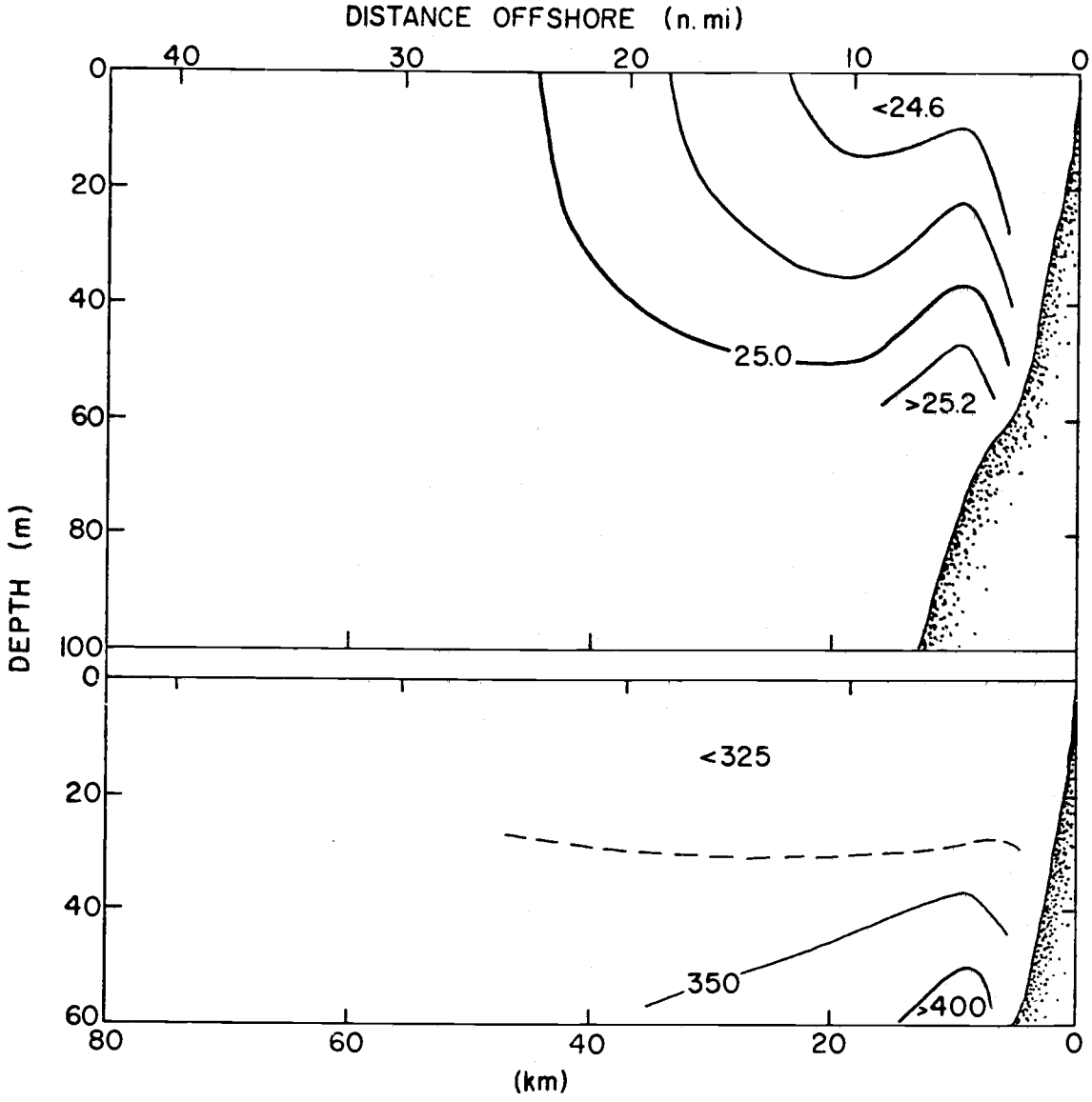

Fig. 5.26. Vertical distribution of density and PCO_2 on the Depoe Bay hydrographic line, 9 January 1970. cf. Fig. 5.14.

set of observations in January or February that are available for this region.

The water was rather well mixed down to more than 40 meters and the isopycnals rather clearly show the effect of river runoff with low density water being evident close inshore. The surface waters were everywhere nearly saturated with respect to atmospheric CO_2 and the range observed was only 8 ppm, from 313 to 321 ppm. A maximum PCO_2 lay at 57 m, 10 kilometers offshore, and had a value of 418 ppm. There was in general a rather close coherence of PCO_2 with density.

Completing an annual cycle, but unfortunately with very large time gaps, a cruise was made in May 1970. Figure 5.27 illustrates the results obtained on the Depoe Bay hydrographic line on 5 May. By this time the early upwelling season was well developed and the isograms were inclined steeply towards shore. The seasonal pycnocline was already somewhat well developed and surface PCO_2's had fallen substantially below atmospheric equilibrium. In the region farther than 5 kilometers offshore the surface waters were undersaturated, with PCO_2 down to 240 ppm. The maximum surface PCO_2, 500 ppm, was observed 2 kilometers offshore. The maximum PCO_2 at depth was 874 ppm, observed 10 kilometers offshore at 55 meters depth. The PCO_2 contours and the isopycnals were generally parallel everywhere.

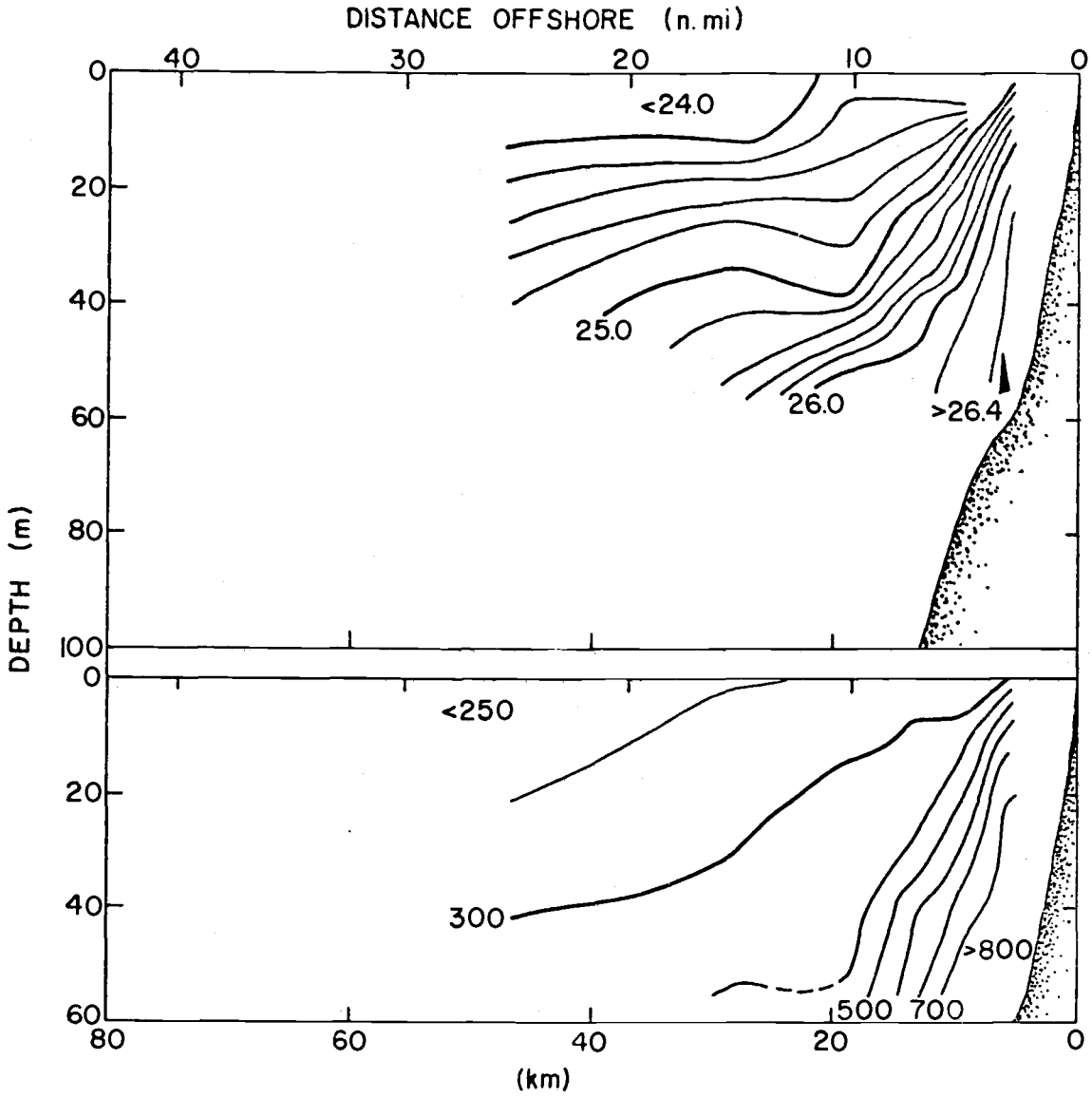

Fig. 5.27. Vertical distribution of density and PCO_2 on the Depoe Bay hydrographic line, 5 May 1970. cf. Fig. 5.14.

Three days later, on the 8th of May, the Depoe Bay line was occupied again. From the data obtained the fragmentary section shown in Fig. 5.28 was constructed. A movement of low density water onshore created a 25 meter deep blob of water of density less than 24.0, 10 kilometers offshore. There were no surface PCO_2 values observed greater than 250 ppm. Two kilometers offshore where the surface PCO_2 three days earlier had been 500 ppm, the observed value had fallen to 230 ppm. The maximum PCO_2 value observed in the section was 870 ppm 50 meters deep, 6 kilometers offshore.

At the Newport hydrographic line, on 6 May 1970 (Fig. 5.29), the early season development of upwelling had taken place. The seasonal pycnocline had broken the surface, forming a front located between 15 and 20 kilometers offshore. A very interesting phenomenon was the appearance at the surface, 14 kilometers offshore, of water having a PCO_2 of 375 ppm. Ten kilometers offshore was centered a low PCO_2 of 225 ppm and inshore of that at 6 kilometers the surface water showed a high PCO_2 of 365 ppm. The maximum PCO_2 observed in the deeper waters was 935 ppm located 6 kilometers offshore at 35 meters. All surface waters offshore of approximately 18 kilometers were undersaturated with respect to the atmosphere.

The sigma-t 26.2 surface corresponded to a PCO_2 of 700 ppm,

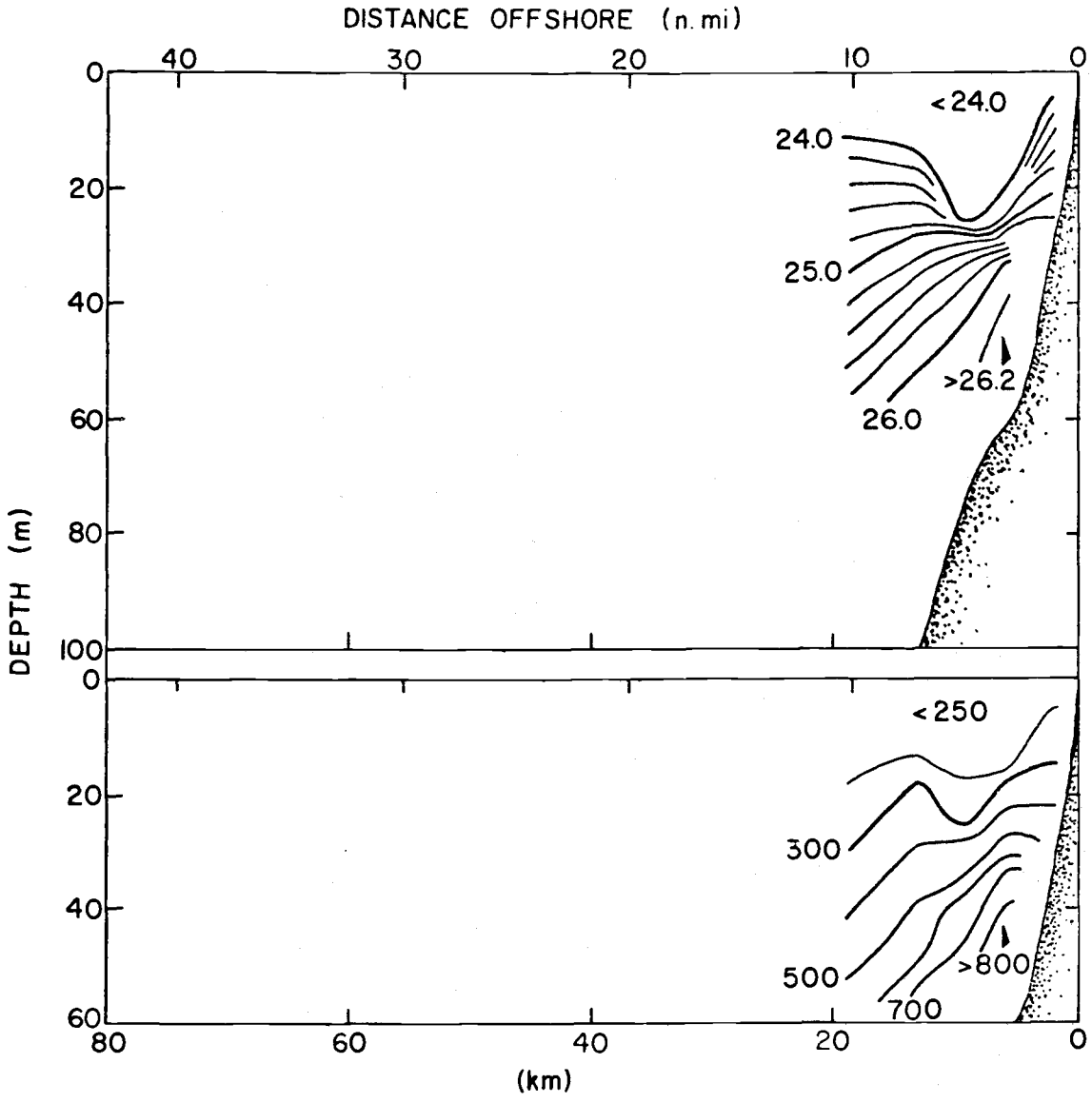

Fig. 5.28. Vertical distribution of density and PCO_2 on the Depoe Bay hydrographic line, 8 May 1970. cf. Fig. 5.14.

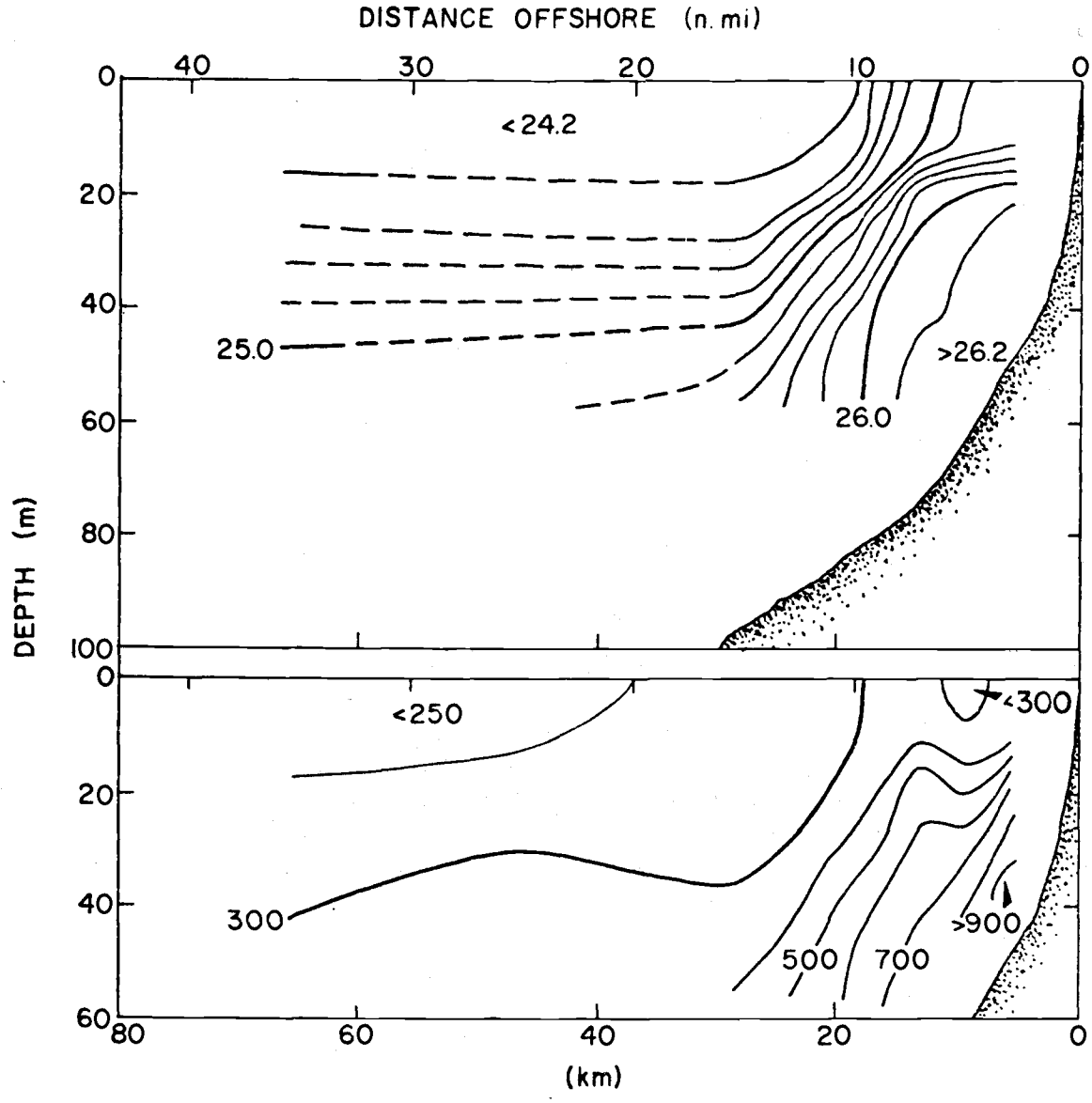

Fig. 5.29. Vertical distribution of density and PCO_2 on the Newport hydrographic line, 6 May 1970. cf. Fig. 5.14.

whereas on the two Depoe Bay sections taken during this cruise this isopycnal corresponded to approximately 800 ppm PCO_2.

5.3 Discussion

5.3.1 PCO_2 as an indicator of upwelling and associated processes.

The surface plots, Figs. 5.2 to 5.5, indicate the locale of the upwelling regime studied. They show, furthermore, that each of these four variables (and therefore several derived variables as well, for example, sigma-t) may be used as indicators of upwelling. Temperature and salinity have been used classically as indicators of upwelling, particularly along the Oregon coast where the vertical structure in both of these variables is favorable for such use. Salinity is perhaps the most nearly conservative of all these variables in the upwelling regime while temperature is definitely influenced by insolation. Oxygen and PCO_2 by contrast, are sensitive indicators of biological processes as well. Therefore, used in conjunction, a set of several of these variables forms an extremely powerful tool in the demarcation of localized upwelling areas.

High precision temperature and salinity recorders have been available for some time and may be employed for the rapid surface mapping of upwelling areas where the vertical structures in these variables are favorable. However it is only very recently that such a recorder has been available to the groups at Oregon State

University, and the instrument is only now being installed aboard R/V YAQUINA at the time of this writing. Oxygen may also be used as an indicator of the biological processes associated with upwelling. However, Teal and Kanwisher (1966) have concluded that PCO_2 is a far more persistent indicator for biological changes than is oxygen. They calculated that oxygen will return to equilibrium with the atmosphere after a biological perturbation approximately 24 times faster than does carbon dioxide. Furthermore, our experience with continuous oxygen recorders had not been as favorable as the experience with carbon dioxide analysis systems in the sense of drift and reproducibility. This argues against the use of both dissolved oxygen itself and the derived apparent oxygen utilization as a method of continuously recorded indication of upwelling and subsequent biological processes.

It is apparent from Figs. 5.6 to 5.9 that pH and PCO_2 are quite coherent in Oregon coastal waters. It would seem that pH might also be used as an indicator of upwelling. This would indeed be quite feasible and appears to be an attractive possibility. The reason for the latter conclusion is that the equipment for pH recording is relatively simple and inexpensive. But it must be said the PCO_2 seems to be intrinsically a more desirable variable to portray graphically rather than pH. This is because it is the carbon dioxide which is being utilized by phytoplankton or released by biological oxidation,

not the hydrogen ion. It would be a relatively simple matter provided a shipboard on-line computer were available to simply re-calculate the pH observations to PCO_2 and in that way express the results to the human observer in the more meaningful PCO_2. The method of doing this theoretically and the results of an attempt to relate PCO_2 to pH theoretically will be treated in more detail in Sect. 5.3.2.

To further discuss the use of PCO_2 as an indicator of upwelling it will be instructive to examine in some detail the relationship of PCO_2 to the density of the waters found off Oregon. This will also assist in the understanding of the vertical distributions of sigma-t and PCO_2 presented in Figs. 5.14 to 5.29.

Figure 5.30 illustrates the co-variance of PCO_2 and density. If one excludes the low salinity waters which have been heavily diluted by the Columbia River effluent, one is struck by the almost linear relationship between density and PCO_2. However, this is a deceptively simple description of the data. It represents a coincidental action of several processes as illustrated in Fig. 5.31. The shaded area in this figure outlines the region in which all PCO_2-sigma-t points fall that have ever been obtained in this work. A very small number of "wild" points have been removed.

Also shown in this figure are vectors illustrating the trajectories that water types would follow if they were subjected to the action of various oceanographic processes. In the first case, that

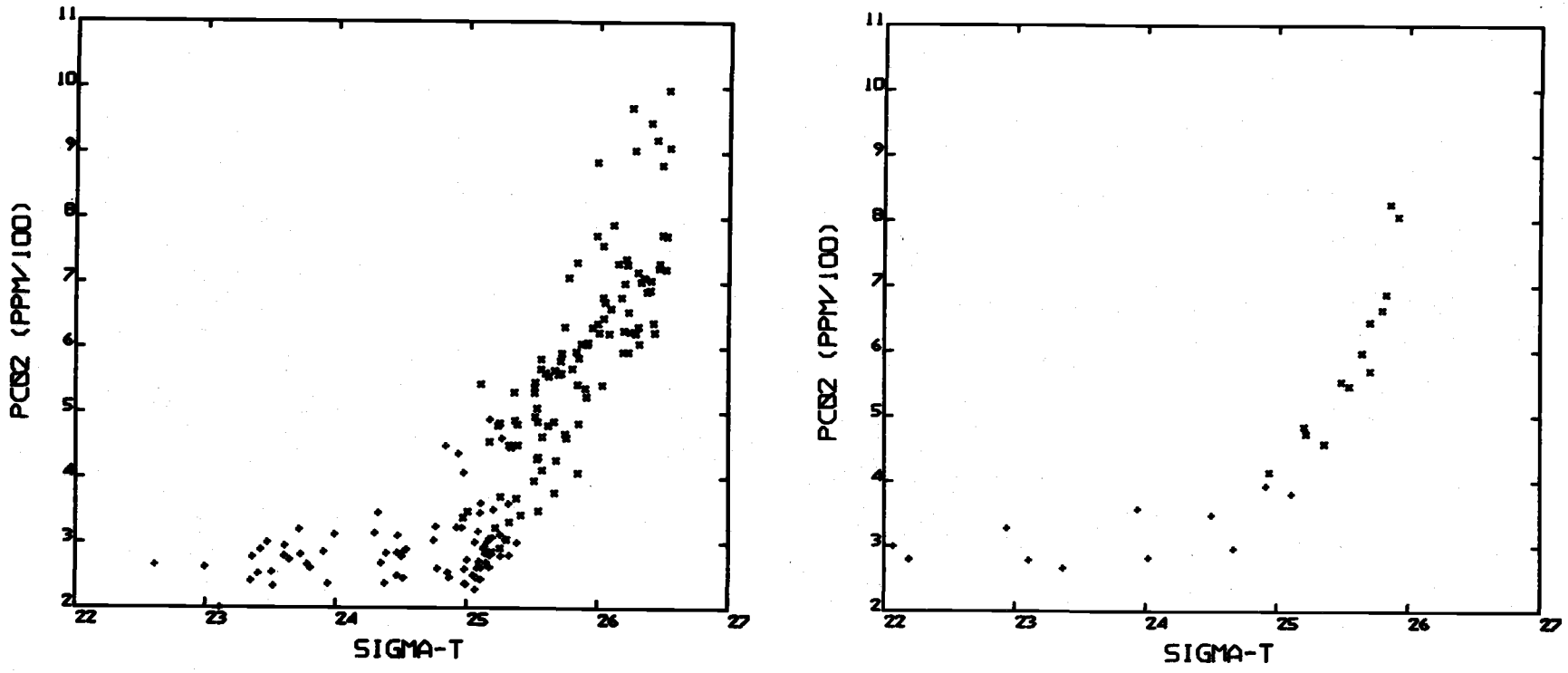

Fig. 5.30. PCO_2 density relationships in Oregon coastal waters during the upwelling season. Points plotted with plus signs in the region of low PCO_2 and sigma-t represent waters of salinity less than 28‰, that is heavily diluted by Columbia River water. a) Data from cruise Y6806C, June 1968, on the Depoe Bay line. b) Data from cruise Y6806C, June 1969, on the Depoe Bay line.

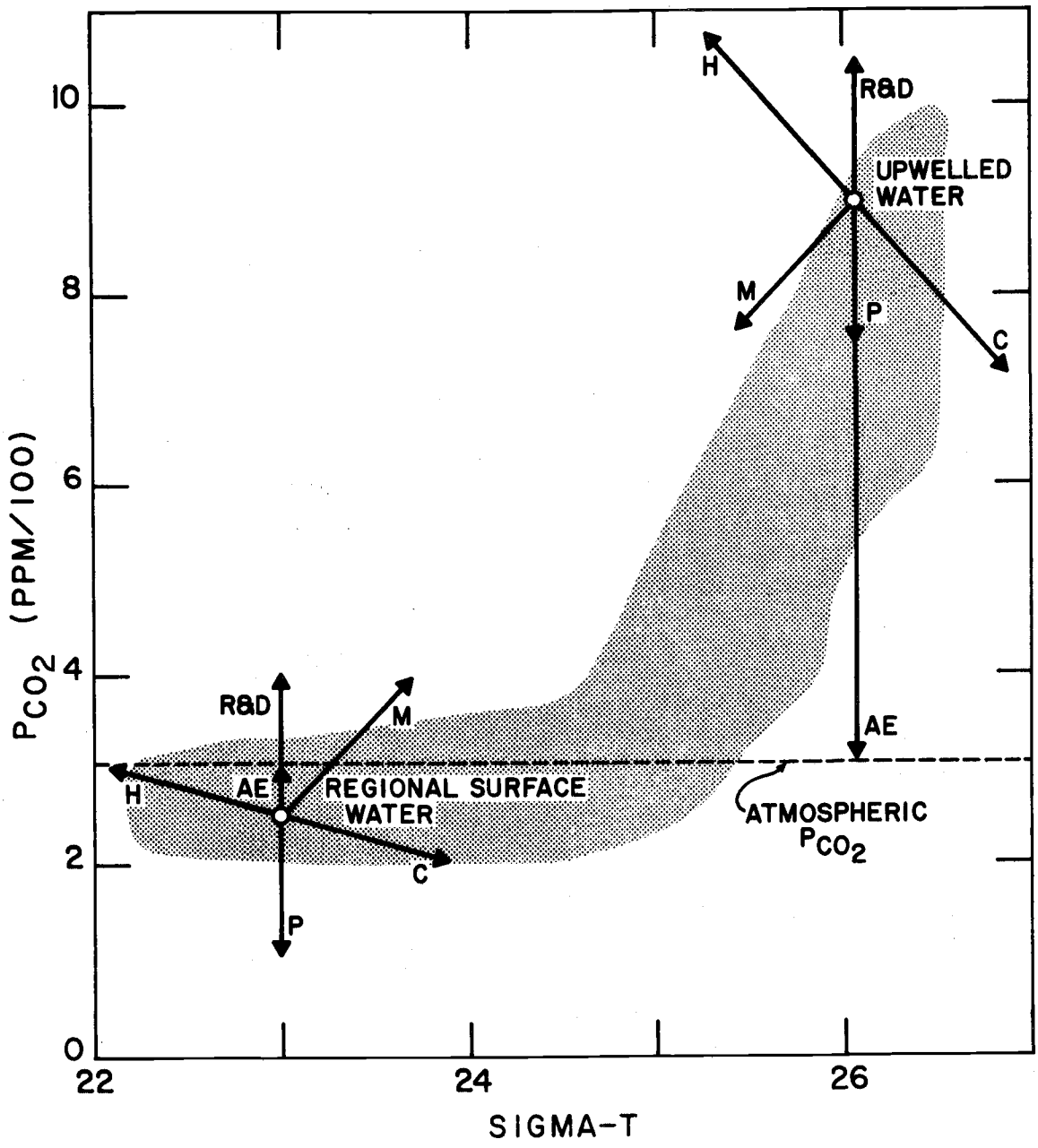

Fig. 5.31. Processes affecting the PCO_2-sigma-t relationship. The hatched area denotes the field of all measured points in Oregon coastal waters during 1968 and 1969. The heating and cooling vectors (labelled H and C, resp.) give the magnitude and direction of the effect of a ± 5° C temperature change. Atmospheric exchange is indicated by AE. Only the directions of the photosynthesis, respiration and decay, and mixing vectors are significant (indicated by P, R&D, and M, respectively).

of the upwelling water, there are shown six process vectors acting upon the water type characterized by PCO_2 900 ppm and sigma-t 26.0. (This is a nearly representative water type whose characteristics have been adjusted so as to move it into an easily manipulated area of the diagram. Actually it should be located at a somewhat higher PCO_2 and sigma-t to be more truly representative of upwelling water.)

The six process vectors shown are the results of hypothetical heating and cooling of the water, mixing of the water with regional surface water, the effects of photosynthesis, and respiration and decay taking place within the water, and finally exchange of carbon dioxide between the water and the atmosphere.

The mixing, photosynthesis, and respiration and decay vectors are quite self-evident and will not be discussed. Atmospheric exchange in the case of the upwelling water can only lead to a decrease of PCO_2. Over the open ocean the atmosphere is generally found to have a PCO_2 of around 310-320 ppm while the upwelling water typically has values of 900 ppm or more and is thus quite supersaturated with respect to the atmosphere. Therefore the exchange of CO_2 of upwelling water with the atmosphere can only lead to a net loss to the atmosphere.

Heating and cooling vectors were calculated as indicated in Sect. 2.7 of this work on the heating effect on PCO_2; the sigma-t component of the vector was taken from readily available

tables (Keala, 1965).

The initial water type for regional surface water has been placed at PCO_2 of 250 ppm and sigma-t 23.0. This was done for illustrative purposes. A more realistic sigma-t value would place the water type at perhaps 24.0 or 24.5. This would not alter any of the process vectors with the exception of the angle of the mixing vector. Because the regional surface water typically has a PCO_2 below that of the atmosphere, the general direction of the atmospheric exchange is now in the direction of penetration of CO_2 from the atmosphere into sea. However, it is important to note that this is not always true and that there are many points in this plot which do lie somewhat above the atmospheric PCO_2 and therefore for those waters the exchange would be in the opposite direction.

An important distinction between the upwelling water and the regional surface water is evident in the angle of the heating and cooling vectors. These have a considerably larger slope in the case of the upwelling water because, as is outlined in Sect. 2.7, the fractional change of PCO_2 with respect to temperature is constant. Therefore the absolute change in the PCO_2 will be an increasing function of PCO_2 itself. If this diagram had been plotted with a logarithmic PCO_2 scale, then one would have observed parallel heating and cooling vectors for the upwelling water and for the regional surface water.

The conclusions to be drawn from this diagram are rather

interesting. First, it would seem to be a remarkable circumstance that the relationship between PCO_2 and sigma-t observed for the inshore upwelling region is quite linear or nearly linear. Obviously there are several processes acting which could produce points lying anywhere in the PCO_2 - sigma-t field. What the linearity of the PCO_2 - sigma-t relationship tells us is something of the predominance of certain processes and the coupling of some of them. Thus, mixing in the frontal zone between the upwelling water and the regional surface and very shallow intermediate waters is certainly an important process and would lead to a linear relationship. Also, as upwelling water rises into the bottom of the euphotic zone, photosynthesis begins to take place; this begins removing carbon dioxide from the water without affecting its density. However, as the water moves higher in the euphotic zone it enters the shallower layers within a few meters or even centimeters of the surface where most of the solar radiation is absorbed and transformed into heat. This raises the temperature of the water and one now begins to see most strongly the influence of the heating vector.

Note that the time sequence of these two processes is first photosynthesis, then warming, as the upwelling water rises into the euphotic zone, through the zone of maximum photosynthesis, and finally into the most surficial few centimeters. This sequence, although probably more complicated, may explain the relative

downwarping, which often is seen, of the PCO_2 isograms compared to the isopycnals (looking onshore in the upper 20 to 30 meters, within 20 kilometers of the coast). This is very striking in Fig. 5.21. It is also apparent in Figs. 5.22, 5.24, 5.27, and 5.28 as further examples. The absence of "seed" phytoplankton populations at some periods in the upwelling water may explain why this phenomenon is not always observed.

If the model of Mooers, Collins and Smith (1972) obtains, wherein there are several layers within the water column in the upwelling area with alternately onshore-offshore movement, then one could certainly expect rather extensive mixing to be occurring between the upwelling, and regional surface, and shallow intermediate waters as the upwelling water rises to the surface.

In total then, one would expect to see a summation of the heating, mixing, and photosynthesis vectors acting as the upwelling water rises to the surface and of course once the water arrives at the surface one can also expect to observe the action of the atmospheric exchange vector. Further, the processes are not independent but always more or less coupled. The resultant apparently lies in the direction shown by the inclined shaded area which is not influenced by excessive Columbia River water dilution.

In the area close to the Columbia River mouth can be seen very localized effects of Columbia River high PCO_2 water. The presentation

of Figs. 5.2-5.4 shows this rather clearly. (See also, Sect. 4.4 and Park et al. (196); Kantz (1973) presents results of seasonal studies of the Columbia River carbon dioxide chemistry.) Apparently, marine phytoplankton activity and dilution by seawater quickly reduce the PCO_2 of the plume water to moderate levels.

In summary, considering the limitations of the several possible indicator variables discussed above and the history of the availability of systems for their measurement at OSU, it has been found that PCO_2 serve as an extremely valuable indicator for upwelling and its associated processes. It has been employed very effectively for this purpose on the several collaborative cruises with biological oceanographers in 1970, 1971, and 1972.

5.3.2 PCO_2 related to pH. The close coherence shown between pH and PCO_2 in Figs. 5.6 to 5.9 led to an attempt to calculate the trajectories, as pH changes for any reason, of points on the pH-PCO_2 diagram which initially would have given a set of temperature, salinity, pH and alkalinity (TA) corresponding to: (a) upwelling water, (b) regional surface water and (c) Columbia River water.

A summary of some of the typical values of the physical and chemical variables encountered for regional (or ambient) surface water, upwelling water, and for surface water in the lower Columbia River estuary is given in Table 5.2. Some of these data will be used

Table 5.2. Ambient surface water, upwelling water, and Columbia River water properties; Y6806C.

Property	Typical Ambient Surface Water	Approximate Upwelling Water	Estuarine Columbia River Water
Temperature	12° C	7.8° C	16° C
Salinity	31.2‰	33.2‰	3‰
Sigma-t	24	26	(~1)
Dissolved O_2 conc.	7 ml/l	4 ml/l	7 ml/l
pH	8.2	7.95	8.0
Alkalinity	2.21 mM	2.23 mM	0.8 mM
PCO_2	highly variable 200-300 ppm	$\geq$ 480 ppm	325 ppm

in calculations in a later section of this chapter. The "typical" values were obtained as follows: 1) Surface water properties observed 20 to 80 kilometers offshore on the Newport and Depoe Bay hydrographic lines were tabulated for the several upwelling season cruises discussed. A subjective attempt was made to identify water which would be lying just offshore of the front, between it and newly upwelling water. This was an effort to identify water which would be mixing

across the front with the upwelling water in the horizontal velocity shear zone separating them. 2) The upwelling water was identified by examination of vertical sections of sigma-t on the Depoe Bay and Newport hydrographic lines. (See Sect. 5.2.4.) Water which was penetrating to or nearly to the surface in relatively unmodified (by insolation or photosynthesis) condition was traced back along its isopycnal in the section to a point approximately 100 kilometers offshore. There, values of the various water properties were read off vertical sections of those properties, measured at the same time as the density data were measured. These data were also tabulated and "typical," or subjective estimations of the modal, values determined.

The values of temperature and salinity obtained in this way for the upwelling water were compared with similar water types identified by Pillsbury (1972) and Pattullo and Denner (1965). They obtained 8° C, 33.5‰ and 8.5° C, 33.5‰ for the temperature and salinity, respectively. As noted in Table 5.2,7. 8° C and 33.2‰ were found in this work.

3) The Columbia River water properties represent a set of "typical" (in the sense of the last paragraphs) values observed in the mouth of the River, just upstream of the entrance jetties. The water there already contains an admixture of about three percent seawater judging by its salinity. The values given are at best gross approximations. The hydrography at this location is strongly determined by

the state of the tides and river flow. The intent is to provide some estimation of very much lower estuarine water which is actively mixing with and diluting the regional surface seawater. In this treatment the variables temperature, salinity, and total alkalinity were held constant as pH changes. PCO_2 was then calculated as a function of these selected fixed variables and incremented hydrogen ion concentrations according to:

$$TA = CA + BA = CA + K'_B C_B/(K'_B + [H^+]) \qquad (5.1)$$

where C_B is total boron concentration, BA is borate alkalinity, and

$$PCO_2 = CA[H^+]^2/\left[K'_1\alpha([H^+] + 2K'_2)\right] \qquad (1.18)$$

The constants, α, K'_1, K'_2, and K'_B, were evaluated using the polynomials described in Appendix I based upon Lyman's (1956) work. The calculation used a program, CO2CALCS, written for the OSU CDC3300 digital computer. The values for temperature, salinity, and alkalinity were taken for the appropriate waters from Table 5.2.

The resulting curves have been plotted in Figs. 5.6 to 5.9. In Fig. 5.6 it may be seen that the observed points scatter about the calculated curves for regional surface water and the upwelling water. There is some spread of points below these curves which is bounded by the Columbia River water curve. However this scattering of the points about the calculated curves is somewhat fortuitous. First of

all there are several points which occurred in the Columbia River estuary and had low salinities which fall away from the Columbia River curve and close to the regional surface water and upwelling water curves. In these cases, however, the titration alkalinity was not the usual 0.8 meq/l which we observe for the Columbia River but was considerably higher, approximately 2.5 meq/l. Because the PCO_2 calculated from Eq. (1.18) is directly proportional to the carbonate alkalinity, one might expect the observed PCO_2 in these cases to be even higher for a given pH than was shown for these points. However, it may well be the case that all of the unusually large titration alkalinity observed for these points was not in fact carbonate alkalinity and so the abnormally large PCO_2 would not be so much greater than that calculated for the usual Columbia River alkalinity. Another factor which must be considered for this figure is the rather crude state of our art in measuring pH's during the time of this cruise as discussed in Sect. 5.2.2.

The much more coherent pH-PCO_2 picture displayed in Fig. 5.7 permits some rather more definite conclusions to be drawn. In the high PCO_2 waters representing the upwelling and recently upwelled water, there exists a systematic discrepancy toward the low PCO_2 side of the upwelling water curve. But the calculated curve has approximately the correct shape and the points are closely parallel to the upwelling water curve. Further, the series of points marked

with small boxes lies in the correct direction toward the Columbia River water curve and these points indeed corresponded to samples having low salinity; that is, they were samples of seawater rather highly diluted with Columbia River water.

The observed points in Fig. 5.8 lay even more closely along the calculated curves for the regional surface water and upwelling water and present a rather satisfactory picture. In this case it may be fairly said that the simple calculation presented here does, in fact, characterize the behavior of the waters off Oregon rather well. This is also true of the October 1969 data presented in Fig. 5.9. Here the observed data scatter rather symmetrically about the upwelling water curve and higher PCO_2's and cluster neatly between the regional surface water and upwelling water curves in the vicinity of atmospheric saturation.

These results are consistent with the open north Pacific Ocean observations shown in Fig. 3.4. There, when PCO_2 was calculated from not only the pH of the individual seawater samples but the individual observed temperature, salinity, and titration alkalinity as well, a close fit to the measured PCO_2 was obtained. A systematic discrepancy of 2.3% was found; that is, the calculated PCO_2 lay 2.3% on the average below the measured PCO_2, and the root mean square deviation from the ideal line of the individual points in that case was 4%.

The rather successful fitting of the observed points to theoretical curves, or put another way, of PCO_2 points calculated from pH and alkalinity to actual, observed PCO_2 values, would indicate that pH observations would provide a fruitful, alternative means for monitoring PCO_2 changes in the oceans as discussed in the previous section.

Another very important conclusion to be derived from this fit of the observed points to the theoretical curves is that the carbonate alkalinity in the regional waters off Oregon remains quite constant. This conclusion follows from the two facts that the carbonate alkalinity was assumed constant in the calculation of each of the curves in Figs. 5.6 through 5.9 and from the close fit of the curves calculated with this assumption to the observed data.

Contemporary efforts toward improving knowledge on the interrelationships among the constitutents of the marine carbon dioxide system should improve our ability to make this calculation even more accurately and precisely (Takahashi et al., 1970).

5.3.3 The AOU-PCO_2 relationship. A procedure was worked out to establish the functional relationship between AOU and PCO_2 in order to better understand the data in Figs. 5.10 to 5.13. Taking the values of T, S, pH and TA for regional surface water in Table 5.2, a pair of PCO_2 and total carbon dioxide values was calculated

using Eqs. (5.1), (1.18), and

$$TCO_2 = CA \frac{(1 + K'_2/[H^+] + [H^+]/K'_1)}{(1 + 2K'_2/[H^+])} \qquad (5.2)$$

[cf. Skirrow (1965, p. 266)].

AOU was assigned the value zero for this set of initial T, S, pH, and TA. (Actually this water was usually somewhat oversaturated with oxygen. For these conditions the PCO_2 is approximately equal to the atmospheric PCO_2. Therefore the calculated curve does not go precisely through the 0, 0 point.) Then the Redfield et al. (1963) model for the oxidation and reduction of hypothetical marine organic matter was used:

$$(CH_2O)_{106} \cdot 16NH_3 \cdot H_3PO_4 + 138O_2 =$$

$$106CO_2 + 16HNO_3 + H_3PO_4 + 122H_2O \qquad (5.3)$$

where $(CH_2O)_{106} \cdot 16NH_3 \cdot H_3PO_4$ represents a hypothetical average molecule of marine organic matter. From this model one derives:

$$\Delta TCO_2/\Delta AOU = 106/138 \text{ (molecules/molecule)}$$

$$= 0.0343 \text{ (m moles } CO_2\text{/ml AOU)} \qquad (5.4)$$

and this was used to calculate a series of incremented TCO_2 values corresponding to increments of AOU. With the new TCO_2 values and the original T, S, and CA, a new pH was calculated for each new TCO_2 value using:

$$[H^+] = (K_1'/2)(TCO_2/CA)\left\{[1 - (CA/TCO_2)] + \left[[1 - (CA/TCO_2)]^2 + 4(K_2'/K_1')(CA/TCO_2)[2 - (CA/TCO_2)]\right]^{\frac{1}{2}}\right\} \qquad (5.5)$$

This equation was taken from Takahashi et al. (1970, Eq. A6) and used after verification. Finally, PCO_2 was calculated for each of the pH values resulting from the increments in AOU, using Eq. (1.18), and the resulting points plotted on Figs. 5.10-5.13. This was done for the upwelling, regional surface, and Columbia River waters as characterized in Table 5.2.

In general the fit to the observed data is quite good, although apparent systematic discrepancies are evident. The scatter is rather large. In the case of Fig. 5.10 for cruise Y6806C the systematic error tends to always be in the direction of the zero AOU line indicating the possibility of active atmospheric exchange. It has been pointed out earlier in this work that Teal and Kanwisher have shown that atmospheric exchange is approximately 24 times faster for oxygen than for carbon dioxide.

The systematic discrepancies become greater at higher AOU's

in Figs. 5.11 and 5.12. This is perhaps because the calculation was made using the temperature, salinity, and total alkalinity for regional surface water whereas the higher AOU's occur in the upwelling or recently upwelled waters. This is probably only part of the answer, because the calculation is not extremely sensitive to temperature and salinity. The fit is quite good for Fig. 5.13, the late season, October 1969, cruise.

Despite the scatter in the data and the apparent systematic discrepancies, the calculated AOU-PCO_2 curves do generally describe the relationship. The fits are generally not as good as in the pH-PCO_2 curves. Larger errors for the oxygen data probably result from two causes: sampling errors are quite severe in dissolved oxygen work. Secondly, the particular modification of the Winkler method of analysis for dissolved oxygen which has been in use at Oregon State University for several years is not as accurate and precise as pH and PCO_2, relative to the observed variations.

5.3.4 The time scales of variations in PCO_2 distributions. Evident in the data presented in Figs. 5.14 through 5.29 are many variations on several time scales in the distributions of PCO_2. It would be impossible to examine all of the variations with time in a detailed fashion. However, in an effort to distill the essence of some of the more dramatic variations shown in those figures, Fig. 5.32 has been

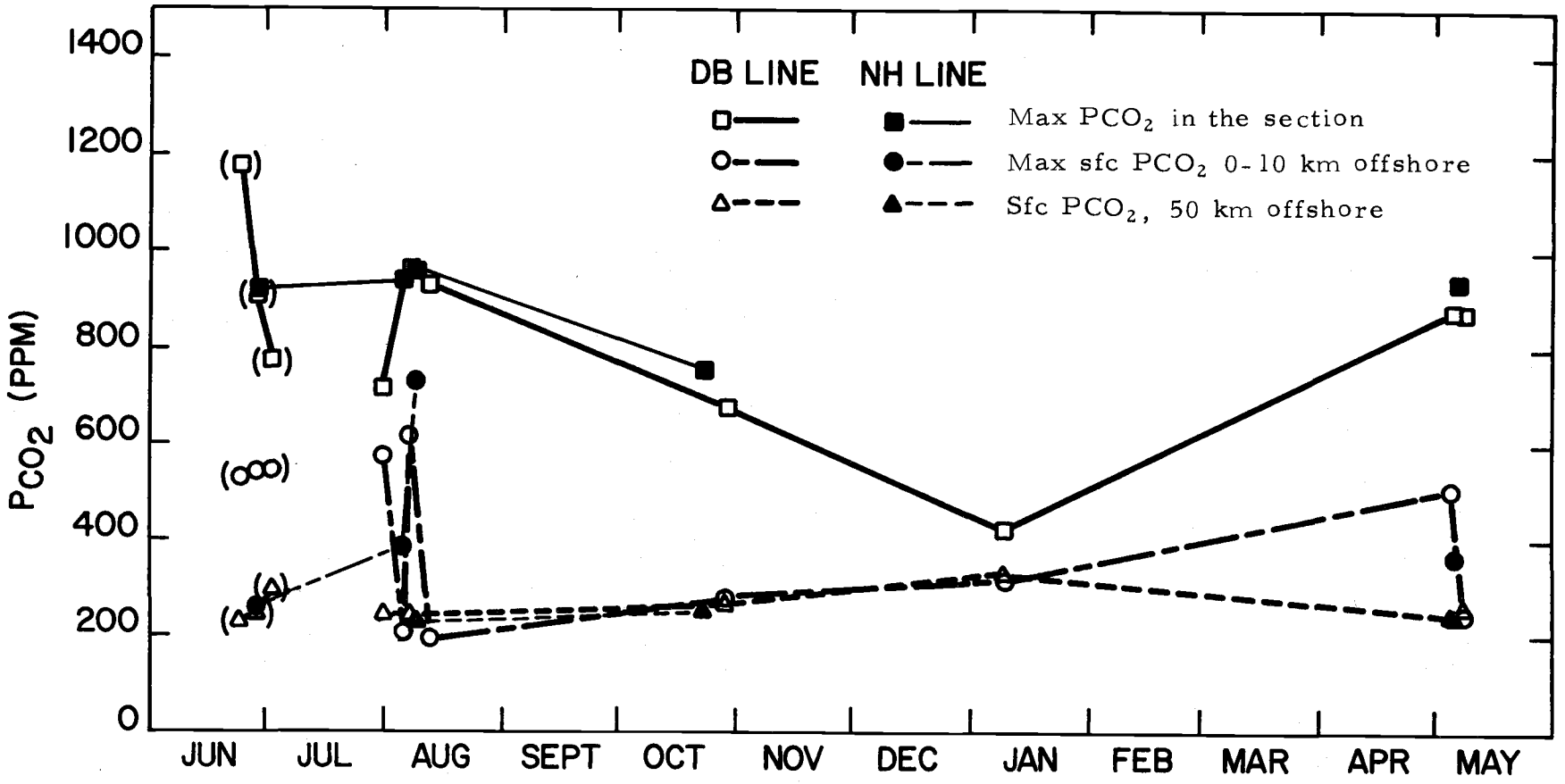

Fig. 5.32. Summary of the time scales of PCO_2 variations off Oregon. The parentheses denote data from 1968. The remaining points are from 1969 and 1970.

constructed. This summarizes the variations in PCO_2 observed on the Newport and Depoe Bay lines at three locations. The first location is in the region of the maximum PCO_2 observed in the entire section. This characteristically occurs near the bottom within five or ten kilometers of the shore. The next feature is the variation at the surface within five kilometers of the coast. Lastly, there have been plotted the surface observations 50 kilometers offshore.

With the use of this figure one can easily examine the variations on the time scales of two to five days, on the scale of seasonal variations, and to a very limited degree, the variation on the annual scale.

The short-term variability can be estimated from the repeated observations made at intervals of from two to five days on several of the cruises. We see that the variation is least at the surface 50 kilometers offshore. This location is more than 30 kilometers from the frontal system. Usually this water displays appreciable dilution by Columbia River water and is somewhat isolated horizontally and vertically from the surrounding ocean water. As the driving winds for upwelling intensify or weaken, this water simply moves somewhat more onshore or offshore and experiences little vertical or horizontal mixing on a dramatic scale within periods of two or three days. We see in Fig. 5.32 that the 50 kilometer offshore surface water points describe rather small fluctuations in PCO_2 amounting to perhaps 50 ppm as a maximum.

The values of PCO_2 at the deep inshore maximum, however, are much more variable on the short time scale. They range over excursions of 200-300 ppm. One would expect this as the result of the variability in the winds and the rather rapid response of the upwelling system to them. As the upwelling is intensified deeper waters more highly charged with carbon dioxide are moved up into the area sampled in this study. As the winds subside the upwelling water tends to sink below the depth sampled in this study and is replaced with water which has experienced more or less photosynthetic removal of carbon dioxide.

The most extreme short-term variations in PCO_2 are displayed by the waters at the surface within ten kilometers of the shore. Here the PCO_2 can vary by as much as 400 ppm in the space of five days.

The inshore surface waters are highly variable owing not only to the variability in upwelling but to the additional variability induced by biological processes as well. These cause an additional, spatial "patchiness" to the source-sink processes acting upon the carbon dioxide.

The seasonal variations are largely obscured by the short-term day-to-day variability. But some trends are evident which are consistent with what one might predict for the region. For example, the PCO_2 at the surface 50 kilometers offshore is lowest in the

summer, approaches atmospheric equilibrium through the fall and in winter, and is again undersaturated with respect to the atmosphere by May. This is consistent with a moderately intense photosynthetic consumption during the summer months in the plume waters which are somewhat isolated from the surrounding waters. The approach to atmospheric equilibrium through the fall and into the winter is consistent with diminished photosynthetic activity and greatly intensified fall and winter storm activity. A decrease to PCO_2's below that of the atmosphere by May is consistent with May being well within the early upwelling season and spring phytoplankton blooms.

The deep inshore maximum is highly variable as upwelling waxes and wanes seasonally. The summer upwelling maintains variable but very high PCO_2's ranging from 700-1200 ppm. Diminished upwelling and intensified vertical mixing in the winter make for a more uniform surface-to-50 meters distribution and as pointed out in the preceding paragraph, equilibration with respect to the atmosphere. Nevertheless one still sees the influence of vertical mixing with high PCO_2 waters from depth, and possibly addition to the water column from the bottom sediments as will be discussed in the following section. By May one sees almost the same picture as in June with early season upwelling already bringing high PCO_2 waters into the 55 meter deep region being sampled.

The seasonality of the inshore surface maximum is quite

interesting. The PCO_2's at the coast in the surface waters exhibit a great day-to-day variability and show many, very high values during the upwelling season. By autumn, upwelling has for the most part subsided in so far as surface manifestations are concerned and the variability in the nearshore surface waters diminishes greatly. These waters now resemble the offshore surface waters (cf. Fig. 5.32, October, January).

The year-to-year variability of PCO_2 in the waters off Oregon is not well established from the data presented here. The day-to-day variability certainly obscures annual variations. To draw conclusions on the annual variations would require a study over several years with very careful attention to long-term reproducibility of the data.

5.3.5 Indications of a carbon trap on the continental shelf off Oregon. It was noted in the discussions of Figs. 5.17, 5.18, 5.19, 5.21 and 5.23 that the PCO_2 contours were much more steeply inclined upward as one approached shore in the region of zero to 25 kilometers offshore. (Although not noted in the presentation of the results, this is also true in Figs. 5.14 and 5.20.) If the deep water were advecting onshore in this region, along the isopycnals, in other words quasi-isentropically, then the water would be moving against the PCO_2 gradient. That is to say, that as the water was moving shoreward

its carbon dioxide partial pressure was increasing. This could only take place: 1) if there were a source of carbon dioxide within the water itself; 2) within waters mixing with it across the isopycnals, or 3) within the sea floor with which it was in contact.

The first possibility, that there might be a source of carbon dioxide within the incipient upwelling water itself is conceivable, but the rate of oxidation of organic material in this water would most likely be somewhat slow. The most labile compounds would have already been oxidized by the time the PCO_2 had attained such high values as 700-900 ppm. However, it is quite possible that as the upwelling water had moved inshore there could have rained into it a substantial stream of biological debris from the overlying waters. This material might then form the carbon source within the incipient upwelling water itself. The second possibility, that of the incipient upwelling water mixing with waters containing carbon is quite similar. In this case, the overlying waters probably have higher biomasses and the mixing process is simply an alternative one to a "fallout" or rainout of biological material from above. The third possibility, that of diffusion or turbulent mixing upward from the sea floor of carbon, is only a reversal of the direction of transport from an external source.

Another explanation could be that there was a carbon dioxide source north or south of these sections in waters of comparable

density. With the data presented here it is not possible to identify a north-south gradient in PCO_2 by comparison of the Newport and Depoe Bay lines. The possibility of the pulp mill effluent which originates in Toledo, Oregon, inland of Newport has also been considered. It would seem that the volume of the ocean affected is far too great for any realistic flow of the pulp mill effluent. In addition, the low density of the effluent would cause it to float toward the ocean surface rather than remain at depth.

Considering the evidence it seems reasonable to postulate as possible, a cyclic process wherein deep water carbon dioxide is continually added to the coastal system during the upwelling season. This takes place as the deeper water moves shoreward at moderate depths and ultimately upwells. In the return, seaward flow at the surface, or near surface, part of the carbon dioxide is removed into the biomass via photosynthesis. Some of this is scavenged or falls out of the water column toward the bottom. Here it enters the sediments and/or the benthos. It is then oxidized in part and returns to the shoreward moving water just above the bottom. The result is a cycle in which carbon dioxide concentrations are built up to high levels in a relatively narrow coastal band. With the cessation of upwelling in the fall the carbon trapped in the sediments and benthos continues to decay and for some time furnishes a continued source of carbon dioxide to the bottom waters.

Certainly, more detailed sampling designed to specifically test for this phenomenon would be desirable. One could envision for this purpose cooperative work between benthic ecologists, microbiologists and chemical and physical oceanographers.

5.4 Summary

From the results and discussion presented in this chapter it was concluded that PCO_2 used with selected hydrographic variables can be a powerful tool for indicating and locating coastal upwelling. Its use complements the use of temperature or salinity or preferably both. pH could be equally well used for this purpose except that it only indirectly indicates the removal or addition of carbon dioxide by biological processes. For many studies this would not be desirable and the data would be more useful when converted to PCO_2.

That monitoring of pH in order to estimate PCO_2 changes is a feasible procedure is borne out by the next part of this study. This showed that the coherent behavior of PCO_2 and pH could be predicted quite satisfactorily.

The coherent behavior of AOU and PCO_2 was less satisfactorily predicted. This was largely a result of the relatively poor precision and accuracy of dissolved oxygen sampling and analysis.

The data presented in this work allowed some insight into the time variations of PCO_2 in the waters off Oregon. It was found that

during the upwelling season the high PCO_2's observed nearshore near the bottom were quite variable, varying by 200-300 ppm. The nearshore surface waters varied even more widely during the upwelling season by up to 500 ppm. In contrast, during the fall and winter the few data presented indicated that there was far less variability on a day-to-day scale in PCO_2. Despite the wide day-to-day variations found, there were indications of seasonal trends with high PCO_2 found during the upwelling season in the near bottom waters inshore and low values being found there in the winter.

The surface waters offshore showed much less variability even during the upwelling season and indicated a predictable gradual rise in PCO_2 from 50 to 70 ppm undersaturation during upwelling season to approximate atmospheric saturation in the winter.

This work also indicates the possible presence of a carbon trap on the continental shelf off Oregon. It is concluded that this might form the basis of a profitable field experiment to look specifically for this feature.

CHAPTER 6

SUMMARY AND CONCLUSIONS

A system for continuous, semi-automated measurement of PCO_2 in ocean surface waters and at depths to 100 meters has been described. The system is relatively simple and portable. It may be operated for periods of several weeks at sea with little malfunctioning. Those malfunctions which have occurred have been repairable at sea because of the simplicity of the system. The portability of the system permits easy transport from the shore laboratories to the ship either by truck or air freight.

The system employs a non-dispersive infrared gas analyzer to measure the concentration of CO_2 in an air stream which has been equilibrated with the seawater whose PCO_2 is desired. The response times of the equilibrator and of the system have been calculated from simplified models and compared with experimentally determined response times. Under varying conditions of air and seawater flow rates through the equilibrator the calculated response times were about 1/2 the observed response times. The discrepancies may be attributed to the oversimplified model employed or to an effect of the air stream drying agent employed.

The system has a response time of 40 seconds which allows a

99% response to horizontal PCO_2 features of scale one kilometer or greater, when operating on a ship traveling at a speed of ten knots. There will be a lag in indicated position of such features of one kilometer under these conditions.

The calibration of the system was accomplished using standard gases furnished by the CO_2 project laboratories at the Scripps Institution of Oceanography. These gases lay in the concentration range of 282-348 ppm. The calibration range was extended with the use of zero concentration gases in the form of commercially available prepurified nitrogen and a simple gas-dilution apparatus. A nonlinear calibration formula was derived to permit operation of the analyzer over almost any desired concentration range rather than only the two ranges for which it had been calibrated by the manufacturer.

The system has a precision of ±1% and an estimated accuracy of ± 5%.

A discussion is presented of the corrections which must be applied to the data as a result of pressure differences which occur in the analyzer between the calibration and seawater measurement modes of operation. Because the air stream must be dried before analysis the observed PCO_2 must be corrected back to the conditions before drying. This correction is discussed.

When a seawater sample is pumped or otherwise transported to the equilibrator, its temperature is generally increased by a few

tenths of a degree Celsius. Magnitudes which have been published for the temperature correction vary from one to seven percent of the value of PCO_2 observed per degree Celsius. In this work, a correction was calculated theoretically for the restraints that the salinity, alkalinity, and total carbon dioxide concentration of the seawater sample are invariant. The resultant correction, approximately +4%/°C, agrees well with that measured directly by Kanwisher (1960), +4.5%/°C, over a more limited temperature, salinity, and alkalinity range.

Measurements of time variations of surface PCO_2 distributions were made in the subarctic North Pacific Ocean. Between October 1968 and March-April 1969 the PCO_2 was observed to increase by an average of 60 ppm. This was attributed to wintertime mixing of deep, high PCO_2 waters into the surface layers which had been depleted in CO_2 during the summer phytoplankton blooms. By October the photosynthetic activity of the phytoplankton had ceased but the PCO_2 of the surface waters remained low because of relatively slow exchange of CO_2 between the atmosphere and sea and because of inhibited vertical mixing through the summer pycnocline. An additional rise in PCO_2 of 18 ppm occurred in a period of 30-45 days in March and April 1969 in part of the region largely because of spring warming of the surface waters.

Not only did the PCO_2 rise 60 ppm from October 1968 to

March-April 1969 but the direction of the air-sea gradient reversed. Thus much of the Pacific subarctic waters observed changed roles from oceanic sinks to sources for atmospheric CO_2 during the half-year period.

The present work has extended the mapping of summertime PCO_2 distributions in surface waters of the Pacific Ocean and Bering Sea. Keeling's (1968) "Global Distribution" chart included data only as far north as 35° N. This work fills in the gap in the subarctic Pacific and the Bering Sea to 55° N. High surface PCO_2 was found along the Aleutian Island arc reflecting conditions of local upwelling and or intense vertical mixing near the passes between the islands. Seasonal depletion of CO_2 by photosynthesis was evident in both the central Bering Sea and central subarctic Pacific. There was also evidence of CO_2 supersaturation in surface waters off the mouths of large rivers such as the Yukon and Kuskokwim.

The use of PCO_2 as a surface indicator of upwelling was tested using data obtained in 1968, 1969, and 1970 off the Oregon and Washington coasts. A very large range of PCO_2 in the surface waters was observed, 155-525 ppm. The PCO_2 correlated with other physical and chemical variables measured and could be explained in terms of the presence of the Columbia River plume, active photosynthesis, and coastal upwelling. Because of the large PCO_2 difference between the PCO_2 of ambient surface waters and the upwelling water and because

of the ease of making continuous underway surface measurements with the PCO_2 system, PCO_2 indeed serves as a convenient indicator of coastal upwelling.

The interrelationship of the observed PCO_2 and pH distributions in the upwelling region off Oregon was examined. It was found that variations in pH and PCO_2 were quite coherent. This leads to two conclusions. First, that pH as well as PCO_2 could serve as an alternate means of monitoring upwelling and biological processes off Oregon. Second, one can infer that the carbonate alkalinity in the waters off Oregon remains relatively constant. This follows from the fact that calculated curves, assuming constant carbonate alkalinity, fitted the observed pH-PCO_2 data quite well.

The covariance of PCO_2 and apparent oxygen utilization was also examined. In this case the relatively poor coherence between these variables argues against the use of dissolved oxygen to monitor the biological processes associated with upwelling. The scatter in the relationship was attributed to two causes. The first cause is the more rapid exchange of oxygen compared to carbon dioxide between the atmosphere and sea. The second cause was probably inferior accuracy and precision in dissolved oxygen measurement compared to PCO_2 measurement.

The PCO_2 system has also been applied to a study of the time scales of PCO_2 variations in the upwelling regions along the Oregon

coast. The range of time scales investigated included a few days to a few months. Evidence is given that even though the regional surface waters may reequilibrate with the atmosphere by January, the near bottom waters at depths of 50 meters are still not in equilibrium. This implies a flux of CO_2 from deep waters or the bottom sediments during most of the year.

Comparison of vertical sections made perpendicular to the coast for density and PCO_2 gave some evidence of existence of a carbon trap on the shelf near the coast. This carbon trap was postulated to be the result of a cyclical process wherein a fraction of the carbon dioxide entering the upwelling region at depth was fixed into organic matter in photosynthesis and trapped in the biomass in the water column over the shelf and in the benthos or sediments at the bottom of the water column. It would seem that a detailed study to confirm or disprove the existence of this carbon trap would be an interesting field for future research.

BIBLIOGRAPHY

Akiyama, T. 1968. Partial pressure of carbon dioxide in the atmosphere and in sea water over the western north Pacific Ocean. Oceanographical Magazine 20(2): 133-146.

Akiyama, T. 1969a. Carbon dioxide in the atmosphere and in sea water in the adjacent seas of Japan. Oceanographical Magazine 21(1): 53-59.

Akiyama, T. 1969b. Carbon dioxide in the atmosphere and in sea water over the western north Pacific Ocean. Oceanographical Magazine 21(2): 121-127.

Akiyama, T. 1969c. Carbon dioxide in the atmosphere and in sea water in the Pacific Ocean east of Japan. Oceanographical Magazine 21(2): 129-135.

Alvarez-Borrego, S. 1970. Chemico-oceanographical parameters of the central north Pacific Ocean. Master's thesis. Corvallis, Oregon State University. 84 numb. leaves.

Alvarez-Borrego, S. and P. K. Park. 1971. AOU as indicator of water-flow direction in the central North Pacific. Journal of the Oceanographical Society of Japan 27(4): 142-151.

Alvarez-Borrego, S., L. I. Gordon, L. B. Jones, P. K. Park, and R. M. Pytkowicz. 1972. Oxygen-carbon dioxide-nutrients relationships in the southeastern region of the Bering Sea. Journal of the Oceanographical Society of Japan 28(2): 71-93.

Anderson, D. H. and R. J. Robinson. 1946. Rapid electrometric determination of the alkalinity of sea water using a glass electrode. Industrial and Engineering Chemistry, Analytical ed. 18: 767-773.

Atlas, E. L., S. W. Hager, L. I. Gordon and P. K. Park. 1971. A practical manual for use of the Technicon AutoAnalyzer® in seawater nutrient analyses; revised. 49 numb. leaves. (Oregon State University, Dept. of Oceanography, Technical report 215, Reference no. 71-22)

Bainbridge, A. 1969. Associate Research Physicist. Scripps Institution of Oceanography, University of California at San Diego. Personal communication. La Jolla, California. 21 January.

Ball, D. S. 1970. Seasonal distributions of nutrients off the coast of Oregon, 1968. Master's thesis. Corvallis, Oregon State University. 71 numb. leaves.

Barraclough, W. E., R. J. Lebrasseur and O. D. Kennedy. 1969. Shallow scattering layer in the subarctic Pacific Ocean: Detection by high-frequency echo sounder. Science 166: 611-613.

Barstow, D., W. Gilbert and B. Wyatt. 1969. Hydrographic data from Oregon waters 1968. 84 numb. leaves. (Oregon State University, Dept. of Oceanography. Data report no. 36, Reference 69-6, on Office of Naval Research Contract N00014-67-A-0369-0007 Project NR083-102)

Bates, R. G. 1964. Determination of pH theory and practice. New York, John Wiley & Sons, Inc. 435 p.

Ben-Yaakov, S. 1970. A method for calculating the in situ pH of seawater. Limnology and Oceanography 15(2): 326-328.

Broecker, W. S. and T. Takahashi. 1966. Calcium carbonate precipitation on the Bahama Banks. Journal of Geophysical Research 71(6): 1575-1602.

Buch, K. 1951. Das Kohlensäure gleichgewichtssystem im Meerwasser. Havsforsknings Institutets Skrift, Helsingfors. No. 151: 3-18 (Photocopy)

Carpenter, J. H. 1966. New measurements of oxygen solubility in pure and natural water. Limnology and Oceanography 11: 264-277.

Culberson, C., R. M. Pytkowicz, and J. E. Hawley. 1970. Seawater alkalinity determination by the pH method. Journal of Marine Research 28(1): 15-21.

Culberson, C. H. 1972. Program DATA. In: Processes affecting the oceanic distribution of carbon dioxide. Doctoral dissertation. Corvallis, Oregon State University. 178 numb. leaves.

Deffeyes, K. S. 1965. Carbonate equilibria: A graphic and algebraic approach. Limnology and Oceanography 10(3): 412-426.

Dodimead, A. J., F. Favorite, and T. Hirano. 1963. Salmon of the North Pacific Ocean: Part II. Review of Oceanography of the Subarctic Pacific Region. International North Pacific Fish Commission Bulletin No. 13. 195 p.

Dyrssen, D. and L. G. Sillén. 1967. Alkalinity and total carbonate in seawater. A plea for p-T-independent data. Tellus 19(1): 113-121.

Edmond, J. M. 1970. The carbonic acid system in sea water. Doctoral dissertation. San Diego, University of California. 174 numb. leaves. (Microfilm-xerograph)

Edsall, J. T. 1969. Carbon dioxide, carbonic acid, and bicarbonate ion: Physical properties and kinetics of interconversion. In: CO_2: Chemical, biochemical, and physiological aspects: Symposium held at Haverford College, Haverford, Pennsylvania 1968. ed. by R. E. Forster, J. T. Edsall, A. B. Otis and F. J. W. Roughton. Washington, D. C. (NASA SP-188) p. 15-27.

Eriksson, E. 1963. Possible fluctuations in atmospheric carbon dioxide due to changes in properties of the sea. Journal of Geophysical Research 68: 3871-3876.

Favorite, F. 1966. Bering Sea. In: The Encyclopedia of Oceanography, ed. by R. W. Fairbridge, Reinhold, New York. p. 135-140.

Fisheries Research Board of Canada. 1970. Data record first Canadian trans-Pacific oceanographic cruise March to May, 1969 biological, chemical and physical data. Biological Station, Nanaimo, British Columbia, Canada. Manuscript Report Series No. 1080. 92 p.

Forster, R. E., J. T. Edsall, A. B. Otis, and F. J. W. Roughton. 1969. CO_2: Chemical, biochemical, and physiological aspects. A symposium held at Haverford College, Haverford, Pennsylvania 1968. Washington, D. C. 291 p. (NASA SP-188)

Garrels, R. M. and M. E. Thompson. 1962. A chemical model for sea water at 25° C and one atmosphere total pressure. American Journal of Science 260: 57-66.

Garrels, R. M. and C. Christ. 1965. Minerals, solutions and equilibria. New York, Harper and Row, 450 p.

Gilbert, W. E., W. M. Pawley and K. Park. 1968. Carpenter's oxygen solubility table and nomograph for sea water as a function of temperature and salinity. Journal of Oceanographical Society Japan 23: 252-255.

Gordon, L. I. and P. K. Park. 1968. Carbon dioxide tension measurements in surface waters off the Oregon coast as an indicator of upwelling. (Abstract) Transactions, American Geophysical Union 49: 642.

Gordon, L. I., J. J. Kelley, D. W. Hood and P. K. Park. 1970. Carbon dioxide in the surface waters of the Bering Sea and northwest Pacific Ocean, late summer. (Abstract) Transactions, American Geophysical Union 51: 326.

Gordon, L. I., P. K. Park, S. W. Hager, and T. R. Parsons. 1971. Carbon dioxide partial pressures in North Pacific surface waters - time variations. Journal of Oceanographical Society Japan 27: 81-90.

Gordon, L. I. and P. K. Park. 1972a. Oregon State University PCO_2 data: 1968. (Oregon State University, School of Oceanography. Data report, in preparation)

Gordon, L. I. and P. K. Park. 1972b. Oregon State University PCO_2 data: 1969. (Oregon State University, School of Oceanography. Data report, in preparation)

Gordon, L. I. and P. K. Park. 1972c. Oregon State University PCO_2 data: 1970. (Oregon State University, School of Oceanography. Data report, in preparation)

Gordon, L. I. and P. K. Park. 1972d. A continuous PCO_2 measurement system. 101 numb. leaves. (Oregon State University, School of Oceanography. Technical Report 240, Reference 72-17, on Office of Naval Research Contract N00014-67-A-0369-0007 Project NR 083-102 and NSF Grants GA 1281 and GA 12113)

Gran, G. 1952. Determination of the equivalence point in potentiometric titrations. Part II. The Analyst 77: 661-671.

Guenther, P. 1971. Staff Research Associate. Scripps Institution of Oceanography, University of California at San Diego. Personal communication. La Jolla, California. 11 February.

Harvey, H. W. 1955. The chemistry and fertility of sea waters. Cambridge, University Press. 224 p.

Ivanenkov, V. I. 1964. Hydrochemistry of the Bering Sea. Akademiya Nauk SSSR, Izdatel'stvo Nauka, Moscow. 137 p.

Kantz, K. W., L. I. Gordon and P. K. Park. 1972. Oregon State University PCO_2 data: 1971. (Oregon State University, School of Oceanography. Data report, in preparation)

Kantz, K. W. 1973. Chemistry and hydrography of Oregon coastal waters and the Willamette and Columbia Rivers: March and June, 1971. Master's thesis. Corvallis, Oregon State University. (in preparation)

Kanwisher, J. 1960. pCO_2 in sea water and its effect on the movement of CO in nature. Tellus 12(2): 209-215.

Kanwisher, J. 1963. On the exchange of gases between the atmosphere and the sea. Deep-Sea Research 10: 195-217.

Keala, B. A. 1965. Table of sigma-t with intervals of 0.1 for temperature and salinity. 186 p. (U. S. Fish and Wildlife Service Special Scientific Report--Fisheries No. 506)

Keeling, C. D. 1965. Carbon dioxide in surface waters of the Pacific Ocean 2. Calculation of the exchange with the atmosphere. Journal of Geophysical Research 70(24): 6099-6102.

Keeling, C. D., N. W. Rakestraw and L. S. Waterman. 1965. Carbon dioxide in surface waters of the Pacific Ocean 1. Measurements of the distribution. Journal of Geophysical Research 70: 6087-6097.

Keeling, C. D. 1968. Carbon dioxide in surface ocean waters. 4. Global distribution. Journal of Geophysical Research 73(14): 4543-4553.

Keeling, C. D. and L. S. Waterman. 1968. Carbon dioxide in surface ocean waters 3. Measurements on Lusiad expedition 1962-1963. Journal of Geophysical Research 73(14): 4529-4541.

Keeling, C. D. and B. Bolin. 1968. The simultaneous use of chemical tracers in oceanic studies II. A three-reservoir model of the North and South Pacific Oceans. Tellus 20(1): 17-54.

Keeling, C. D. and L. S. Waterman. 1968. Shipboard carbon dioxide project. Report no. 3. January 1, 1968. 185 numbered leaves. (University of California, San Diego, Scripps Institution of Oceanography)

Kelley, J. J. 1968. Carbon dioxide in the seawater under the Arctic ice. Nature 218(5144): 862-864.

Kelley, J. J. 1970. Carbon dioxide in the surface waters of the North Atlantic Ocean and the Barents and Kara Seas. Limnology and Oceanography 15(1): 80-87.

Kelley, J. J. and D. W. Hood. 1971. Carbon dioxide in the Pacific Ocean and Bering Sea: upwelling and mixing. Journal of Geophysical Research 76(3): 745-752.

Kelley, J. J., L. L. Longerich, and D. W. Hood. 1971. Effect of upwelling, mixing, and high primary productivity on CO_2 concentrations in surface waters of the Bering Sea. Journal of Geophysical Research 76(36): 8687-8693.

Kern, David M. 1960. The hydration of carbon dioxide. Journal of Chemical Education 37: 14-33.

Li, Y-H., T. Takahashi, and W. S. Broecker. 1969. Degree of saturation of $CaCO_3$ in the oceans. Journal of Geophysical Research 74(23): 5507-5525.

Li, Y-H. and T-F. Tsui. 1971. The solubility of CO_2 in water and sea water. Journal of Geophysical Research 76(18): 4203-4207.

List, R. J., Ed. 1966. Smithsonian Meteorological Tables. Sixth Revised Edition. Smithsonian Miscellaneous Collections, vol. 114 (whole volume) Smithsonian Institution, City of Washington. 527 p.

Lyman, J. 1956. Buffer mechanism of sea water. Doctoral dissertation. La Jolla. University of California, Los Angeles. 196 numbered leaves. (Photocopy)

Miyake, Y. and Y. Sugimura. 1969. Carbon dioxide in the surface water and the atmosphere in the Pacific, the Indian and the Antarctic Ocean areas. Records of Oceanographic Works in Japan 10(1): 23-28.

Mooers, C. N. K., C. A. Collins, and R. L. Smith. 1972. The dynamic structure of the frontal zone in the coastal upwelling region off Oregon. Submitted to the Journal of Physical Oceanography.

Munk, W. H. 1966. Abyssal recipes. Deep-Sea Research 13: 707-730.

Murray, C. N and J. P. Riley. 1971. The solubility of gases in distilled water and sea water--IV. Carbon dioxide. Deep-Sea Research 18: 533-541.

Pak, H., G. F. Beardsley, Jr., and R. L. Smith. 1970a. An optical and hydrographic study of a temperature inversion off Oregon during upwelling. Journal of Geophysical Research 75(3): 629-636.

Pak, H., G. F. Beardsley, Jr., and P. K. Park. 1970b. The Columbia River as a source of marine light-scattering particles. Journal of Geophysical Research 75(24): 4570-4578.

Park, K., J. G. Pattullo, and B. Wyatt. 1962. Chemical properties as indicators of upwelling along the Oregon coast. Limnology and Oceanography 7(3): 435-437.

Park, P. K., G. H. Kennedy, and H. H. Dobson. 1964. Comparison of gas chromatographic method and pH-alkalinity method for determination of total carbon dioxide in sea water. Analytical Chemistry 36: 1686.

Park, K. 1965a. Gas chromatographic determination of dissolved oxygen, nitrogen, and total carbon dioxide in sea water. Journal of Oceanographical Society Japan 21: 28-29.

Park, K. 1965b. Total carbon dioxide in sea water. Journal of Oceanographical Society Japan 21: 54-59.

Park, K. 1967. Nutrient regeneration and preformed nutrients off Oregon. Limnology and Oceanography 12(2): 353-357.

Park, P. K. 1969. Oceanic CO_2 system: An evaluation of ten methods of investigation. Limnology and Oceanography 14(2): 179-186.

Park, P. K., G. R. Webster and R. Yamamoto. 1969a. Alkalinity budget of the Columbia River. Limnology and Oceanography 14(4): 559-567.

Park, P. K., L. I. Gordon, S. W. Hager and M. C. Cissell. 1969b. Carbon dioxide partial pressure in the Columbia River. Science 166: 867-868.

Park, P. K., L. I. Gordon, and S. Alvarez-Borrego. 1972. The carbon dioxide system of the Bering Sea. Presented at the Bering Sea Symposium section on Dynamics of Chemical Parameters. Dr. Y. Kitano, Convener. 31 January-4 February 1972, Hakodate, Japan. 82 p. (preprint)

Parsons, T. R. and G. C. Anderson. 1970. Large scale studies of primary production in the North Pacific Ocean. Deep-Sea Research 17: 765-776.

Pattullo, J. and W. Denner. 1965. Processes affecting seawater characteristics along the Oregon coast. Limnology and Oceanography 10(3): 443-450.

Pawley, W. 1969. Computer Programmer. Oregon State University, Dept. of Oceanography. Personal communication. Corvallis, Oregon. 1 April.

Pillsbury, D. and J. Bottero. 1971. Average nearshore sections from the Newport hydrographic line during the upwelling season. Unpublished. Corvallis, Oregon State University, Dept. of Oceanography. 43 p.

Pillsbury, R. D. 1972. A description of hydrography, winds, and currents during the upwelling season near Newport, Oregon. Doctoral dissertation. Corvallis, Oregon State University. 163 numb. leaves.

Pytkowicz, R. M., D. R. Kester and B. C. Burgener. 1966. Reproducibility of pH measurements in sea water. Limnology and Oceanography 11(3): 417-419.

Pytkowicz, R. M. and D. R. Kester. 1966. Oxygen and phosphate as indicators for the deep intermediate waters in the northeast Pacific Ocean. Deep-Sea Research 13: 373-379.

Pytkowicz, R. M. 1968. The carbon dioxide-carbonate system at high pressures in the oceans. Oceanography and Marine Biology Annual Reviews, 6: 83-135.

Redfield, A. C., B. H. Ketchum and F. A. Richards. 1963. 2. The influence of organisms on the composition of seawater. In: The sea. Vol. 2. ed. by M. N. Hill, New York, John Wiley & Sons. p. 26-77.

Reed, R. K. and N. P. Laird. 1971. Thermohaline inversions near the Subarctic Boundary in the western Pacific. Unpublished manuscript. Seattle, Washington. 16 p.

Revelle, R. and H. E. Suess. 1957. Carbon dioxide exchange between atmosphere and ocean and the question of an increase of atmospheric CO_2 during the past decades. Tellus 9(1): 18-27.

Schonzeit, M. H. 1973. Relationships between lower trophic levels and hydrography during an upwelling season off Oregon. Master's thesis. Corvallis, Oregon State University. 102 numb. leaves.

Seki, H. 1970. Microbial biomass in the euphotic zone of the North Pacific subarctic water. Pacific Science 24: 269-274.

Skirrow, G. 1965. The dissolved gases - carbon dioxide. In: Chemical oceanography. Vol. 1. ed. by J. P Riley and G. Skirrow, London and New York, Academic Press. p. 227-322.

Smith, R. L. 1968. Upwelling. Oceanography and Marine Biology Annual Reviews 6: 11-46.

Sokolnikoff, I. S. and R. M. Redheffer. 1958. Mathematics of physics and modern engineering. New York, McGraw-Hill. 810 p.

Stefánsson, U. and F. A. Richards. 1963. Processes contributing to the nutrient distributions off the Columbia River and Strait of Juan de Fuca. Limnology and Oceanography 8: 394-410.

Stefánsson, U. 1968. Dissolved nutrients, oxygen and water masses in the Northern Irminger Sea. Deep-Sea Research 15: 541-575.

Stephens, K. 1970. Automated measurement of dissolved nutrients. Deep-Sea Research 17: 393-396.

Strickland, J. D. H. and T. R. Parsons. 1968. A practical handbook of seawater analysis. Fisheries Research Board of Canada, Ottawa. Bulletin 167. 311 p.

Stumm, W. and J. J. Morgan. 1970. Aquatic Chemistry. New York, Wiley, 1970. 583 p.

Sugimura, Y. and Y. Hirao. 1970. Carbon dioxide in the atmosphere and in the surface sea water. In: Preliminary report of the Hakuho Maru cruise KH-68-4 (Southern Cross Cruise), ed. by Y. Horibe, Tokyo, Ocean Research Institute, University of Tokyo, p. 67-68.

Sugiura, Y. and H. Yoshimura. 1964. Distribution and mutual relation of dissolved oxygen and phosphate in the Oyashio and the northern part of Kuroshio regions. Journal of Oceanographical Society Japan 20: 14-23.

Sugiura, Y. 1965. On the reserved nutrient matters. La mer; Bulletin de la Société franco-japonaise d' océanographie 2(2): 87-91.

Sverdrup, H. U., M. W. Johnson and R. H. Fleming. 1942. The oceans. New York, Prentice-Hall, Inc. 1087 p.

Swinnerton, J. W., V. J. Linnenbom, and C. H. Cheek. 1962. Determination of dissolved gases in aqueous solution by gas chromatography. Analytical Chemistry 34: 483-485.

Takahashi, T. 1961. Carbon dioxide in the atmosphere and in Atlantic ocean water. Journal of Geophysical Research 66: 477-494.

Takahashi, T., R. F. Weiss, C. H. Culberson, J. M. Edmond, D. E. Hammond, C. S. Wong, Y. Li and A. E. Bainbridge. 1970. A carbonate chemistry profile at the 1969 GEOSECS intercalibration station in the eastern Pacific Ocean. Journal of Geophysical Research 75(36): 7648-7666.

Teal, J. M. and J. Kanwisher. 1966. The use of PCO_2 for the calculation of biological production, with examples from waters off Massachusetts. Journal of Marine Research 24(1): 4-14.

U. S. Weather Bureau. 1953. Relative humidity-psychrometric tables, Celsius (Centigrade) temperatures. Rev. ed. by Technical Investigators Section, Station Facilities and Meteorological Observations Division. Washington, D. C. 32 p.

Waterman, L. S. 1965. Carbon dioxide in surface waters. Nature 205: 1099-1100.

Weiss, R. F. 1970. Dissolved gases and total inorganic carbon in seawater: Distribution, solubilities, and shipboard gas chromatography. Doctoral dissertation. San Diego, University of California. 130 numb. leaves.

Wickett, W. P. 1969. Water masses encountered in March and April during Transpac 69 cruise. Paper presented at 16th annual meeting of International North Pacific Fisheries Commission (Document Number 1233), September 30, Vancouver, British Columbia, Canada. 3 p.

Wong, C. S. 1968. The distribution of inorganic carbon in the eastern tropical Pacific Ocean. Doctoral dissertation. San Diego, University of California. 123 numb. leaves. (Microfilm-xerograph)

Wooster, W. S., A. J. Lee and G. Dietrich. 1969. Redefinition of salinity. Deep-Sea Research 16: 321-322.

Wyatt, B., W. Gilbert, L. I. Gordon and D. Barstow. 1970. Hydrographic data from Oregon waters 1969. 155 numb. leaves. (Oregon State University, Dept. of Oceanography. Data report no. 42, Reference 70-12, on Office of Naval Research Contract N00014-67-A-0369-0007 Project NR 083-102)

Wyatt, B., R. Tomlinson, W. Gilbert, L. Gordon and D. Barstow. 1971. Hydrographic data from Oregon waters 1970. 134 numb. leaves. (Oregon State University, Dept. of Oceanography. Data report 49, Reference 71-23, on Office of Naval Research Contract N00014-67-A-0369-0007 Project NR 083-102 and NSF Grant GA 12113)

Wyatt, B., R. Tomlinson, W. Gilbert, L. Gordon and D. Barstow. 1972. Hydrographic data from Oregon waters 1971. 77 numb. leaves. (Oregon State University, Dept. of Oceanography. Data report no. 53, Reference 72-14 on Office of Naval Research Contract N00014-67-A-0369-0007 Project NR 083-102 and NSF Grant GA 12113)

Wyrtki, K. 1962. The oxygen minima in relation to ocean circulation. Deep-Sea Research 9: 11-23.

APPENDICES

APPENDIX I

POLYNOMIAL FIT TO TEMPERATURE AND CHLORINITY OF BUCH'S CO_2 SOLUBILITY AND LYMAN'S CARBONIC AND BORIC ACID DISSOCIATION CONSTANTS

Introduction

To facilitate theoretical calculations by computer in the carbonic acid system in seawater it is helpful to have the necessary "constants" expressed as mathematical functions of the seawater temperature and salinity. The constants required are α, the solubility of CO_2 in seawater; K'_1 and K'_2, the apparent first and second dissociation constants of carbonic acid in seawater; and K'_B, the dissociation constant of boric acid in seawater. I was not aware of any published mathematical expressions for these constants at the time I began this work. Since that time various workers have derived and published equation (for instance: Li et al., 1969; Weiss, 1970). In the present work the salinity range of the seawaters sampled exceeds that of the published equations, particularly at low salinities where our seawaters have been diluted extensively by river runoff. For these reasons I derived expressions for $\ln\alpha$, pK'_1, pK'_2, and pK'_B as polynomials in temperature and chlorinity over the ranges encountered in

our work.

Method and Results

The constants $\ln\alpha$, pK'_1, pK'_2 and pK'_B were fitted by the method of least squares to polynomial functions of temperature T and chlorinity Cl through the use of Program POLY2VAR (Pawley, 1969). A single run of the program tests the fit of the data to polynomials of six different specified degrees. The objective was a 1% fit to the input data for α, K'_1, and K'_2, within a reasonable number of terms in the polynomial. K'_B required a fit to 5% or better, but the fit obtained was almost as close as for K'_1 and K'_2. The selection of the degree of the polynomial finally used was based upon minimizing the resultant sum of the squares of the differences between the values computed from the polynomial and the original data. When the sums did not minimize, a degree was selected wherein a further change in degree (to a higher order polynomial) did not appreciably change the resultant sum of the squares of the differences.

The polynomial equation for α is a function of $1/T°K$ and Cl based on values of α from Buch (1951). Harvey gave α for temperature 0-30° C and for chlorinity 0-21‰. The sum of the squares of the differences (see Table 1) minimized for the polynomial of degree 3, 2 in $1/T°K$ and Cl, respectively. The other five degrees tested were: 2, 1; 2, 2; 3, 1; 4, 1 and 4, 2. The polynomial is given as Eq. (1)

in Table 1.

The polynomials for pK'_1, pK'_2 and pK'_B are based on values from Lyman (1956). Lyman presents values of $pK'_1 = -\log_{10}K'_1$, $pK'_2 = -\log_{10}K'_2$, and $pK'_B = -\log_{10}K'_B$ for temperature 0-35°C and chlorinity 0-36‰. A good fit to these data was not obtained for a single polynomial for the full range of chlorinity. Accordingly, the pK's are linearly interpolated for the chlorinity range 0-1‰ and two separate polynomials are used for the chlorinity range 1-16‰ and 16-25‰. Equations were not fitted for the chlorinity range 25-36‰ since this was outside the range of the chlorinity data from the cruises. The polynomials for the pK's are functions of temperature in °C and chlorinity in ‰. The sum of the squares of the differences for each polynomial is given in Table 2.

The polynomials for the constants, and the linear interpolation for the pK's for Cl 0-1‰, have been incorporated into SUBROUTINE CONSTANT for which temperature and salinity are provided as input. Values for chlorinity (Cl = S/1.80655), α, K'_1, K'_2 and K'_B are returned as output.

Table 1.

$$\ln \alpha = -1.868560E+1 + 1.092676E+4 \frac{1}{T°K} - 3.156749E+6 \left(\frac{1}{T°K}\right)^2 + 3.755901E+8 \left(\frac{1}{T°K}\right)^3$$
$$+5.557664E-2\ CL - 2.969025E+1 \left(\frac{1}{T°K}\right)CL + 3.291232E+3 \left(\frac{1}{T°K}\right)^2 CL$$
$$+4.729467E-6\ CL^2 - 6.871322E-3 \left(\frac{1}{T°K}\right)CL^2 \quad (1)$$

Chlorinity (CL) 1-16

$$pK'_1 = 6.515016E0 - 9.852755E-3\ T - 6.944827E-5\ T^2 + 5.308594E-6\ T^3 - 3.409073E-8\ T^4$$
$$-5.034762E-2\ CL + 5.404861E-4\ T\ CL + 6.537938E-6\ T^2\ CL - 2.482184E-7\ T^3 CL$$
$$+3.480640E-3\ CL^2 - 5.439522E-5\ T\ CL^2 + 1.803763E-7\ T^2\ CL^2$$
$$-1.025132E-4\ CL^3 + 1.634544E-6\ T\ CL^3 \quad (2)$$

CL 16-25:

$$pK'_1 = 6.340147E0 - 8.955418E-3\ T + 7.551020E-5\ T^2$$
$$-1.004432E-2\ CL + 5.705409E-5\ T\ CL \quad (3)$$

CL 1-16:

$$pK'_2 = 1.019643E1 - 1.322139E-2\ T + 4.122661E-5\ T^2 - 5.123750E-7\ T^3 + 2.651502E-8\ T^4$$
$$-1.542677E-1\ CL + 3.616125E-4\ T\ CL - 1.770241E-6\ T^2\ CL - 2.262948E-7\ T^3\ CL$$
$$+1.475184E-2\ CL^2 - 3.839890E-5\ T\ CL^2 + 3.015831E-7\ T^2\ CL^2$$
$$-4.993383E-4\ CL^3 + 1.351080E-6\ T\ CL^3 \quad (4)$$

CL 16-25:

$$pK'_2 = 9.802809E0 - 7.888585E-3\ T + 1.629283E-4\ T^2 - 3.434345E-6\ T^3$$
$$-2.312676E-2\ CL - 4.318717E-4\ T\ CL - 3.254867E-6\ T^2\ CL$$
$$+1.010936E-4\ CL^2 + 1.054850E-5\ T\ CL^2 \quad (5)$$

CL 1-16:

$$pK'_B = 9.449362E0 - 1.293920E-2\ T + 9.423519E-5\ T^2 - 5.050592E-8\ T^3$$
$$-5.171520E-2\ CL + 5.210158E-5\ T\ CL - 5.444828E-7\ T^2 CL$$
$$+2.555487E-3\ CL^2 + 9.956743E-7\ T\ CL^2$$
$$-6.696407E-5\ CL^3 \quad (6)$$

CL 16-25:

$$pK'_B = 9.262718E0 - 1.259625E-2\ T + 7.551020E-5\ T^2$$
$$-1.634087E-2\ CL + 5.572434E-5\ T\ CL \quad (7)$$

Table 2. Degree of polynomial and sum of squares of differences.

Constant	Degree T*, Cl	Range T(°C)	Range Cl(‰)	Sums of Squares of Differences
ln α	3 , 2	0-30	0-21	4.9204E-4
pK'_1	4 , 3	0-35	1-16	1.5996E-4
	2 , 1	0-35	16-25	3.7828E-4
pK'_2	4 , 3	0-35	1-16	2.4954E-4
	3 , 2	0-35	16-25	7.0853E-4
pK'_B	3 , 3	0-35	1-16	2.9401E-4
	2 , 1	0-35	16-25	8.2522E-4

* Actually fitted to $\frac{1}{T°K}$

APPENDIX II

GLOSSARY

a	subscript denoting air phase
A	empirical constant in nonlinearity equation for IRA
AH	absolute humidity
a_{H^+}	hydrogen ion activity
$AIRPCO_2$	the CO_2 concentration in the original undried air stream
AOU	apparent oxygen utilization
atm	atmosphere
B	constant of integration in response time equation
C	Celsius, carbon, or concentration of CO_2 in ppm
C'	concentration of CO_2 at ambient atmospheric pressure
C_a	concentration of CO_2 in air phase
CA	carbonate alkalinity
C_E	concentration in equilibrator in ppm
C_i	concentration of CO_2 in incoming water
Cl	chlorinity
C_m	concentration of the mixture in ppm
CO_2	carbon dioxide
C_o	concentration of CO_2 in incoming water at $t \leq 0$

C_s	concentration of span gas for calibration, in ppm
C_w	concentration of CO_2 in water phase
C_x	unknown gas concentration in ppm
C'_x	the linearly calculated part of the gas concentration
C_z	concentration of zero gas for calibration, in ppm
C_0	zero gas concentration
C_{610}	nominal concentration of 610 gas
DBT	dry bulb temperature °C
e	base of Naperian logarithm system
E	east
E-4	10^{-4}
F	air flow rate in ml/sec
F_0	flow rate of 0 gas
F_{610}	flow rate of 610 gas
hr	hour
i	subscript denoting incoming water
IRA	infrared analyzer
k	empirical constant in nonlinearity equation for IRA
K'_B	apparent dissociation constant of boric acid in seawater
K'_1	apparent dissociation constants of carbonic acid in seawater
K'_2	
l	liter

LIRA	Mine Safety Appliances Company Model 200 LIRA infrared gas analyzer
m	meter or slope of linearly calculated part of concentration
mb	millibars
meq	milliequivalents
mg	milligram
min	minute
ml	milliliters
MSA	Mine Safety Appliances Company
N	North, or number of molecules of CO_2
N_a	number of molecules of CO_2 in air phase
N_w	number of molecules of CO_2 in water phase
O_{obs}	dissolved oxygen concentration in ml/l in water sample measured by Winkler method
O_{sat}	oxygen solubility
OSU	Oregon State University
O_2	oxygen
P	pressure
PCO_2	partial pressure of carbon dioxide, in either air, fresh or seawater, or a calibration gas
pH	nominally the logarithm of the reciprocal of the hydrogen ion activity. We actually employ the operational definition, $$pH = pH_s + (E - E_s)/(2.303RT/F)$$

where: E is the electromotive force (e. m. f.) of a cell formed by a glass electrode and a reference electrode (usually a calomel or silver-silver chloride half cell). pH_s is the pH of a standard buffer solution and E_s is the e. m. f. measured for the cell when the electrodes are immersed in the standard buffer. R, T, and F are the gas constant, the absolute temperature of the cell in °K, and the Faraday constant, respectively (Bates, 1964, p. 32).

ppm — parts per million

$P_{sv}(T)$ — saturated vapor pressure in mb relative to pure water at temperature T in °K

$P_{sv\text{-}sw}(T_w)$ — saturated vapor pressure in mb of seawater in the equilibrator at temperature T_w in °K

R — $= C_s - C_z$, calibration range. The difference between the CO_2 concentrations of the span and zero calibration gases

RH — relative humidity

R_m — $= (R_z + R_s)/2$, point on recorder chart midway between the zero gas reading R_z and span gas reading R_s

R_s — recorder reading of span gas

R_x — recorder reading of unknown gas

R_z — recorder reading of zero gas

S — salinity

$SEAPCO_2$ — the PCO_2 in the equilibrator air stream

sec — seconds

sigma-t — density at temperature t minus one, times 1000:

$$\sigma_t = (\rho - 1)\ 1000$$

t — time or temperature °C

T	temperature ° Kelvin
TA	total alkalinity
TCO_2	total CO_2
T_w	temperature of seawater in equilibrator in ° K
t_x	flow time in sec for 100 ml of gas being measured
t_0	flow time in sec for 100 ml of 0 gas
t_{610}	flow time in sec for 100 ml of 610 gas
V	volume of CO_2
V_a	volume of CO_2 in air phase
V_w	volume of CO_2 in water phase
w	subscript denoting water phase
W	west
WBT	wet bulb temperature ° C
WHOI	Woods Hole Oceanographic Institution
α	solubility of carbon dioxide in seawater
$\delta PCO_2/\delta t$	increase of PCO_2 with increase of temperature ° C
ΔC_m	the maximum departure from linearity of the IRA response at mid range
ΔC_x	nonlinearity correction to gas concentration
ΔP_{eq}	difference from atmospheric pressure in the IRA cell when the equilibrator air stream is being measured
ΔP_{ref}	difference from atmospheric pressure in the IRA cell when a reference gas is being measured
Δt	change in temperature, ° C

μ	volume mixing ratio
ρ	flow rate
ρ_a	air flow rate
ρ_w	water flow rate
σ_t	see sigma-t
τ	the response of the system or flushing time of the equilibrator
τ_a	response time of the concentration of CO_2 in the air loop to changes in PCO_2 of the incoming water
τ_{a+w}	response time calculated from Eq. 2.11
τ_e	1/e or 37% response time
τ_{PCO_2}	response time of the PCO_2 trace
τ_t	flushing time of water in equilibrator as deduced from temperature
τ_w	flushing time of water in equilibrator from Eq. 2.9
τ_{50}	the 50% response time
τ_{99}	the 99% response time
%	percent
‰	parts per thousand or per mil

APPENDIX III

VITA

Louis I. Gordon

Born 17 August 1928

B. S., University of California, Los Angeles	1951
M. S., Scripps Institution of Oceanography, University of California, Los Angeles	1953
United States Army Chemical Corps	1953-1955
Graduate Research Assistant, Scripps Institution of Oceanography	1955-1958
Graduate Research Chemist, Scripps Institution of Oceanography	1958-1963
Associate Specialist in Marine Geochemistry, Scripps Institution of Oceanography	1963-1966
Graduate Assistant, Oregon State University	1966-1969
Instructor, Oregon State University	1969-

Membership in Professional and Honorary Societies:
American Association for the Advancement of Science, American Geophysical Union, American Society of Limnology and Oceanography, Phi Lambda Upsilon, and Sigma Xi

Publications:

1963 Nitrous oxide in the ocean and the marine atmosphere. Geochimica et Cosmochimica Acta 27: 949-955. (H. Craig and L. I. Gordon)

Isotopic exchange effects in the evaporation of water. Journal of Geophysical Research 68(17): 5079-5087. (H. Craig, L. I. Gordon, and Y. Horibe)

1964 Isotopic oceanography: Deuterium and oxygen 18 variations in the ocean and the marine atmosphere. In: Proceedings of Symposium on Marine Geochemistry, University of Rhode Island. Occasional Publication No. 3-1965, p. 277-374. (H. Craig and L. I. Gordon)

1965 Deuterium and oxygen 18 variations in the ocean and the marine atmosphere. In: Proceedings of Spoleto Conference on: Stable isotopes in oceanographic studies and paleotemperatures, ed. by E. Tangiorgi. V. Lischi e F., Pisa, Italy, p. 9-130. (H. Craig and L. I. Gordon)

1968 A practical manual for use of the Technicon Analyzer in seawater nutrient analyses. Final Report Bureau of Commercial Fisheries Contract 14-17-0001-1759. Oregon State University, Dept. of Oceanography, Reference 68-33. 31 p. (S. W. Hager, L. I. Gordon, and P. K. Park)

Carbon dioxide tension measurements in surface waters off the Oregon coast as an indicator of upwelling. Transactions American Geophysical Union 49: 642. (L. I. Gordon and P. K. Park)

1969 Carbon-13: carbon-12 ratios in dissolved and particulate organic matter in the sea. Deep-Sea Research 17: 19-27. (P. M. Williams and L. I. Gordon)

Carbon dioxide partial pressure in the Columbia River. Science 166: 867-868. (P. K. Park, L. I. Gordon, S. W. Hager, and M. C. Cissell)

1970 Carbon dioxide in the surface waters of the Bering Sea and northwest Pacific Ocean, late summer. Transactions of the American Geophysical Union 51: 326. (L. I. Gordon, J. J. Kelley, D. W. Hood, and P. K. Park)

1971 CO_2 partial pressure in the surface waters of the north Pacific Ocean between Canada and Japan, March-April 1969. In: Proceedings of the Joint Oceanographic Assembly September 1970: The ocean world, ed. by M. Uda. Japan Society for the Promotion of Science, Tokyo, Japan. p. 401-402. (P. K. Park, L. I. Gordon, S. W. Hager, and T. R. Parsons)

Carbon dioxide partial pressures in north Pacific surface waters--time variations. Journal of Oceanographical Society of Japan, 27(3): 81-90. (L. I. Gordon, P. K. Park, S. W. Hager, and T. R. Parsons)

A practical manual for use of the Technicon AutoAnalyzer® in seawater nutrient analyses; revised. Dept. of Oceanography, Oregon State University, Corvallis. Reference 71-22. 49 p. (E. L. Atlas, L. I. Gordon, S. W. Hager, and P. K. Park)

Hydrographic data from Oregon waters, 1970. Dept. of Oceanography, Oregon State University, Corvallis. Reference 71-23. 134 p. (B. Wyatt, R. Tomlinson, W. Gilbert, L. Gordon, and D. Barstow)

1972 The carbon dioxide system of the Bering Sea. In: The International Bering Sea Symposium, Hakodate, 1972. University of Alaska Press. In press. (P. K. Park, L. I. Gordon, and S. Alvarez-Borrego)

The expendable bathyoxymeter. Limnology and Oceanography 17: 288-292. (H. Jeter, E. Føyn, J. M. King, and L. I. Gordon)

An at-sea comparison of manual and AutoAnalyzer® analyses of phosphate, nitrate, and silicate. Limnology and Oceanography. In press. (S. W. Hager, E. L. Atlas, L. I. Gordon, A. W. Mantyla, and P. K. Park)

Oxygen-carbon dioxide-nutrients relationships in the southeastern region of the Bering Sea. Journal of Oceanographical Society of Japan 28(2): 71-93. (S. Alvarez-Borrego, L. I. Gordon, L. B. Jones, P. K. Park, and R. M. Pytkowicz)

A continuous PCO_2 measurement system. School of Oceanography, Oregon State University, Technical Report 240. Reference 72-17. (L. I. Gordon and P. K. Park)

A sample changer for automated seawater nutrient analysis systems. Ocean Engineering. In press. (R. D. Tomlinson and L. I. Gordon)

Carbon dioxide in the surface waters of the Bering Sea and north Pacific Ocean. Submitted to Marine Chemistry. (L. I. Gordon, J. J. Kelley, D. W. Hood, and P. K. Park)

Oregon State University PCO_2 data 1968. School of Oceanography, Oregon State University, Data Report. In preparation. (L. I. Gordon and P. K. Park)

Oregon State University PCO_2 data 1969. School of Oceanography, Oregon State University, Data Report. In preparation. (L. I. Gordon and P. K. Park)

Oregon State University PCO_2 data 1970. School of Oceanography, Oregon State University, Data Report. In preparation. (L. I. Gordon and P. K. Park)

Oregon State University PCO_2 data 1971. School of Oceanography, Oregon State University, Data Report. In preparation. (K. W. Kantz, L. I. Gordon, and P. K. Park)

An instruction manual for use of the Technicon AutoAnalyzer® in precision seawater nutrient analyses, Manual for instruction of GEOSECS technicians. Dept. of Oceanography, Oregon State University. In preparation. (J. C. Callaway, R. D. Tomlinson, L. I. Gordon, and P. K. Park)